International Atomic Energy Agency

INDC(IND)–30
Distr. G

INDC INTERNATIONAL NUCLEAR DATA COMMITTEE

# PROCEEDINGS OF THE WORKSHOP ON NUCLEAR DATA EVALUATION PROCESSING AND TESTING

## KALPAKKAM
## AUGUST 4, 5, 1981

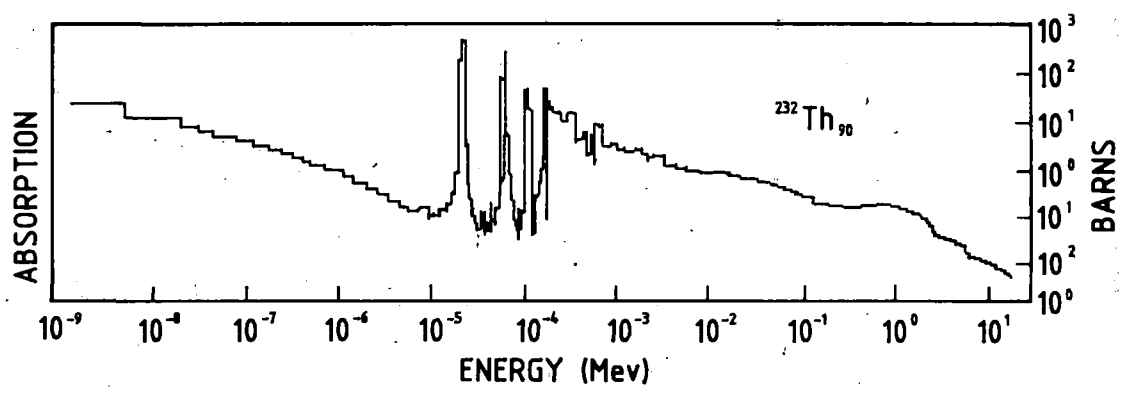


COMPILED BY S. GANESAN



IAEA NUCLEAR DATA SECTION, WAGRAMERSTRASSE 5, A-1400 VIENNA

# PROCEEDINGS OF THE

# WORKSHOP ON NUCLEAR DATA EVALUATION

# PROCESSING AND TESTING

KALPAKKAM

AUGUST 4, 5, 1981

COMPILED BY S.GANESAN

Reactor Research Centre

Kalpakkam

TAMILNADU 603 102

## FOREWORD

The present Workshop on Nuclear Data Evaluation, Processing and Testing has been primarily organised with the objective of enabling the scientists working in this area of Nuclear Data from various laboratories to come together, review the present status of work in the respective groups, discuss the future requirements of our programme and identify specific areas where a coordinated effort can be effectively implemented. The response hasbeen fairly good with the participation of scientists from Bhabha Atomic Research Centre, Bombay, I.I.T., Kanpur and from the Reactor Research Centre, Kalpakkam, the institutions actively persuing the nuclear science and technology programmes, as expected.

It is clear from the papers presented in the Workshop that a significant amount of work on Nuclear Data Evaluation is in progress in the groups working on basic nuclear physics whereas the areas of processing and testing nuclear data have been persued by reactor physics groups concerned with the reactor design. This is the first time that such a workshop on Nuclear Data has been organised on a national level and we hopethe discussions generated in the workshop have provided the impetus required for close collaborative work between the various groups working on Nuclear Data, in the future.

It is a pleasure to thank Shri N.Srinivasan, Director, RRC for inaugurating the workshop and for having provided all the required support and Dr. M.K.Mehta, Head, Nuclear Physics Division for giving the Key Note address and generating the lively discussions among the participants. The active co-operation received from the members of the organizing committee and other colleagues is gratefully acknowledged.

R.Shankar Singh
Convenor
Organising Committee

## PREFACE

The papers presented at the Workshop on Nuclear Data Evaluation, Processing and Testing have been compiled and presented in this volume. Where full paper was not available due to unavoidable reasons, the abstract or summary has been included. The Workshop gave the opportunity to the Indian Nuclear Data Community to discuss in depth the current needs and future course of action in this important field.

It is hoped that this volume will help to disseminate the contents of the Workshop among wider section of the Indian Nuclear Data Community.

I take this opportunity to express my sincere thanks to S/Shri R. Shankar Singh, V. Gopalakrishnan, A. K. Jena and M. M. Ramanadhan for their valuable co-operation in and contribution to organization of this Workshop.

Thanks are due to Shri N. Srinivasan and Shri S. R. Paranjpe for their support and encouragement.

S. Ganesan
(SECRETARY)

CONTENTS

| Paper No. | Title |
|---|---|
| 14 | Comments on $^{9}Be$ (n, 2n) Cross Section Data in the Context of Fission and Fusion Systems |
| 15 | Evaluation of Thermal Reactor Cross Sections through Integral Measurements |
| 16 | Evaluations of Gamma Production Cross Sections in Coupled Neutron - Gamma Cross Section Sets |
| 17 | Effect of Gamma Source Spectra on Gamma Transport Near Interfaces |
| 18 | Fusion Blanket Neutronics |

---

## ORGANISING COMMITTEE

| | | |
|---|---|---|
| S/SHRI. | R. SHANKAR SINGH | (Convenor) |
| | S. GANESAN | (Secretary) |
| | A.K. JENA | |
| | V. GOPALAKRISHNAN | |
| | M.M.RAMANADHAN | |

Paper to be presented at Workshop on Nuclear Data Evaluation, Processing and Testing, August 4, 5, 1981, R.R.C., Kalpakkam.

# NUCLEAR DATA REQUIREMENTS FOR A FAST REACTOR PROGRAMME

by

S. Ganesan and R. Shankar Singh
Fast Reactor Group
Reactor Research Centre
Kalpakkam 603102
TAMIL NADU, INDIA.

## INTRODUCTION

This paper briefly discusses the nuclear data requirements for the Indian Fast Reactor Programme. Plans to construct a 500 MWe Fast Breeder Reactor (FBR) by the middle of next decade followed by a series of FBRs by the year 2010 are underway. In this context, the scope of this paper is limited by the discussion on the nuclear data requirements and the target accuracies for the complete fuel cycle involving core design, operation and fuel reprocessing as well as safeguards and safety of FBRs. The current status of availability of various nuclear data for our FBR programme in India as pointed out. Suggestions are made regarding how we should handle the nuclear data needs in future.

## II STATUS AT RRC.

### II.1. AVAILABLE NUCLEAR DATA FILES.

At RRC and at BARC, evaluated nuclear data libraries have been procured [1] through IAEA and have been processed in the recent past to obtain multigroup sets. For example KEDAK-3 (1976) and ENF-B/IV (1975) are available at RRC. Some of the elements in ENDF/B-IV have been processed by the fast reactor nuclear data processing code RAMBHA[2] developed at RRC. The various nuclear data files for core design and shielding and other aspects of complete fuel cycle of FBR available as on today at RRC are given below.

A. General Evaluations

(i) ENDF/B-III, seven standard nuclides
(ii) ENDF/B-IV, General files
(iii) UKNDL-402
(iv) KEDAK2 and KEDAK3
(v) The Livermore Library ENDL

.....2

B. Dosimetry reactions

(i) UKNDL, dosimetry file
(ii) SAND II and DETAN-74

C. Fission Product Libraries

(i) The Australian library of evaluated neutron cross sections for fission product nuclei - point data.

(ii) The Bologna Library of evaluated neutron cross sections for fission product nuclei.

(iii) The ENDF/B Library for fission product cross sections (and decay data).

(iv) The Dériller's library of fission product yield ( and decay data)

(v) The Japanese Library for fission product cross sections.

D. Multigroup Cross section Libraries

(i) 25 Group Cadarache Cross Section Library.
(ii) n-γ coupled cross section library DLC-37
(iii) 100 Group Cross Section Library DLC-2E
(iv) Modified ANL-32 group set
(v) 605-Group Legendre Coefficient ELMOE Library
(vi) n-γ coupled Cross Section Library DLC-23D (CASK)

.....3

## II.2 CREATION OF INDIAN EVALUATED NUCLEAR DATA FILE.

For an indigenous nuclear data programme, we must aim to develop our own evaluated nuclear data file. Considering the limitations of available man power and experimental facilities such as accelerators, to start with, we can have as base the ENDF/B data that we already have for the various nuclides which are relevant for $^{239}Pu$-$^{238}U$ and $^{232}Th$-$^{233}U$ fuel cycles. The aim should be to develop our own file by improving specific nuclear data as and where improved evaluations and / or differential nuclear data measurements are made in India or reported in the open literature. Such an approach is a must for India in the long run since we are

- unable to procure improved and latest versions of ENDF/B as and when they are released.

- in a better position to understand and recognize readily the defects and omissions in the available data files. (For instance in ENDF/B-IV there is no unresolved resonance data for $233_U$; For $^{232}Th$, the data of ENDF/B-IV and ENDF/B-III are same below 50 KeV etc.)

## II.3 CREATION OF AN INDIGENOUS PROCESSING CODE SYSTEM

The creation of a multi group cross section set is best done by an indigenously developed processing code. This helps to clearly understand and improve on a continuing basis the methods followed by the various individual

.....4

modules of the processing code. The development of RAMBHA[2] at RRC is such an effort. It is expected that from the point of view of reducing the computing time without sacrificing the accuracy, efforts will be made to improve the individual modules based on the published experiences and our own numerical experimentations. The details of the first version of fast reactor nuclear data processing code RAMBHA will be discussed in a separate paper in this Workshop.

## III. TARGET ACCURACIES [3-13]

At this point, we examine the details of accuracy required in nuclear data evaluations and the corresponding uncertainties in the neutronic parameters of FBRs. The general requirement on the predictional capability of integral parameters for FBRs in various countries is centred around the following values:

| | | |
|---|---|---|
| $K_{eff}$ | : | 0.7% |
| Breeding Ratio | : | ±6% |
| Maximum sodium void effect | : | ±20% |
| Control Rod Worth | : | ±6% |
| Doppler effect | : | ±15% |
| Power Distribution (both for local/average and peak/average) | : | ±4% |

.....5

Table - I

Estimated Uncertainties

( 2 $\sigma$ level )

| Causes/Sources of Uncertainty | Prototype Fast Reactors* | | Commercial Fast Reactors** | |
|---|---|---|---|---|
| | $D_{eff}$ | Breeding Gain | $K_{eff}$ | Breeding Gain |
| From the experience obtained in critical assemblies | 0.4 - 0.7% | 5 - 6% | 0.7 - 0.9% | 5 - 6% |
| Extrapolation to power reactor | 0.7% | 5 - 6% | 0.9% | 4% |
| Burnup related effects (End of cycle) | 1% | 2% | 1.3% | 4% |
| Fuel specifications | 1% | - | 1% | - |
| Total (fresh fuel) | 1.3% | 7% | 1.5% | 7% |
| Total (Burnt up fuel) | 1.7% | 7% | 1.9% | - |

* Prototype Fast Reactors in the range of 250-300 MWe

** Commercial Fast Reactors are expected to produce power in the range of 1200-1300 MWe

.....6

It is also accepted that the requirement for any of the neutronic parameters mentioned above is not met without a critical assembly. Table I gives the estimated uncertainties in Keff and breeding gain as arrived at by laboratories that have supporting critical experiments program. The uncertainties for us will be larger than these values atleast for the first few core loadings.

According to Hafele et.al.,[14] "the prediction of Keff is within 3% to 4% (critical mass 15% to 20%) if a particular reactor case is calculated and the group constant set is chosen from among the sets in use. If one instead chooses or prepares the group constant set with care but without special experimental assistance, the prediction of Keff is within 1.5 to 2.5% (critical mass 8% to 10%). If in addition to the latter case the results of a similar critical experiment are available it should be possible to predict Keff within 0.5% to 1% (critical mass less than 5%).

Thus considering the fact that we do not have a critical facility our uncertainty for Keff may be higher than 1% from nuclear data consideration alone. The differences in fabrication uncertainties in Indian conditions as compared to those in advanced nations will have to be appropriately added to the uncertainty assigned to Keff obtained by analyses of selected fast critical assemblies of other nations. For cores involving $^{232}Th$-$^{233}U$ fuel, additional uncertainties arise as the fast critical assemblies constructed in other nations either have $^{238}U$ - $^{239}Pu$ fuel or do not have relation to our requirements of composition and size.

.....7

## IV. REQUIREMENTS OF NUCLEAR DATA.

### IV.1 CORE DESIGN

As mentioned already the requirements of accuracy of nuclear data are more stringent in India as the critical experiments program is absent. Table II gives the required accuracy of the cross section corresponding to target accuracies of $\pm 1\%$ in Keff and $\pm 2\%$ in breeding ratio as given by Bobkov et.al [15]., These numbers for $^{239}Pu$ and $^{238}U$ closely agree with those reported by Weisbin et.al independently)

The generation of our own multigroup data set using RAMBHA code system and ENDF/B-IV (or RRC DF[16]) will lead to a 'non-adjusted' multigroup data set. Extensive analyses of fast critical assemblies should be performed to validate this new data set. At present, in view of limited man power and computation time, it has only been possible to generate multigroup cross sections for specific elements such as $^{232}Th$, Fe, $^{238}U$ etc and add them to the Cadarache set. It has been recognized that there is a need to obtain better group constants for the higher isotopes of $^{241}Pu$ and $^{242}Pu$ and for Ni, Fe and Cr, as the Cadarache set is not satisfactory for these elements [17]. It is also known that the Cadarache set will not work satisfactorily for $^{232}Th$-$^{233}U$ fuel systems. Thus evaluations of the relevant isotopes of this fuel cycle are to be completed and validated. Thus in parallel, the indigenous programme of generation and testing of multigroup cross sections for all fissile, fertile and structural isotopes by processing the latest basic neutron nuclear interaction data should continue. Some of the assemblies proposed to be analysed have been listed already [17].

..... 8

TABLE II

DIFFERENTIAL CROSS SECTION ACCURACY REQUIREMENTS (PER CENT).

(After Ref. 15)

| | 0,8 < E < 10 MeV | | | | 0,1 < E < 0,8 MeV | | | | 0 < E < 0,1 MeV | | | |
|---|---|---|---|---|---|---|---|---|---|---|---|---|
| | I | II | III | IV | I | II | III | IV | I | II | III | IV |
| **$^{239}$Pu** | | | | | | | | | | | | |
| $\bar{\sigma}_c$ | - | 50* | 50* | 41 | 41 | 9,5 | 10 | 6,5 | 6,7 | 3,7 | 5,0 | 2,5 | 3,6 |
| $\bar{\sigma}_f$ | 2,6 | 4,0 | 6,0 | 10* | 1,3 | 2,3 | 4,0 | 6,0 | 1,1 | 2,0 | 4,0 | 4,0 |
| $\bar{\nu}_f$ | 1,2 | 1,2 | 1,5 | 1,9 | 0,4 | 0,7 | 0,5 | 0,9 | 0,5 | 0,8 | 0,7 | 1,2 |
| **$^{238}$U** | | | | | | | | | | | | |
| $\bar{\sigma}_c$ | 9,3 | 10 | 19 | 19 | 2,8 | 6,0 | 4,3 | 4,7 | 2,2 | 4,0 | 2,6 | 4,4 |
| $\bar{\sigma}_f$ | 1,8 | 3,4 | 2,1 | 2,6 | | | | | | | | |
| $\bar{\nu}_f$ | 1,0 | 2,5 | 1,3 | 1,7 | | | | | | | | |
| **Steel** | | | | | | | | | | | | |
| $\bar{\sigma}_c$ | 20 | 20 | 25 | 25 | 15 | 18 | 17 | 18 | 11 | 15 | 12 | 13 |
| **$^{240}$Pu** | | | | | | | | | | | | |
| $\bar{\sigma}_c$ | 45 | 45 | 50* | 50 | 14 | 15 | 17 | 17 | 6,5 | 7,1 | 9 | 9 |
| $\bar{\sigma}_f$ | 3,5 | 5,0 | 4,4 | 6,5 | 5,3 | 7,0* | 6,6 | 6,6 | 7,0* | 7,0* | 7,0* | 7,0* |
| $\bar{\nu}_f$ | 2,0 | 2,1 | 2,4 | 2,5 | 3,0* | 3,0* | 3,0* | 3,0* | 3,0* | 3,0* | 3,0* | 3,0* |
| **$^{241}$Pu** | | | | | | | | | | | | |
| $\bar{\sigma}_f$ | 10* | 10* | 10* | 10* | 5 | 5,4 | 6,2 | 6,2 | 3,7 | 3,8 | 4,5 | 5,0 |
| $\bar{\nu}_f$ | 4,0* | 4,0* | 4,0* | 4,0* | 2,3 | 2,3 | 2,9 | 3,0* | 1,2 | 1,3 | 1,5 | 1,6 |
| **Flux** | | | | | | | | | | | | |
| | 1,3 | 1,7 | 2,0 | 2,7 | 1,1 | 1,8 | 2,5 | 2,7 | 2,0 | 3,0 | 2,1 | 2,5 |
| | 50* | 50* | 50* | 50* | 14 | 16 | 17 | 17 | 7,0 | 8,0 | 9,3 | 10 |

Required accuracy $\bar{\nu}_f^{52}\ \bar{\sigma}_f$ - 0,3%

I and II Requirements for prediction of both keff and BR
III and IV Requirements for prediction of BR

I and II Requirements when integral measurements are not included
II and IV Requirements when integral measurements are taken into account.

Fast reactor benchmarks could be analysed by both RRC and BARC teams independently using same multigroup structure and diffusion and transport codes. This exercise when completed will bring out the spread in the calculated values of neutronic parameters calculated using

(1) Cadarache cross section set
(2) RRC set generated by RAMRHA
(3) BARC set generated using $MC^2$ and ENDF/B-IV

The uncertainties in safety related reactivity coefficients in FBRs due to nuclear data considerations can be reduced by following considerations:

- More accurate data on resonance parameters are desirable in resolved and unresolved resonance region and better processing methods of these data. This is for Doppler effect predictions
- The energy cross section gradients must be known accurately to ± 3% to determine sodium voiding reactivity accurately.
- The elastic and inelastic cross sections and transfer matrices which determine the spectrum and spectral gradients should be evaluated to high accuracy, as it is believed that the underprediction of low energy component in fast spectrum has led to underestimation of Doppler effect.

For determination of control rod worths to ± 5% accuracy, the typical requirements for the absorber material (such as B, Cd, Ta etc.) are that the capture cross sections should be known to ± 5% and scattering cross sections to ± 10%.

## IV.2 REQUIREMENTS OF NUCLEAR DATA FOR OTHER REACTOR PARAMETERS

The typical fast reactor requirements for properties other than major neutronic parameters are as follows[12]

| Parameter | percentage accuracy |
|---|---|
| Decay Heat | 2 to 5 |
| Activity of components | 10 |
| Fluence | 5 |
| Displacement damage cross sections | 5 |
| Dose Gradients | 10 |
| Helium and Hydrogen Production cross sections | ±20 to ±50 |

The various data requirements are given in Table III. Dosimetry measurements are used to give information about the total flux and flux spectrum. The cross section requirements from this angle are also given in Table III. Activation reactions in structural materials and coolant are required to determine the induced activity satisfactorily. The standard cross sections given in Table III should be known to the highest accuracy possible as other cross sections are obtained relative to the cross section used as a standard. Presently the accuracy required for helium producing reactions is not so stringent as the mechanisms of radiation damage has higher non neutronic uncertainties in interpretations.

## III.3 NUCLEAR DATA REQUIREMENTS FOR SHIELDING CALCULATIONS[19]

In shielding calculations, use is made of the group constants, the generation of which do not generally takes into account the strong spatial variation of neutron spectrum in the shield. Thus for example the use of a simplified slowing down model in the generation of group constants is a main source of error in calculating the neutron penetration in fast reactors. To ensure ± 50% accuracy in the flux at the outer boundary of the shield the total interaction cross section must be known for all the isotopes comprising the shield (such as steel, sodium, carbon) within ± 1% accuracy in the range 1MeV - 1eV. The radiative capture cross section should be known within ± 10% for those

Table III

LIST OF CROSS SECTIONS AND REQUESTED ACCURACIES

I Fast Reactor Core Design

Isotopes : Fissile : $^{233}U$, $^{235}U$, $^{239}Pu$
Fertile : $^{232}Th$, $^{238}U$
Structural : Fe, Cr, Ni

| Parameter | Fissile isotopes | Structural isotopes | Fertile Isotopes |
|---|---|---|---|
| $\nu_f$ | 0.3% | - | 1% |
| $\sigma_f$ | 2% | - | 2% |
| $\sigma_c$ or $\alpha$ | 4% | 5-10% | 3% (1.5% in ratio to $\sigma_f$ of $^{239}Pu$) |
| $\sigma_t$ , $\sigma_s$ | 2% | 5% ($\sigma_s$) | 5% |
| $\sigma_{in}$ | 10% | ± 5% | 5% |
| $\sigma_{n,2n}$ | 10% | - | 10% |
| Resonance Parameters | 10% | 20% | 3% |
| $\nu$ delayed | 3% | - | 5% |

The above requirements for $^{241}Pu$ and $^{240}Pu$ are less stringent (by a factor of two)

Table IIIcontd.

II CONTROL ABSORBERS

Isotopes: $^{10}B$, $^{11}B$, Ta, Cd, Eu, Gd, Er, Hf

$\sigma_c$ : ± 5% )
$\sigma_s$ : ±10% ) for $^{10}B$ and $^{11}B$

For the other isotopes which are proposed to be control rod materials the same requirements arise in future.

III FISSION PRODUCT NUCLEAR DATA

Bulk Reactivity Effects ± 5% to 10%

This leads to $\sigma_c$ : ± 10%

and $\sigma_s$ : ± 30%

Burnup Monitoring, Integral decay heat and delayed neutron emission

$\sigma_c$ to be known to ± 10% for the following

$^{97}Mo$, $^{99}Tc$, $^{101}Ru$, $^{104}Ru$, $^{106}Ru$, $^{105}Pd$, $^{107}Pd$, $^{129}I$, $^{131}Xe$, $^{135}Xe$,

$^{133}Cs$, $^{135}Cs$, $^{144}Ce$, $^{143}Nd$, $^{145}Nd$, $^{147}Nd$, $^{147}Pm$, $^{149}Sm$, $^{151}Sm$

'able III cont'd.

IV ACTIVATION REACTIONS

The requested accuracy is ± 10%

$^{58}Ni(n,p)\ ^{58}Co$; $^{50}Cr(n,\gamma)\ ^{51}Cr$; $^{54}Fe(n,p)\ ^{55}Mn$; $^{58}Fe(n,\gamma)\ ^{59}Fe$;

$^{59}Co(n,\gamma)\ ^{60}Co$; $^{60}Ni(n,p)\ ^{60}Co$; $^{75}As(n,\gamma)\ ^{76}As$; $^{98}Mo(n,\gamma)^{99}Mo$ ;

$^{181}Ta(n,\gamma)\ ^{182}Ta$; $^{23}Na(n,\gamma)\ ^{24}Na$; $^{23}Na(n,2n)\ ^{24}Na$; $^{40}A(n,\gamma)\ ^{41}A$ ;

V DOSIMETRY CROSS SECTIONS

Standards $^{27}Al(n,\alpha)\ ^{24}Na$; $^{237}Np(n,f)$F.P. $^{56}Fe(n,p)\ ^{56}Mn$; $^{58}Ni(n,2n)\ ^{57}Ni$;

$^{63}Cu(n,2n)\ ^{62}Cu$, $^{197}Au(n,\gamma)\ ^{198}Au$, $^{238}U(n,f)$ F.P. $^{239}Pu(n,f)$ F.P.

VI STANDARDS

$^{3}He(n,p)\ ^{6}Li(n,\alpha)$, $^{10}B(n,\alpha)\ ^{12}C$: $\sigma_t, \sigma_s$ $^{197}Au(n,\gamma)$;

$^{235}U(n,f)\ ^{252}Cf$: $\nu$ and fission spectrum

VII HELIUM PRODUCTION CROSS SECTIONS

All isotopes and impurities present in stainless steel ;

$^{58}Ni(n,\gamma)\ ^{59}Ni(n,\alpha)$ ; Such two step reactions also need this cross sections to be known

elements especially below 10keV for a good (±10%) prediction of heat generation and capture gamma radiation fluxes. In the shielding of FBRs the capture gamma yield is due mainly to the absorption of neutrons. We need to perform a few more sensitivity studies to assess our complete requirements.

## III.4 NUCLEAR DATA REQUIREMENTS FOR OUT-OF-PILE PART OF FUEL CYCLE[19]

The importance of actinides in fuel cycle is well known.

a) In the core itself the build up of actinides changes reactivity. The errors in the cross sections of $^{236}U$, $^{237}Np$, $^{238}Pu$ and Am isotopes lead to 500 pcm error in criticality of FBR fuelled with plutonium. The minor actinides other than Pu isotopes contributes 1% to the generation of power and $^{241}Am$ isotope may have an effect on the internal breeding gain by about 0.02 at the end of fuel life. When Pu from PHWR is fed into LMFBR, the higher isotopes $^{240}Pu/^{241}Pu/^{242}Pu$ contribute 6/8/1% to reactor power.

b) The prediction of radiation and heat generation depends on the neutron, $\gamma$, $\alpha$ and $\beta$ sources of spent fuel and this has to be known for shielding and cooling purposes, during transport, reprocessing and refabrication. The $\alpha$ and $\gamma$ activity mainly due to $^{242}Cm$ and $^{244}Cm$ pose problems in fabrication and handling of fuel. The inadequate knowledge of effective cross sections used in the calculations of isotopic composition leads at present to 50% error. The study of actinide depletion is important as the actinide waste would represent a hazard risk for 100,000 years and longer while the risk from fission products decreases to acceptable levels within decay periods of 1,000 years.

A study of sensitivity analysis of the actinide production and burnup in fast reactors should be taken up in order to arrive at the information on the required accuracy of nuclear data for actinides.

## V RECOMMENDATIONS AND CONCLUDING REMARKS

From the broad overview of nuclear data requirements presented above we recommend the following for satisfying the requirements of our fast reactor programme.

1. The absence of fast critical experiments programme leads to the requirement of a more careful evaluation and watching of the developments in international efforts in the field of neutron induced nuclear data evaluation. The analyses of selected critical experiments could be performed by two independent selected groups in India to enable healthy criticism and cross-checking.

2. Efforts to obtain the detailed information on critical assemblies must be initiated through international bodies like IAEA or ENEA/OECD.

3. A co-ordinated all-India effort in the long run and RRC-BARC collaboration in the immediate future will be very helpful for successful implementation of indigeneous evaluation processing and validation of nuclear data for applications to fast reactors.

4. Sensitivity studies are required to be performed to assess the nuclear data requirements in Indian context for some of the shielding, out-of-pile and in-pile cases.

References

1. M.L.Sharma, ' A note on the Numerical Nuclear Data Files Available at Reactor Physics Section', Unpublished Note FRG-RP-161/1978.

2. S.Ganesan et al., 'Development of a New Fast Reactor Processing Code RAMBHA at RRC' paper P-5 in this Workshop.

3. P.Greebler et al. 'Implications of Nuclear Data Uncertainties to LMFBR Design' GEAP 13643(1970).

   See also p.928 in New Developments in Reactor Physics and Shielding CONF - 720901 (1972) USA.

4. C.R.Weisbin et al. (Editors) 'A Review of the Theory and Application of Sensitivity and Uncertainty Analysis', Proceedings of a Seminar - Workshop, Oak Ridge, Tennessee, August 22-24, 1978, ORNL/RSIC - 42 (1979) USA

5. E.Kiefhaber, 'Evaluation of Integral Physics Experiments in Fast Zero Power Facilities' in Advances in Nuclear Science and Technology Vol.8, Academic Press (1975).

6. L.G.Lesage et al. 'Assessment of Nuclear Data Files via Benchmark Calculations - A Report on the NEACRP/IAEA International Comparison Calculation of A Large LMFBR', Advances in Reactor Physics, Silver E.G. (Ed). Proceedings of an American Nuclear Society Topical Meeting, Gatlinburg, Tennessee, CONF-780401 (1978)
   See also the final report ANL-80-78 (1980).

7. F.G.Perey et al. 'Estimated Data Covariance Files of Evaluated Cross Sections -- Examples for $^{235}U$ and $^{238}U$' in Advanced Reactors: Physics, Design Economics Pergamon Press (1975).

8. M.Salvatores, 'Recent Developments in Cross-section Adjustment Techniques Advances in Reactor Physics Silver E.G.(Ed) P.269-283, Proceedings of an American Nuclear Society Topical Meeting, Gatlinburg, Tennessee CONF-780401 (1978) USA

9. F.G.Perey et al. 'Estimated Data Covariance Files of Evaluated Cross-sections - Examples for $^{235}U$ and $^{238}U$ in Advanced Reactors : Physics, Design and Economics' J.M.Kallfelz and R.A.Karam (Eds) Pergamon Press (1975).

10. G. de Saussure and R.N. Perez 'Present Status of Cross-Section data of the Fissile and Fertile Isotopes for Fast Reactors' in AdvancedReactors : Physics, Design and Economics, J.M.Kallfelz and R.A. Karam (Eds) Pergamon Press (1975).

11. C.R.Weisbin et al. 'Application of Sensitivity and Uncertainty Methodology to Fast Reactor Integral Experiment Analysis' Nucl. Sci. Engg., 66, 307 (1978).

12. J.L.Rowlands, 'Nuclear Data for Reactor Design, Operation and Safety' in Proceedings of the International Conference on Neutron Physics and Nuclear Data for Reactors and Other Applied Purposes, Harwel, UK, Sep. 25-29 (1978).

13. S.Ganesan 'Target Accuracy and Sensitivity Analysis' Radiation Physics Vol.3, Nov. 1980, Newsletter Published by Indian Society for Radiation Physics.

14. W.Hafele et al., 'Fusion and Fast Breeder Reactors,' International Institute for Applied Systems Analysis, Austria (1977).

15. Yu. G. Bobkov et al,'Planning of Neutron Data Experiments and Evaluations for Reactors' INDC (CCP)-46/ IAEA Vienna.

16. Activity Reports of Reactor Physics Section for the years 1978, 1979 and 1980 RRC, Kalpakkam

17. S.Ganesan and R.Venkatesan,'Analysis of Fast Critical Assemblies in Support of Criticality, Predictions for FBR-500' Note No.FRG/01100/RP-209 (12-2-1981).

18. Differential and Integral Nuclear Data Requirements for Shielding Calculations' IAEA-207 (1978) Vienna Proceedings of a Specialists Meeting held in Vienna 12-15 October 1976.

19. H.Mitani et al. J.Nucl. Sci. & Tech. (1980); JAER 1 - M 8133 (1979).
See also S. Ganan, 'General Survey of

# USE OF THEORETICAL MODELS IN NUCLEAR DATA EVALUATION

S.K. Gupta

Nuclear Physics,Division, Bhabha Atomic Research Centre,

Bombay 400085.

Abstract:

A brief overview of nuclear models for neutron nuclear cross section predictions is presented starting with basic concepts. Resonance reactions, optical model, statistical model and level statistical parameters, preequilibrium model, gamma emission and fission theory are reviewed.

1. Introduction

Nuclear Data[1] find numerous applications such as in

a thermal and fast fission reactors

b plants for nuclear fuel febrication end reprocessing

c fusion reactors

d shielding of reactors and accelerators

e nonenergy applications such (i) nuclear activation analysis (ii) radioisotopes as tracers (iii) production of radioisotopes (iv) nuclear particle irradiation such as in cancer therapy.

f nuclear physics to enhance an understanding of the nuclear phenomena.

Due to immense importance of nuclear data, every possible effort to obtain these data is rigorously persued. The primary effort is in directly measuring them but the experimental generation of nuclear data in its entirety is inadequate obviously on grounds of feasibility and economics. It is here that the nuclear models and systematics play a crucial role in providing a unified or concept-economic understanding of the measured data. This understanding finally promotes confidence in using experimental data by removing discrepant data. It further fills gaps by interpolation of the data as a function of energy and by predictions in the extrapolated energy and mass-number domains.

There exist two hard core beliefs in life (i) direct experiment and (ii) rigorous theory. An experimentalist believes that only the experiments can lead to reality while a theorist insists that he can tell all about the reality by a fabric of logical structures. An evaluator of nuclear data believes in using the best of both the worlds and provides a balanced objective view-point to the user of nuclear data.

The nucleus consists of neutrons and protons. In cross sections for neutron nuclear reactions which comprise a large segment of data-needs, an incident neutron interacts with the target nucleus and may produce one of the several end-products. To exemplify, a neutron interacting with a target nucleus undergoes interactions with its consituent nucleons and comes out without any change in the internal state of the target giving rise to elastic scattering. Other possible modes are inelastic scattering, radiative capture, fission, (n,p), (n,$\alpha$), (n,2n) reactions and so on. The interaction probability is represented by cross section which varies with energy. In a naive picture of a nucleus interacting with a neutron, the neutron undergoes an interaction with the average potential produced by the whole nucleus. This potential depends on the distance between the neutron and the centre of the nucleus. The remaining part of the interaction between the neutron and the centre of the nucleus. The remaining part of the inter-

action between the neutron and the constituent nucleons can be envisaged as giving rise to successive collisions with them. The first collision gives rise to the doorway state in which the incident neutron loses energy and a nucleon inside the nucleus gains energy leaving a hole behind. If the doorway state does not decay by disintegration another collision will give rise to three excited particles and two holes. Every further collision increases the number of particles and holes by two units. If at any stage there are n excited particles and holes collectively called as excitons each has an average energy E/n where E is the excitation energy of the composite system. Thus if a intermediate state formed does not decay, it leads to a state where the energy is shared between several excitons each having much less than the energy of the incident nucleon. This state is the compound state which does not have any memory about its formation. The compound state lives for a long time and its decay is that of a fully equilibrized system. As the excitation energy increases the system sometimes decays before reaching the equilibrium and this gives rise to the preequilibrium component. The equilibrium emission is characterized by low-energy and almost isotropically emitted particles while the preequilibrium emission is characteristic of high energy particles emitted in the forward peak.

The interrelationships between various model is best illustrated in the Fig.1 where the model applicability is shown for various energy regions.

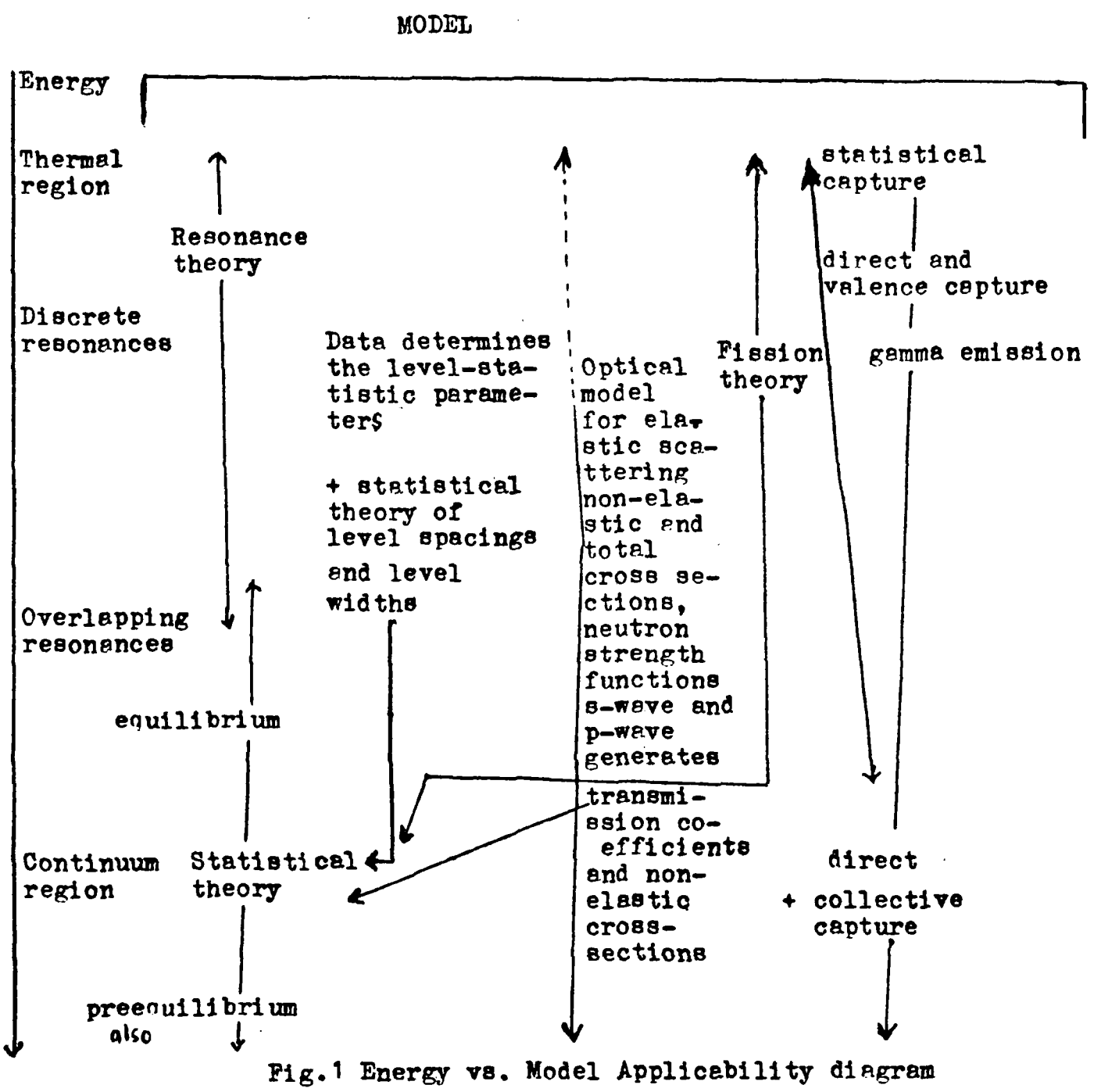


Fig.1 Energy vs. Model Applicability diagram

## 2. Resonance Reactions

At low neutron energies of the order of electron-volts in heavy nuclei, of the order of kiloelectron volts in medium nuclei and of the order of million-electron-volts in light nuclei isolated resonances are observed as a function of energy in the cross-section excitation function. A resonance represents a positive energy near-eigenstate of the compound system and is further characterized by a definite angular momentum and parity, its total and various partial decay widths. Resonance theories[2)] aim at describing the cross sections in terms of these parameters rather than aim at predicting the parameters. A detailed prediction of the resonance parameters is not possible. The advantage of using resonance parameters to generate cross-sections leads to an economy in description. Resonance-region cross-sections are doppler-broadened for use in reactor physics calculations. This can determine preference in using one approximation over another. The R-matrix theory separates out explicitly the energy dependence of the resonance-parameters but sometimes it is computationally tedious as the inversion of large matrices may be involved. The unitarity of the scattering matrix is guaranteed in this theory. The Kapur-Peierls' theory has an implicit energy-dependence in the resonance parameters and the unitarity of the scattering matrix may not be guaranteed. However it may be computationally advantageous to use the Kapur-Peierls' theory.

## 3. Optical Model

The average potential felt by a neutron due to the whole nucleus is complex in the optical model. The imaginary part of the potential describes loss of the flux from the incident channel, however, it can reappear as the compound elastic contribution. The imaginary part arises due to the formation of the doorway state or its genetic offspring the compound nucleus. The latter can decay either in the elastic channel or in the nonelastic channels. As the energy increases nonelastic processes dominate and determine the imaginary potential. The optical model predicts total, elastic, differential elastic, reaction cross sections and generates transmission coefficients and wave functions. The latter form an input to other cross-section calculations such as the statistical model and the distorted wave Born Approximation calculations. Recently Chatterjee, Murthy and Gupta[3] have published an analytic parameterization of the optical reaction cross sections for light projectiles. Optical model predicts polarization cross sections as well when the spin-orbit potential is also included.

In phenomenological analyses[4] the optical potential is chosen to be of analytic form which involves strength and geometry parameters. These parameters behave systematically with mass number and energy. The determination of

global optical parameters is quite useful for the prediction of the nuclear data. As an example the comparison for 14 MeV total, elastic and nonelastic cross section is shwon in figs. 2 and 3. A new potential proposed by Murthy and Gupta[5] seems to work satisfactorily.

Presently there exist several calculations which aim to predict the optical potential[5] starting from the nucleon-nucleon potential. The calculations are reasonably successful and predict the total optical potential reasonably well.

When the low-lying excited states of a nucleus are similar in their nuclear structure differing only in deformation or vibration degree of freedom, the generalized optical model employing coupled Schrödinger equations is used.

4. Statistical model and level-statistical parameters.

With increase in energy the number of levels in the compound nucleus increases rather exponentially. The level-widths also increase. When the ratio of the mean level width to the mean level spacing is larger than unity, the statistical model description results. This is usually known as the Hauser-Feshbach model[7]. Moldauer's level-width fluctuation correction should also be applied to the H-F model.

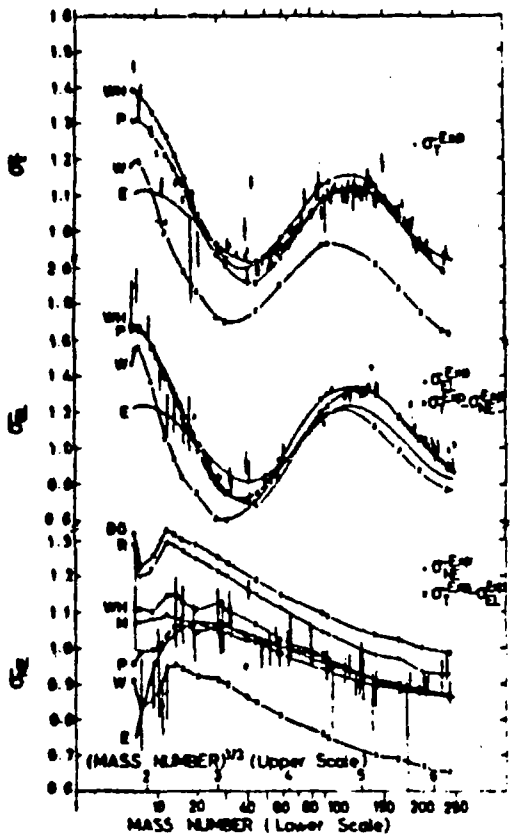


Fig. 1. 2

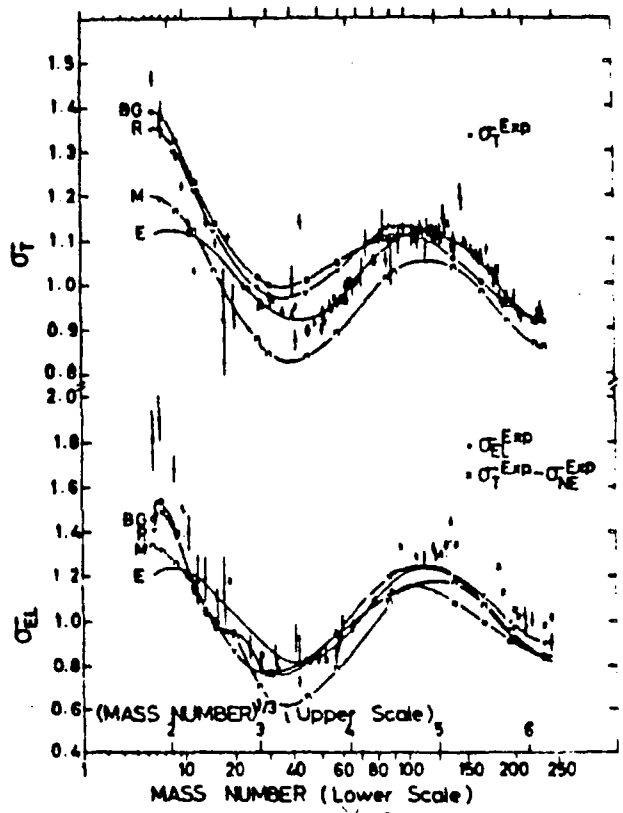


Fig. 2. 3

Figs 2 and 3. Total, elastic and non-elastic cross sections for 14 MeV neutrons are plotted in black-nucleus units. Experimental data, empirical curves (E) of Angeli *et al.* and predictions of various optical potentials due to Becchetti-Greenlees (BG), Rapaport *et al.* (R), Wilmore-Hodgson (WH), Mani *et al.* (M) and Watson *et al.* (W) and also of the potential proposed in the present work (P) are shown. Calculated points for specific nuclei are joined to guide the eye.

When the number of levels in the residual nucleus also becomes large, the discrete ensemble is replaced by a discrete plus a continuum or by a continuum ensemble. To obtain the continuum of the levels i.e. the level density, experimental information on the level spacing available at neutron binding energy from the resolved resonance data is combined with a theoretical model to obtain the level density at other energy. There are uncertainties in obtaining the mean level spacing from the experimental data and recently an intercomparison exercise has begun.[8] Kataria, Ramamurthy and Kapoor[9] have also proposed a new level-density formula.

In the cases where levels in the residual nucleus are replaced by the continuum and if angular momentum effects can also be ignored the Weisskapf-Ewing evaporation model results. This model is attractive due to its simplicity and finds an application in several calculations as for $(n,\gamma)$, $(n,n')$, $(n,2n)$, $(n,3n)$, $(n,p)$, $(n,\alpha)$, $(n,f)$ reactions etc.

## 5. Preequilibrium model

The statistical model assumes a decay from a fully equilibrized system, however as the energy increase, the composite system decays even while the system is equilibriating. This decay is described by the preequilibrium model which treats an equilibrating system in a statistical manner. In one version of the preequilibrium models[10], the exciton model the n exciton state either makes a transition into neighbouring $n \pm 2$ state or decays by emitting a particle. The preequilibrium phenomenon is found to be a necessary ingradient in explaining the increase or decrease in several cross sections.

In the master-equation approach the statistical (equilibrium) model and the preequilibrium models get unified. The master equations describe the equilibrating system as a function of time. However the time-integrated master equations[11] are adequate to obtain the cross sections by calculating mean lives of each exciton state. The mean lives as a function of exciton number represent both the preequilibrium and the equilibrium parts. The one-component equations without distinguishing between neutrons and protons are described by three term master equations. The time-integrated version of these equations give rise to a tridiagonal system of linear simultaneous equations. Chatterjee and I have obtained a continued fraction solution of these equations.

The angle-dependent master equations in the framework of exciton model have also been proposed and now their solution can be obtained[11] in a similar manner.

The role of angular momentum in preequilibrium models has been investigated meagrely and is probably most explicit in Feshbach-Kerman-Koonin version.[12] A clear distinction is maintained between multi-step direct and multi-step compound processes in this approach.

6. Gamma Emission

It is adequate to treat only the electric dipole transitions in the radiative transitions. In gamma-ray transmission coefficients the Weisskopf profile or the Brink-Axel profile is used. At lower energies apart from statistical capture[13], the direct capture and valence mechanisms also dominate in certain mass-energy region. At higher energies ( $\sim$ 10-15 MeV) the direct and collective mechanisms[15] dominate.

7. Fission theory

Fission is quite a complex phenomenon though its understanding is based on rather a simple concept. An excited equilibrized nucleus prefers to break into two almost similar parts was rather unexpected. If such a nucleus is assumed to be a liquid drop which is undergoing deformation and its

energy passes through a maximum as a consequence of competition between the surface energy and the Coulomb energy, the problem of understanding fission[16] becomes an exercise in barrier penetration. Though a fissioning nucleus undergoing continuous deformation develops a neck after traversing the barrier and breaks into one of the several possible pairs of fission fragments, the barrier region has only a few transition states determining the fission cross section and hence the fission is characterized by a few degrees of freedom. The effect of nuclear shells makes the barrier to be double-humped and gives rise to several interesting phenomena. A vast part of the fission theory deals with the calculation of the barrier parameters such as heights and widths for the two or more humps. Once a definite prescription of calculating the fission transmission coefficients in terms of the fission barrier parameter is defined, the fission theory joins the mainstream of the nuclear reaction theory.

According to the excitation energy the compound nucleus traverses the barrier. When the excitation energy increases so that the residual nucleus, after emitting a neutron, can undergo fission called second chance fission. Similarly after the emission of a neutron emission the second residual nucleus can undergo the third chance fission. These situations can be handled in a sequential manner in the

statistical theory. A semi-empirical formula was proposed for calculating the second and third chance fission by Jhingan et al.[17)]

## 8. Conclusions

Presently nuclear theory is quite powerful and is undergoing further development to predict nuclear cross sections and related quantities more precisely. In this brief over-view we have presented some facets of nuclear model useful in predicting nuclear data. Optimal results will be obtained in using the existing models and the experimental results in a complementary manner.

References

1) J.J. Schmidt in Nuclear Theory for Applications, IAEA - SMR-43, Published by ICTP, Trieste 1980 (abbreviated hereafter as NTA 1980), p. 1

2) M.S. Moore, NTA 1980, p. 31, F. Fröhner, NTA 1980 p. 59

3) A. Chatterjee, K.H.N. Murthy and S.K. Gupta, Pramana 16 (1981) 391.

4) A. Prince, NTA 1980, p. 149

5) K.H.N. Murthy and S.K. Gupta, Annals of Nucl. Energy (1981 in press).

6) C. Mahaux, NTA 1980 p. 97

7) P.A. Moldauer, NTA 1980 p. 180

8) P. Ribon and P. Johnston, March 1981, NEANDC (E)213-AL

9) S.K. Kataria, V.S.Ramamurthy and S.S. Kapoor, Phys. Rev. C18 (1978) 549; S.K. Kataria and V.S. Ramamurthy, Phys. Rev. C22 (1980) 2263, Nucl. Phys. A349 (1980) 10.

10) M. Blann, Ann. rev. Nucl. Sci. 25(1975) 123.

11) S.K. Gupta and A. Chatterjee, Int. Conf. on Nuclear Cross sections for Technology, Knoxville (October 1979); A. Chatterjee and S.K. Gupta, Z. Phys. A - Atoms and Nuclei 301 (1981 in press)

12) H. Feshbach, A. Kerman and S. Koonin, Ann. Phys. 125 (1980) 729.

13) G. Reffo, NTA 1980, p. 205

14) J.R. Bird, B.J. Allen, J.W. Boldeman, M.J. Kenny and A.R. de L. Musgrove, Int. Conf. on Interactions of Neutrons with Nuclei, Lowell 1976, p. 76

15) G. Longo and F. Sapovetti, Nuclear Theory in Neutron Nuclear Data Evaluation Vol. I, IAEA 1976, p. 191.

16) S. Bjornholm and J.E. Lynn, Rev. Mod. Phys. 52 (1980) 725.

17) M.L. Jhingan, R.P. Anand, S.K. Gupta and M.K. Mehta Annals of Nucl. Energy 6 (1979) 495.

# Calculation of Displacement Cross Sections in Stainless Steel Using SETR Cross Section Set

C.P.Reddy and S.M.Lee

Reactor Physics Section

## 1. Introduction

Any component which resides in a neutron field undergoes radiation damage. There are different ways to quantify the amount of neutron exposure. The units usually used to measure the exposure of materials to fast neutrons is the number of displacements per atom. ( dPa ) and fluence above 0.1 Mev (nvt). In most of the studies where effects of radiation damage are studied using accelerators, correlations are obtained between the number of times the atom is displaced and the effects of radiation damage like swelling, radiation embrittlement etc. So it is required of a core design engineer to specify the displacements per atom in all the components during their life time, which requires knowledge of displacement cross sections. In the present paper displacement cross sections are given, calculated using TRN model[4] and SETR cross sections. The authors discuss the reasons for choosing TRN model, breifly describe the model. Also we discuss mode adapted for calculating displacement cross sections and compare the results with the other published results.

## 2. Basis for the selection of the model

There are many models discussed in the literature for calculating displacement cross sections. To name some important ones are Kinchin and Pease model[1], Half Nelson model[2], Torrens-Robinson and Norgett simulation model[3] and Torrens, Robinson and Norgrette standard model[4]. In table 1 we compare[5] the multigroup displacement cross sections given by the different models. Half Nelson model gives approximately half the values of Kinchin and Pease model whereas TRN simulation and TRN standard model compare

well with each other and also with the Kinchin-Pease model at higher energies. Experimental results show that TRN model is a better approximation[6]. Also IAEA is now recommending TRN model as a standard of damage dose.

3. The Torrens-Robinson-Norgett model

According to TRN model number of displacements $n_d(E_p)$ produced by primary knock on atom of recoil energy $E_p$ is given by

$$n_d(E_p) = \frac{\beta(E_p - E_{inelastic})}{2E_d} \rightarrow (1)$$

For low energies

$$n_d(E_p) = 0 \quad \text{for } (E_p - E_{inelastic}) < E_d$$

$$= 1 \quad \text{for } E_d \leq (E_p - E_{inelastic}) < 2E_d$$

where $E_d$ is the displacement threshold energy for stainless steel $E_d = 36$ ev and $\beta = 0.8$

$E_{inelastic}$ is the energy lost by the primary knock on atom due to inelastic scattering and it is given by

$$E_{inelastic} = \frac{E_p k g(\epsilon)}{1 + k g(\epsilon)} \rightarrow (2)$$

where

$$g(\epsilon) = \epsilon + 0.40244\ \epsilon^{3/4} + 3.4008\ \epsilon^{1/6}$$

$$k = \frac{0.0793\ Z_1^{2/3}\ Z_2^{1/2}\ (A_1 + A_2)^{3/2}}{\left(Z_1^{2/3} + Z_2^{2/3}\right)^{3/4} A_1^{3/2}\ A_2^{1/2}}$$

$$\mathcal{E} = AE_p \qquad (E_p \text{ in ev})$$

$$A = \frac{0.8853 A_2}{27.2 Z_1 Z_2 (Z_1^{2/3} + Z_2^{2/3})^{1/2}(A_1 + A_2)} \quad ev^{-1}$$

$A_1$, $Z_1$ = The atomic weight and atomic number of the recoiling heavy ions

$A_2$, $Z_2$ = like quantities for the matrix atoms.

for any alloy

$$A_2 = \sum_{i=1}^{N} n_i A_i \Big/ \sum_{i=1}^{N} n_i$$

$$Z_2 = \sum_{i=1}^{N} n_i Z_i \Big/ \sum_{i=1}^{N} n_i$$

$n_i$ = number density of ith element in the alloy and

$A_i$, $Z_i$ = are atomic weight and atomic number of ith element in the alloy.

To calculate displacement rate capture reactions inelastic scattering and anisotropy are ignored. Only elastic scattering is taken into account. These approximations are valid for fast reactors. Then maximum fraction of energy taken by the primary knock on atom of ith

type is

$$\mu_i = \frac{4A_i}{(1+A_i)^2} \qquad \rightarrow (3)$$

So the range of energy of the primary knock on atom is 0 to $\mu E$. where $E$ is the energy of the neutron. Then the number of displacements per a scattering incident of a neutron of energy $E$ is given by

$$\eta_d(E) = \frac{1}{\mu E} \int_0^{\mu E} \eta_d(E_p)\, d E_p \qquad \rightarrow (4)$$

Then the displacement group cross section is

$$\sigma_{d,g} = \frac{\int_{\Delta E_g} \sigma_{el}(E)\, \eta_d(E)\, \phi(E)\, dE}{\int_{\Delta E_g} \phi(E) dE} \qquad \rightarrow (5)$$

$\sigma_{el}(E)$ elastic scattering cross section

4. Mode of Calculations

We have taken elastic scattering cross sections from 25 group SETR cross section set. Instead of evaluating integral in the equation 5 we have assumed $\sigma_{el}$ as constant ovet the group and energy of the neutron as the middle energy of the group.

Integral in the equation 4 is done by reducing it to a summation by dividing the energy range from 0 to $\mu E$ into small regions and assuming the $\eta_d(E_p)$ as constant in each of these small regions.

We also have 574 group cross sections in SETR cross section

library covering a range upto 2.23 Mev. We also calculated displacement cross sections for 574 groups. For the sake of comparison we have collapsed these cross sections into 25 groups, using the standard spectrum given in the Table 2.

## 5. Results

In table 3 we present results of 25 group displacement cross section for iron, 574 group cross sections collapsed in to 25 groups along with J.I.Bramman et al. results[5]. Results agree well. Small differences seen are due to approximations used and difference in the cross section set. In table 4 we present the displacement cross sections generated using 25 group SUTR version II cross section and 574 fine group SUTR version II cross sections collapsed into the 25 group format. Both the results agree well. The differences are due to the approximations while calculating broad group cross sections.

## 6. Acknowledgements

We acknowledge Mr. M.L.Sharma for his kind help in retreiving 574 fine group cross sections. We acknowledge Mr. K.Shankar Singh for the interest he has shown in the work.

## 6. References


1. Kinchin, G.H. and Pease R.S. Rep. Prog. Phys. 18, 1, (1955).

2. Nelson, R.S. AERE Harwell Report R 6092, (1969).

3. Torrens I.M. and Robinson M.I., 'Radiation induced voids in metals' (Ed. J.W.Corbett and S.C.Ianiello) USAEC Symposium, Series 26 (1972).

4. Norgett M.J., Robinson M.T and Torrens I.M., AERE Harwel Report TP 494.

5. Bramman, J.I. et al., 'Radiation damage unit for fast reactor steels', Irradiation Embrittlement and creep in fuel cladding and core components', BNES Conf. London (1972).

6. J.Ravier, 'Sections Efficaces Multigroupes et JEU SEH a 25 groupes PNR/SEH-66-050/JR (1966).

Table 1

Multigroup displacement cross sections

| Neutron energy group | Lower energy of group in keV | Group Cross Sections in barns | | | |
|---|---|---|---|---|---|
| | | Kinchin & Pease | Half-Nelson | THN Simulation | THN Standard |
| 1 | 3680 | 2278 | 1433 | 2789 | 2120 |
| 2 | 2230 | 2246 | 1241 | 1809 | 1381 |
| 3 | 1350 | 1876 | 882.1 | 1112 | 836 |
| 4 | 821 | 1479 | 649.9 | 727.7 | 554.3 |
| 5 | 498 | 1249 | 577.8 | 607.1 | 442.8 |
| 6 | 302 | 911.6 | 454.8 | 468.8 | 338.3 |
| 7 | 111 | 444.8 | 235.0 | 241.2 | 175.3 |
| 8 | 40.9 | 262.4 | 144.1 | 156.9 | 105.0 |

Table 2

Standard Spectrum

| Energy Range | Shape of the flux |
|---|---|
| 14.5 Mev to 2.23 MeV | fission source spectrum |
| 2.23 MeV to 821 keV | $1/E^2$ |
| 821 kev to 67.4 kev | $1/E$ |
| 67.4 kev to 2.04 kev | $1/\sqrt{E}$ |
| 2.04 kev to 275 ev | constant |
| 275 ev to 0.414 | E |
| Thermal group | Maxwellian spectrum |

Table 3

Comparison of displacement cross sections for Iron

| Lower energy of the group | Braman et al[7] cross sections | 25 group cross section | 574 collapsed into 25 groups |
|---|---|---|---|
| 3.68 MeV | 2120 | 2632 | - |
| 2.23 " | 1381 | 1422 | - |
| 1.35 " | 836 | 814.0 | 715 |
| 821 keV | 534.3 | 497.4 | 482.0 |
| 498 " | 442.8 | 396.3 | 434.0 |
| 302 " | 338.3 | 296.7 | 352.0 |
| 111 " | 175.3 | 209.0 | 189 |
| 40.9 " | 105.3 | 159.0 | 208 |
| 24.8 " | - | 141.0 | 143 |
| 15.0 " | - | 66.5 | 95.0 |
| 9.12 " | - | 143.0 | 71.6 |
| 5.53 " | - | 14.7 | 131.6 |

Table 4

Displacement cross sections of Stainless Steel

| Lower energy of the group | 25 group cross sections | 574 group cross sections collapsed into 25 groups |
|---|---|---|
| 3.68 Mev | 2731 | - |
| 2.23 " | 1493 | - |
| 1.35 " | 398 | 812 |
| 821 Kev | 581 | 588 |
| 498 " | 427 | 469 |
| 302 " | 312 | 375 |
| 183 " | 221 | 215 |
| 111 " | 189 | 235 |
| 67.4 " | 149.1 | 153 |
| 40.9 " | 76.1 | 192 |
| 24.8 " | 117 | 68.0 |
| 15.0 " | 42.7 | 109 |
| 9.12 " | 33.7 | 40.7 |
| 5.53 " | 30.5 | 34.5 |
| 3.36 " | 15.7 | 23.0 |
| 2.04 " | 6.17 | 9.22 |

WORKSHOP ON NUCLEAR DATA EVALUATION, PROCESSING AND TESTING.

August 4, 5 1981

# DEVELOPMENT OF A NEW FAST REACTOR PROCESSING CODE RAMBHA AT RRC

S. Ganesan, V. Gopalakrishnan, M.M. Ramanadhan, P.B. Rao, M.L. Sharma,

R. Vaidyanathan and R. Shankar Singh.

Reactor Research Centre

Kalpakkam-603 102

Tamil Nadu, INDIA

## Abstract

RAMBHA is a FORTRAN IV computer code system that generates complete set of multigroup constants including self-shielding factors and transfer cross sections, using the differential neutron nuclear cross section data set available in the ENDF/B-IV format for applications to fast reactor calculations. The code averages the point data in the 3rd file (including contributions from the floor corrections for the resonance region) into the given 25 groups. Resonance parameter data are retrieved from the second file; the infinite dilution cross sections as well as self shielded cross sections are computed and the self shielding factors are obtained at given temperatures and background dilution cross sections. The code gets $\bar{\nu}$ from the first file and takes the transfer probabilities from the 5th file. Interpolations, wherever necessary, are carried out respecting the schemes specified in the data file. Standard spectra appropriate to a large fast reactor are used for flux weighting required for averaging. The code has options to include or exclude different modules. The methods or algorithms used in the various modules of the code are explained in brief in the following sections. Typical preliminary results are presented and compared with available multigroup constant set. Self shielding factors computed by RAMBHA code system are compared with available experimented data for $^{239}Pu$.

## 1. INTRODUCTION

Since five years the different modules of the fast reactor processing code RAMBHA[1] were written and individually commissioned. Recently integrated one shot generation of the complete set of multigroup cross sections has been successfully completed for typical fissile, fertile and structural isotopes. This paper briefly documents the functions of various modules with typical results obtained. The primary aim of developing this code system is to enable us generate ourselves the required multigroup data sets for isotopes for which data is not available in the presently available Cadarache[2] multigroup cross section set. The code system can also be used to update the cross sections of some isotopes such as $^{240}Pu$ or Fe or $^{233}U$ for which it is known that the recent differential evaluations of cross sections have undergone much improvements. It is also hoped that the availability of our own nuclear data processing code system will enable us to have better basic understanding of the effect of certain specific changes in fast neutron cross sections on neutronic parameters of fast reactor system by enabling us to perform detailed sensitivity studies directly starting from the differential cross sections.

## II RESONANCE DATA PROCESSING OF DATA GIVEN IN ENDF/B-IV FORMAT[3]

The code takes the resonance parameters for resolved and unresolved resonance region, given isotopwise for any material, in the 2nd file and computes the infinitely diluted as well as self shielded group cross sections. Presently for the resolved resonance region only

SLBW formalism will be accepted in full but MLBW formalism will also be treated ignoring the level interference in scattering.

The SLBW formalism gives the following expressions for an isotope for the capture, fission and scattering Doppler broadened cross sections.

$$\sigma_{ck}(E,T) = \sigma_{ok}\frac{\Gamma_{\gamma k}\psi(\theta,x)}{\Gamma} \qquad (1)$$

$$\sigma_{fk}(E,T) = \sigma_{ok}\frac{\Gamma_{fk}\psi(\theta,x)}{\Gamma} \qquad (2)$$

and $$\sigma_{sk}(E,T) = \sum_{l}\sigma_{sk,l}(\theta,x) \qquad (3)$$

where $\sigma_{sk,l}(\theta,x)$

$$= 4\pi\lambda^2(2l+1)\sin^2\delta_l + \sigma_{ok}\left[\frac{\Gamma_{nk}}{\Gamma}\psi(\theta,x) - 2\sin^2\delta_l\,\psi(\theta,x) + \frac{1}{2}\sin 2\delta_l\,\chi(\theta,x)\right] \qquad (4)$$

E being the Energy,

T the temperature,

$\Gamma_{\gamma k}$ Capture width at $K^{th}$ resonance

$\Gamma_{fk}$ fission width at $K^{th}$ resonance

$\Gamma_{nk}$ neutron width at $K^{th}$ resonance

$\Gamma = \Gamma_{fk} + \Gamma_{nk} + \Gamma_{\gamma k}$

$\sigma_{ok}$ peak cross section for $K^{th}$ resonance

$\delta_l$ phase shift,

$\ell$ angular momentum, indicating the partial wave

$\psi, \chi$ Doppler broadened line shape functions to be evaluated for given temp.

The method of evaluation of any of the above parameters is the same as that followed in the code DOPSEL[4].

Unresolved Resonance Region

In this region since the resonance parameters are not specifically known, the statistics of the resolved resonance parameters are made use of. The cross sections are then obtained by averaging the quantities on the r.h.s. of eqns.(1) through (4) over appropriate distribution functions for the partial widths and the level spacings. For describing the statistics of the partial widths, the Porter-Thomas distribution functions are used.

ENDF/B-IV gives energy dependent or independent parameters for the unresolved resonance region. All these parameters are made use of in getting the group averaged cross sections.

Infinite dilution cross sections

Under the narrow resonance approximation the infinite dilution group cross section for any process in the resolved energy region is calculated as

$$\sigma_x^g = \frac{\sum_{k \in g} \pi \sigma_{0k} \Gamma_{xk} / (2E-k)}{\Delta u_g} \qquad (5)$$

where $\sum_{k \in g}$ stands for summation over the resonance region belonging to the energy group $g$, $\sigma_{ok}$ is the peak cross section of $K^{th}$ resonance, $E_{ok}$ is the energy at which $K^{th}$ resonance occurs and $\Delta u_g$ is the lethargy width of group $g$. $\Gamma_{xk}$ denotes the partial width of $K^{th}$ resonance for the process x.

In the unresolved region the infinite dilution cross section is given by

$$\sigma_x^g = 2\pi^2 \lambda^2 \sum_{l,J} g_J \left\langle \frac{\bar{\Gamma}_n \bar{\Gamma}_x}{\bar{\Gamma}} \right\rangle_{(l,J)} \Big/ \langle D \rangle^{(l,J)} \qquad (6)$$

the symbols having usual meaning and the averaging done over Porter Thomas distribution.

Self shielded cross section

Resolved resonance region The self shielded or effective cross section (temp. and dilution dependent) using the NR approximation is given by

$$\bar{\sigma}_x^g = \frac{\sum_{k \in g} \frac{\sigma_p^{eff} \Gamma_{xk} J_k^*(\theta_k, \beta_k, a_k, b_k)}{E_{ok}}}{\Delta u_g - \sum_{k \in g} \frac{\Gamma_k J_k^*(\theta_k, \beta_k, a_k, b_k)}{E_{ok}}} \qquad (7)$$

$J_k^*$ is known as generalised resonance integral[5]. The evaluation of this function including the overlap correction is done exactly in the same manner as in ref.4.

Unresolved resonance region

$$\tilde{\sigma}_x^{g} = \sum_N \tilde{\sigma}_{xN}^{g}$$

where $N$ stands for a particular $(\ell, J)$ sequence and $x$ for the process.

$$\tilde{\sigma}_{xN}^{g} = \frac{\frac{\sigma_p^{eff}}{\langle D \rangle_N} \langle \Gamma_{xk} J_k^* \rangle}{1 - \sum_N \left[ \frac{1}{\langle D \rangle_N} \langle \Gamma_{tk} J_k^* \rangle_N \right]} \qquad (8)$$

The method of evaluation of the above has been explained in ref.4 which closely follows Ref.5.

Floow corrections

Since the resonance parameters do not adequately represent the cross sections in the resonance region ENDF B/IV gives the floor corrections that one to be added to the cross sections obtained using resonance parameters resolved or unresolved. The floor corrections are given as point data in the 3rd file, that are averaged using flux weighting and are added to the group cross sections obtained using resonance parameters at the group level. The method of averaging is explained under 'point data averaging'. The corrections are made for both self shielded and infinite dilution cross sections.

Point data averaging

ENDF/B gives the point data cross sections in the 3rd file which are averaged as follows;

$$\sigma_g = \frac{\int_{E_{g+1}}^{E_g} \sigma(E)\,\phi(E)\,dE}{\int_{E_{g+1}}^{E_g} \phi(E)\,dE} \qquad (9)$$

The weighting spectrum used in different energy regions are as follows:

| region | | | spectrum |
|---|---|---|---|
| 14.5 MeV | - | 2.23 MeV | $E.e^{-E/1.4x10^6}$ |
| 2.23 MeV | - | 4.98 KeV | $E^{-2}$ |
| 4.98 KeV | - | 40.9 KeV | $E^{-1}$ |
| 40.9 KeV | - | 1.23 KeV | $E^{-0.5}$ |
| 1.23 KeV | - | 22.6 eV | 1.0 |
| 22.6 eV | - | 0.414 eV | E |
| .414 eV | - | 0 | $Ee^{-E/0.0253}$ |

The integration is performed using Gauss Quadrature and any interpolation scheme that is specified in the file is strictly followed.

All the cross sections outside the resonance region are averaged from the point data in this method.

$\sigma_{tr}^{g}$ Transport cross sections

This is obtained using the formula

$$\sigma_{tr} = \sigma_t - \bar{\mu}\sigma_s \qquad (10)$$

$\sigma_t$, $\bar{\mu}$, $\sigma_s$ are obtained at same energy points by proper interpolation from the point data given and $\sigma_{tr}$ computed at those points. Then they are averaged to get $\sigma_{tr}^{g}$ using flux weightings as explained earlier. In the resonance region, since $\bar{\mu}$ does not change significantly, $\sigma_{tr}^{g}$ is obtained using

$$\sigma_{tr}^{g} = \sigma_t^{g} - \bar{\mu}\sigma_s^{g} \qquad (11)$$

in which $\sigma_t^{g}$ and $\sigma_s^{g}$ are actual group cross sections including floor corrections.

In the resonance region, self shielded and $\infty$ dilution $\sigma_{tr}^{g}$ would be obtained by using self shielded $\sigma_t^{g}$, $\sigma_s^{g}$ and $\infty$ dilution $\sigma_t^{g}$, $\sigma_s^{g}$ correspondingly.

$\nu\sigma_f$: $\bar{\nu}$ values are represented in file 1 of ENDF B either in a tabular form or in a polynomial form. If tabular representation is given, $\bar{\nu}_g$ is obtained by energy weighting:

$$\bar{\nu}_g = \int_{E_{g+1}}^{E_g} \bar{\nu}(E)\,dE \Big/ \int_{E_{g+1}}^{E_g} dE \qquad (12)$$

If a polynomial representation is found $\bar{\nu}_g$ is got by analytical integration. Here $\nu$ is represented in the file as $\bar{\nu}(E) = \sum_{n=1}^{NC} C_n E^{n-1}$ where NC is the no of coeffs.

51

Then $\langle \bar{\nu}\sigma_f \rangle_g$ is obtained using

$$\langle \bar{\nu}\sigma_f \rangle_g = \bar{\nu}_g \, \sigma_f^g \qquad (13)$$

where $\sigma_f^g$ is the actual group cross section including floor corrections.

We may get self shielded or $\infty$ dilution $\langle \nu\sigma_f \rangle_g$ by using self shielded or $\infty$ dilution $\sigma_f^g$ correspondingly.

Self Shielding factors

The self shielded as well as $\infty$ diluted cross sections are thus obtained for the capture, scattering, fission, total, transport cross sections and $\langle \bar{\nu}\sigma_f \rangle_g$ values and the self shielding factors for anygroup is obtained as

$$f_x^g = \frac{\bar{\sigma}_x^g \text{ (Self shielded)}}{\langle \sigma_x^g \rangle \text{ (infinitely diluted)}} \qquad (14)$$

where $x$ represents any reaction process.

Transfer matrices

Inelastic : This is made to include the contributions from the $(n,n')$ reactions exciting continuum energy levels, $(n,n')$ reactions exciting discrete energy levels, $(n,2n)$ reactions and $(n,3n)$ reactions. The methods adopted in computing the respective contributions follow those of MIGROS-3

ENDF/B gives the pointwise cross sections for different discrete

52

excitation levels for the ( n, n' ) reactions. The transfer cross section from $g^{th}$ to $g'^{th}$ group is obtained as

$$\sigma^{in}_{g\to g'} = \sum_j \frac{\int_{E_L}^{E_H} \sigma_j^{in}(\epsilon)\,\phi(\epsilon)\,d\epsilon}{\int_{E_{g+1}}^{E_g} \phi(\epsilon)\,d\epsilon} \qquad (15)$$

where $E_L = Max\left(E_{g+1}, E_{g'+1} + \frac{A+1}{A}E_j\right)$

$$E_H = Min\left(E_g, E_g + \frac{A+1}{A}E_j\right)$$

is the threshold for the level

ENDF/B gives, for the (n, n' ) reaction exciting continuum levels, (n, 2n) and (n, 3n ) reactions, the pointwise cross section in file 3 and the transfer probabilities in file 5. The transfer probabilities may be given in one of so many ways of which the code presently can handle tabulated probabilitiesagainst incident and final energies and tabulated nuclear temperature ( $\theta$ ) against incident energy (evaporation model). The transfer cross section from group $g$ to $g'$ is obtained by

$$\sigma^{x}_{g\to g'} = \frac{\int_{E_{g+1}}^{E_g}\int_{E_{g'+1}}^{E_{g'}} \sigma^{x}(E)\,\phi(E)\,p(E\to E'\epsilon g')\,dE\,dE'}{\int_{E_{g+1}}^{E_g}\phi(E)\,dE} \qquad (16)$$

$$x = (n,n'),\ (n,2n) \text{ or } (n,3n)$$

The integration is carried out first and $p(E\to g')$ is obtained.

53

If $P(E \to E')$ is given in the file

$$P(E \to g') = \int_{Eg'+1}^{Eg'} P(E \to E')\, dE' \qquad (17)$$

If $\theta(E)$ are given the sink integration becomes analytic.

$$P(E \to g') = \int_{Eg'+1}^{Eg'} \frac{E'}{I} e^{-E'/\theta(E)}\, dE' \qquad (18)$$

where, $I$, the normalization constant is given by

$$I = \theta^2(E)\left[1 - e^{-(E-U)/\theta(E)}\left(1 + \frac{E-U}{\theta(E)}\right)\right] \qquad (19)$$

$$(0 \leq E' \leq E - U)$$

$U$ being the threshold.

Transfer Matrices :

Elastic

Isotropic scattering is assumed for the present and Bucholz's method is used. The transfer cross section from group $g$ to $g'$ for any moment $l+1$ is given by

$$\sigma_{g \to g'}^{l} = \frac{\int_{Eg+1}^{Eg} \phi(E)\, dE \int_{Eg'+1}^{Eg'} \sigma(E \to E')\, P_l[\mu(E \to E')]\, dE'}{\int_{Eg+1}^{Eg} \phi(E)\, dE} \qquad (20)$$

$$\sigma(E \to E') = \sigma_s(E)\, f(E, \mu_c)\, 2\pi\, d\mu_c \qquad (21)$$

$$= \frac{1}{2\pi}\, \sigma_s(E)\, d\mu_c$$

54

using the relation

$$\mu_L = \frac{1}{A}\left[\mu_L^2 - 1 + \mu_L\left(a^2+\mu_L^2\right)^{1/2}\right] \quad \text{where } a^2 = A^2-1 \tag{22}$$

it can be shown that

$$\int_{E_{g'+1}}^{E_{g'}} P_0(\mu_L)\,\sigma(E\to E')\,dE' = \frac{\sigma(E)}{2A}\left[x(x+\gamma)\right]\Big|_{\mu_L^L}^{\mu_L^U} \tag{23}$$

and

$$\int_{E_{g'+1}}^{E_{g'}} P_1(\mu_L)\,\sigma(E\to E')\,dE' = \frac{\sigma(E)}{2A}\left[\frac{2}{3}\left(x^3+\gamma^3\right) - a^2\gamma\right]\Big|_{\mu_L^L}^{\mu_L^U} \tag{24}$$

where $\gamma = (a^2+x^2)^{1/2}$

and the sink integration is purely analytic.

$$\mu_L = \frac{1}{2}\left[(A+1)\left(\frac{E'}{E}\right)^{1/2} - (A-1)\left(\frac{E}{E'}\right)^{1/2}\right] \tag{25}$$

$\mu_L^L$ and $\mu_L^U$ correspond to the lower and upper energy limits of the sink group subject to the condition that

$$E \geq E' \geq \alpha E$$

where $\alpha = (A-1)^2/(A+1)^2$

Tables 1-3 give the preliminary results obtained using RAMBHA code system. In these tables values from SETR set are also given to

enable detailed comparison with the results of RAMBHA code system.

## CONCLUSION AND REMARKS

Results of analysis of fast critical experiments will be performed using the new multigroup cross section set obtained using RAMBHA code system.

The experience has considerably increased our confidence in the development of a large nuclear data processing code system.

Several improvements are planned to be incorporated in the second version. These will greatly increase the versatality of RAMBHA code system and attempt to remove many of the approximations used in the first version reported in this paper.

## REFERENCES

1. S.Ganesan et al., Section 1.13 in 'Activity Report (1979-1980)', RRC-45 (1981)
2. J.Ravier and J.M.Chaumont, p.47-53, ANL-7320 (1966).
3. D.Garber et al., ENDF-102, (1975).
4. S.Ganesan, P.B.Rao and R.S.Singh, RRC-6 (1975).
5. R.N.Hwang, Nucl. Sci. Eng., 52, 157 (1973).
6. I.Broeders and B.Kreig Section 6 in KfK-2388 (1977).
7. J.A.Bucholz, Nucl. Sci. Eng. 74, 163 (1980).

Table 1

INFINITE DILUTION CROSS SECTIONS FOR $^{239}Pu$

| GRP.No. | SCATTERING | | CAPTURE | | FISSION | | TOTAL | |
|---|---|---|---|---|---|---|---|---|
| | RAMBHA | SETR | RAMBHA | SETR | RAMBHA | SETR | RAMBHA | SETR |
| 1 | .42686+1 | .42867+1 | .14618-2 | .13000-2 | .18244+1 | .18210+1 | .75573+1 | .76850+1 |
| 2 | .42768+1 | .49053+1 | .38404-2 | .28000-2 | .13797+1 | .17560+1 | .77941+1 | .79180+1 |
| 3 | .37747+1 | .43926+1 | .10657-1 | .83000-2 | .19179+1 | .18520+1 | .71345+1 | .73830+1 |
| 4 | .41548+1 | .44559+1 | .25233-1 | .32000-1 | .17390+1 | .17500+1 | .70952+1 | .73270+1 |
| 5 | .53211+1 | .53197+1 | .78716-1 | .10100 | .16268+1 | .17000+1 | .78336+1 | .81750+1 |
| 6. | .65658+1 | .66837+1 | .14042 | .19400 | .15527+1 | .16600+1 | .88316+1 | .94200+1 |
| 7 | .76871+1 | .82468+1 | .18980 | .24100 | .14921+1 | .15960+1 | .98420+1 | .10770+2 |
| 8 | .87031+1 | .95173+1 | .21761 | .28000 | .15331+1 | .15400+1 | .10821+2 | .11880+2 |
| 9 | .95480+1 | .99410+1 | .29609 | .30200 | .15890+1 | .14200+1 | .11712+2 | .12150+2 |
| 10 | .10229+2 | .10912+2 | .41307 | .34800 | .16037+1 | .14020+1 | .12487+2 | .13030+2 |
| 11 | .10572+2 | .11882+2 | .47973 | .52100 | .15956+1 | .14680+1 | .12874+2 | .14220+2 |
| 12 | .11416+2 | .12149+2 | .94528 | .73900 | .18708+1 | .15730+1 | .14430+2 | .14770+2 |
| 13. | .11814+2 | .12086+2 | .13076+1 | .98100 | .20463+1 | .18000+1 | .15295+2 | .15080+2 |

...../-

Table 1 contd.

| GRP. No. | SCATTERING | | CAPTURE | | FISSION | | TOTAL | |
|---|---|---|---|---|---|---|---|---|
| | RAMBHA | SETR | RAMBHA | SETR | RAMBHA | SETR | RAMBHA | SETR |
| 14 | .12329+2 | .11753+2 | .18660+1 | .14920+1 | .23819+1 | .25500+1 | .16587+2 | .15800+2 |
| 15 | .12885+2 | .12066+2 | .26362+1 | .23290+1 | .28881+1 | .31050+1 | .18409+2 | .17500+2 |
| 16 | .13487+2 | .11111+2 | .37245+1 | .3779 +1 | .36217+1 | .40200+1 | .20833+2 | .18910+2 |
| 17 | .14121+2 | .11114+2 | .52383+1 | .47020+1 | .46381+1 | .52240+1 | .23997+2 | .21040+2 |
| 18 | .14772+2 | .11114+2 | .73265+1 | .58800+1 | .60166+1 | .79460+1 | .28116+2 | .24940+2 |
| 19 | .154269+2 | .67510+1 | .10180+2 | .12241+2 | .78604+1 | .11658+2 | .33467+2 | .30650+2 |
| 20 | .24558+2 | .80930+1 | .13664+2 | .12563+2 | .10794+2 | .13224+2 | .49016+2 | .33880+2 |
| 21 | .14982+2 | .14730+2 | .18297+2 | .14170+2 | .17889+2 | .17640+2 | .51168+2 | .46540+2 |
| 22 | .14237+2 | .16020+2 | .32515+2 | .33600+2 | .34566+2 | .38370+2 | .81348+2 | .87990+2 |
| 23 | .10545+2 | .16020+2 | .39068+2 | .54770+2 | .57639+2 | .81270+2 | .10725+3 | .15206+3 |
| 24 | .11553+2 | .11140+2 | .57342+1 | .69700+1 | .19007+2 | .28840+2 | .36294+2 | .46950+2 |
| 25 | .77316+1 | .94000+1 | .23985+3 | .27400+3 | .56598+3 | .74060+3 | .81356+3 | .10240+4 |

Table - 2

ELASTIC SCATTERING TRANSFER MATRICES FOR $^{239}Pu$

| GRP No. | $\sigma$ (G to G) | | G $\sigma$ G Removal | |
|---|---|---|---|---|
| (G) | RAMBHA | SETR | RAMBHA | SETR |
| 1 | .41887 + 1 | .42604 + 1 | .0799 | .26270 - 1 |
| 2 | .41977 + 1 | .48720 + 1 | .0791 | .33240 - 1 |
| 3 | .36944 + 1 | .43490 + 1 | .0803 | .43540 - 1 |
| 4 | .40666 + 1 | .44001 + 1 | .0882 | .55840 - 1 |
| 5 | .52078 + 1 | .52354 + 1 | .1133 | .84290 - 1 |
| 6 | .64443 + 1 | .65854 + 1 | .1358 | .98300 - 1 |
| 7 | .75563 + 1 | .81666 + 1 | .1308 | .13020 |
| 8 | .85526 + 1 | .93709 + 1 | .1505 | .14640 |
| 9 | .93873 + 1 | .98353 + 1 | .1607 | .15880 |
| 10 | .10054 + 2 | .10736 + 2 | .179 | .17610 |
| 11 | .10395 + 2 | .11709 + 2 | .177 | .17360 |
| 12 | .11205 + 2 | .11971 + 2 | .211 | .17740 |
| 13 | .11653 + 2 | .11901 + 2 | .161 | .18040 |
| 14 | .12096 + 2 | .11569 + 2 | .233 | .18440 |
| 15 | .12641 + 2 | .11883 + 2 | .244 | .18290 |
| 16 | .13231 + 2 | .10921 + 2 | .256 | .19000 |
| 17 | .13852 + 2 | .10916 + 2 | .269 | .19800 |
| 18 | .14575 + 2 | .10936 + 2 | .197 | .17800 |
| 19 | .15170 + 2 | .65700 + 1 | .257 | .18100 |
| 20 | .24231 + 2 | .79070 + 1 | .327 | .18600 |
| 21 | .149082 + 2 | .14659 + 2 | .0738 | .71000 - 1 |
| 22 | .14200 + 2 | .15979 + 2 | .037 | .41000 - 1 |
| 23 | .10499 + 2 | .16015 + 2 | .046 | .50000 - 2 |
| 24 | .11549 + 2 | .11136 + 2 | .004 | .35000 - 2 |
| 25 | .76994 + 1 | .94000 + 1 | - | - |

Table - 3

SELF SHIELDING FACTORS FOR $^{239}Pu$ T = 300°K, = 100b

| GRP | CAPTURE | | SCATTERING | | FISSION | | TOTAL | |
|---|---|---|---|---|---|---|---|---|
| | RAMBHA | SETR | RAMBHA | SETR | RAMBHA | SETR | RAMBHA | SETR |
| 12 | 1.01 | 1.0 | .932 | 1.0 | 1.001 | 1.0 | .948 | 1.0 |
| 13 | 1.00 | .984 | .948 | .991 | .997 | .983 | .960 | .993 |
| 14 | .991 | .973 | .955 | .990 | .990 | .972 | .964 | .987 |
| 15 | .966 | .956 | .951 | .984 | .976 | .956 | .957 | .976 |
| 16 | .925 | .925 | .935 | .972 | .956 | .928 | .937 | .956 |
| 17 | .864 | .888 | .906 | .957 | .924 | .894 | .900 | .930 |
| 18 | .783 | .890 | .864 | .957 | .884 | .901 | .847 | .886 |
| 19 | .685 | .749 | .813 | .903 | .835 | .772 | .779 | .826 |
| 20 | .592 | .670 | .851 | .875 | .776 | .700 | .762 | .756 |
| 21. | .458 | .585 | .726 | .858 | .584 | .641 | .581 | .693 |
| 22 | .295 | .362 | .715 | .738 | .505 | .451 | .458 | .473 |
| 23. | .238 | .262 | .901 | .685 | .296 | .327 | .334 | .342 |
| 24. | 1.00 | .747 | 1.00 | .989 | 1.00 | .857 | 1.00 | .872 |

# Multi-Band Methods for Neutron/Photon Transport Calculations

S.GANESAN and M.M.RAMANADHAN

Reactor Research Centre

Kalpakkam 603 102

Tamil Nadu, India

# I. INTRODUCTION

In the design of nuclear reactors, it is common to use the various multigroup transport codes. The method used in these codes is to divide the neutron energy into a number of segments or groups, and assign an average cross sections for all energies within each of these groups. Though the results from these approximations are close enough to experimental results in certain energy groups, it has been proved that, where the actual cross section varies significantly within a group, there is a loss of accuracy and the existing multigroup codes fail. The conventional approach to improving this multigroup approximation is to divide the energy range into narrower segments so that the average cross sections will more closely approximate the true cross sections. Significantly increasing the number of energy groups makes the computation far more time consuming and expensive.

It is claimed that the multiband method greatly improves the accuracy in such type of cases.

The multiband method[1-6] is an upgrading or improvement over the existing multigroup codes without actually replacing them, thus avoiding the time and expense of developing a completely new formulation. The older codes remain largely intact with only a change in the method of determining the cross section to be applied to particular interactions.

In the multiband method, instead of assigning a single average cross section for each broad group, it provides mathematical interpretations or rules for allowing a multiple choice of cross section in

each group, with a list of probabilities for governing these choices. It differs from the probability table method in that, the latter method preassigns ranges of total cross sections and explicitly determines the probability of each range. Whereas in multiband method it attempts to minimise the number of cross section bands and at the same time provides exact solutions to certain limiting transport cases. The number of bands is dictated by the extent of variations of cross sections with energy groups.

The multigroup calculations is sufficient to perform multiband calculations since the information needed for determining the proper cross section choices and probability values are already available and inbuilt in the multigroup data. Thus this method permits rapid implementation with a minimum of developmental effort.

Starting from G energy groups and using B bands in each group results in a coupled set of G x B multigroup multiband equations. These can be solved for the neutron flux by the existing transport codes. Once the multiband cross sections are determined a multigroup processor must provide only the source and transfer matrices to describe the multiband equations completely.

## II. Definition and Calculation of Multiband Parameters

The self shielded cross section in any energy group G is defined as

$$\left\langle \Sigma_i(\Sigma_0, N) \right\rangle_G = \frac{\int_{E_G}^{E_{G+1}} \frac{\Sigma_i(E)\, S(E)\, dE}{(\Sigma_T(E)+\Sigma_0)^N}}{\int_{E_G}^{E_{G+1}} \frac{S(E)\, dE}{(\Sigma_T(E)+\Sigma_0)^N}} \qquad (1)$$

where

$G$ = group index

$(E_G, E_{G+1})$ = the energy range of group G

$\Sigma_i(E)$ = Cross section for reaction $i$ at energy E

$S(E)$ = the energy dependent neutron spectrum

$\Sigma_T(E)$ = Total cross section for the particular case of $\Sigma_i(E)$

$\Sigma_0(E)$ = Background cross section (combined effect of all other materials and geometry)

$N$ = an integer that differs for each legendre moment of the flux ($N=1$ for scalar flux $\phi$, $N=2$ for scalar current $J$ etc.)

To define multiband weights and cross sections, the definitions of group averaged cross section (Eqn.(1)) is transformed from a integral over energy to a integral over cross section.

The transformed eqn. is written as

$$\left\langle \Sigma_i(\Sigma_0, N) \right\rangle_G = \frac{\int_{E_G}^{E_{G+1}} \int_{\Sigma_T^*} \delta(\Sigma_T^* - \Sigma_T(E))\, \Sigma_i(E) \frac{\delta(E)}{(\Sigma_T(E)+\Sigma_0)^N}\, d\Sigma\, d\Sigma_T^*}{\int_{E_G}^{E_{G+1}} \int_{\Sigma_T^*} \delta(\Sigma_T^* - \Sigma_T(E)) \frac{\delta(E)}{(\Sigma_T(E)+\Sigma_0)^N}\, dE\, d\Sigma_T^*} \qquad (2)$$

64

where $\delta\left(\Sigma_T^* - \Sigma_T(E)\right)$ is Dirac delta function

$\Sigma_T^*$ is the entire range of total cross section in the group.

If the integration over $\Sigma_T^*$ is performed first eqn(1) is recovered. However if the integration over energy E is performed first, the equivalent eqn. is

$$\left\langle \Sigma_i\left(\Sigma_{o,N}\right)\right\rangle = \frac{\int_{\Sigma_T^*} \Sigma_i\left(\Sigma_T^*\right) \frac{P\left(\Sigma_T^*\right)}{\left(\Sigma_T^* + \Sigma_o\right)^N} d\Sigma_T^*}{\int_{\Sigma_T^*} \frac{P\left(\Sigma_T^*\right)}{\left(\Sigma_T^* + \Sigma_o\right)^N} d\Sigma_T^*} \qquad (3)$$

where

$$P\left(\Sigma_T^*\right) = \frac{\int_{E_G}^{E_{G+1}} \delta\left(\Sigma_T^* - \Sigma_T(E)\right) S(E)\, dE}{\int_{E_G}^{E_{G+1}} S(E)\, dE} \qquad (4)$$

and

$$\Sigma_i\left(\Sigma_T^*\right) P\left(\Sigma_T^*\right) = \int_{E_G}^{E_{G+1}} \delta\left(\Sigma_T^* - \Sigma_T(E)\right) \Sigma_i(E)\, S(E)\, dE \qquad (5)$$

Eqns.(4) and (5) defines the total cross section probability density $P\left(\Sigma_T^*\right)$ and cross section for each reaction $i$ as a function of the total cross sections $\Sigma_i\left(\Sigma_T^*\right)$.

It can be realized that since the definition of the group averaged cross section as an integral over total cross section (eqn.3) has been derived from the normal definition as an integral over energy (eqn.1) merely by introducing definitions, but no approximations,

the two forms are exactly equivalent.

Eqn.(3) can be rewritten compactly in the form

$$\left\langle \Sigma_i(\Sigma_o, N) \right\rangle = \frac{\left\langle \frac{\Sigma_i P}{(\Sigma_T+\Sigma_o)^N} \right\rangle}{\left\langle \frac{P}{(\Sigma_T+\Sigma_o)^N} \right\rangle} \qquad (6)$$

By assuming that the probability density $P(\Sigma_T^*)$ is given by a series of Dirac delta function $\sum_{t=1}^{B} P_t \delta(\Sigma_n - \Sigma_T')$ Eqn.(3) is reduced to a coupled set of non linear algebraic eqns.

$$\left\langle \Sigma_i(\Sigma_o, N) \right\rangle = \frac{\sum_t^B \frac{\Sigma_{it} P_t}{(\Sigma_{Tt}+\Sigma_o)^N}}{\sum_t^B \frac{P_t}{(\Sigma_{Tt}+\Sigma_o)^N}} \qquad (7)$$

The above procedure is analogous to that used in the multigroup method, in which the continuous energy is replaced by a number of discrete energy values. The quantities $P_t, \Sigma_{it}$ and $\Sigma_{Tt}$ are known as multiband parameters where $P_t$ is the band weight, $\Sigma_{it}$ is the band average cross section for reaction $i$ for each of the B bands into which the range of total cross section is divided, $\Sigma_{Tt}$ is the band average total cross section.

If the band cross sections $\Sigma_{it}$ and $\Sigma_{Tt}$ and the band weights $P_t$ are known by eqn.(7) the self-shielded cross section corresponding to any $(\Sigma_o, N)$ combination can be determined. Conversely if the values of the self shielded cross sections are known, eqn.(7) represents a system of coupled, non linear algebraic eqns. that must be

solved for the band cross sections $\Sigma_{it}$ and $\Sigma_{Tt}$ and for the band weights $P_t$.

## III SOLUTION OF THE MULTIBAND EQUATIONS

It has been shown by Cullen that very few isotopes require more than two bands per group (one band per group is just the multigroup method). Further for two bands the solutions will be analytical, and extremely economical.

The solution of the multiband equations for the case of two bands is given below for the sake of illustration.

From eqn.(7) with $x$ = Total, for two bands. The total cross section eqn. have four unknowns and

The first three equations are

$$1 = P_1 + P_2 \qquad (8)$$

which is equivalent to a normalised probability distribution,

$$\langle \Sigma_T \rangle = P_1 \Sigma_{T1} + P_2 \Sigma_{T2} \quad \text{which is} \qquad (9)$$

equivalent to conservation of the unshielded flux weighted cross section and

$$\left\langle \frac{1}{\Sigma_T} \right\rangle = \frac{P_1}{\Sigma_{T1}} + \frac{P_2}{\Sigma_{T2}} \qquad (10)$$

which is equivalent to conservation of the distance to collision or totally shielded flux weighted cross section.

For the fourth eqn. two methods could be used

$$\text{Method I} : \left\langle \frac{1}{\Sigma_T^2} \right\rangle = \frac{P_1}{\Sigma_{T1}^2} + \frac{P_2}{\Sigma_{T2}^2} \qquad (11)$$

which is equivalent to conservation of totally shielded current weighted cross section.

Method II : $$\left\langle \frac{1}{\Sigma_T+\Sigma_0} \right\rangle = \frac{P_1}{\Sigma_{T_1}+\Sigma_0} + \frac{P_2}{\Sigma_{T_2}+\Sigma_0} \qquad (12)$$

which is equivalent to partially shielded, flux weighted cross section.

## IV USE OF MULTIBAND PARAMETERS IN THE SOLUTION OF LINEAR NEUTRON TRANSPORT EQUATION(5)

The time independent linear Boltzmann equation can be written in the following form

$$\vec{\Omega}\,\vec{\nabla} N(\vec{r},\vec{\Omega},E) + \Sigma_T(E) N(\vec{r},\vec{\Omega},E) = \int_{E'}\int_{\Omega'} f(\vec{\Omega}',E'\to\vec{\Omega},E) N(\vec{r},\vec{\Omega}',E') d\Omega' dE' + S(\vec{r},\vec{\Omega},E) \qquad (13)$$

where

$N(\vec{r},\vec{\Omega},E)$ = angular flux

$S(\vec{r},\vec{\Omega},E)$ = angular source

$\Sigma_T(E)$ = total cross section (usually a function of position by Zone)

$f(\vec{\Omega}',E\to\vec{\Omega},E)$ = transfer function per unit flux from $(\vec{\Omega}',E')$ to $(\vec{\Omega},E)$ (usually a function of position by zone)

The transfer function contains the contributions from all physical processes and is written as follows

$$f(\vec{\Omega}',E'\to\vec{\Omega},E) = \sum_I m_I(E')\Sigma_I(E')\,g_I(\vec{\Omega}',E'\to\vec{\Omega},E) \qquad (14)$$

where the summation is over various physical reaction processes.

$(I = \text{elastic}, (n,n'), (n,2n)$ etc.)

and

$m_I(E')$ = multiplicity for process I

(e.g. $m_I$ = 1 for elastic; $(n,n')$
= 2 for $(n,2n)$
= $\nu(E)$ for fission etc

$\Sigma_I(E')$ = cross section for process I
(e.g. $\Sigma_{el}$, $\Sigma_{n,n'}$ etc)

$g_I(\vec{\Omega}', E \to \vec{\Omega}, E)$ = normalized (where integrated over all $(\Omega, E)$) transfer law which defines the kinematics for process I (e.g. exact correlation for elastic, fission spectrum for fission, temperature model etc.)

A fully defined problem of course includes boundary conditions that specify the incident source on all exterior [illegible] surfaces and the continuity of the angular flux across all interior boundaries (indeed in the absence of concentrated sources, at all interior points)

In the usual multigroup approach the continuous energy range is divided into a number of adjacent intervals: $E_1 < E_2 < E_3 < E_{max}$

Equation (14) is integrated over each energy interval to define a coupled set of equations

$$\bar{\Omega}\cdot\bar{\nabla}N_K(\bar{r},\bar{\Omega})+\Sigma_{T_K}N_K(\bar{r},\bar{\Omega})$$

$$=\frac{\Sigma}{T}\int_{\bar{\Omega}'}f(\bar{\Omega}',\bar{r}\to\bar{\Omega},K)N_K(\bar{r},\bar{\Omega}')+\delta_K(\bar{r},\bar{\Omega}) \quad (15)$$

where the group integral angular flux and source and group averaged cross section and transfer matrix are defined by

$$N_K(\bar{r},\bar{\Omega})=\int_{E_K}^{E_{K+1}}N(\bar{r},\bar{\Omega},E)\,dE \quad (16)$$

$$\delta_K(\bar{r},\bar{\Omega})=\int_{E_K}^{E_{K+1}}\delta(\bar{r},\bar{\Omega},E)\,dE \quad (17)$$

$$\Sigma_{IK}N_K(\bar{r},\bar{\Omega})=\int_{E_K}^{E_{K+1}}\Sigma_I(E)N(\bar{r},\bar{\Omega},E)\,dE \quad (18)$$

($I$ = elastic, total, etc.)

and

$$\int\left(\bar{\Omega}', \bar{r} \rightarrow \Omega, \kappa\right) N_k\left(\bar{r}, \bar{\Omega}'\right) = \int_{E_k}^{E_{k+1}} \int_{E_j}^{E_{j-1}} f\left(\bar{\Omega}', E' \rightarrow \bar{\Omega}, E\right) N\left(\bar{r}, \bar{\Omega}', E'\right) d E' d E \qquad (19)$$

In principle the multigroup equations are exact but to actually use the equation it is necessary to calculate the group averaged cross sections and the transfer matrix in advance. This requires assuming a functional form for the flux $N\left(\bar{r}, \bar{\Omega}, E\right)$ within each group.

It may readily be seen from Eqs.(15) through(18) that since $N\left(\bar{r}, \bar{\Omega}, E\right)$ is a function of energy, direction and position the actual group averaged cross sections and transfer matrix will also be a function of position (i.e. spatial self shielding) and direction. However the normal procedure in defining the group averaged data is to use a single, spatially averaged 'weighting function' in each spatial zone of the problem in an attempt to compensate for spatial effects. This procedure has the advantage of allowing pseudocomposition independent multigroup libraries to be generated for a wide variety of materials and yet the libraries are kept to a reasonable size. The weighting function used to define the group averaged data is usually made up of two components : slowly varying energy spectrum and a rapidly varying self-shielding factor,

$$N\left(\bar{r}, \bar{\Omega}, E\right) = M(E)\, \omega\left[\bar{r}, \Sigma_T(E)\right] \qquad (20)$$

The energy spectrum, $M(E)$ is usually $1/E$ at low energies a fission spectrum at intermediate energies and a fusion spectrum at high energies. The self shielding factor, $\omega\left[\bar{\Omega}, \Sigma_T(E)\right]$, may be either a single Bonderenko-type factor, $1/[\Sigma_T(E)+\Sigma_0]$ or separate factors for each legendre moment of the flux. With these weighting factors, the definitions of the multigroup cross section and transfer matrix become

$$N_K(\bar{\Omega}) = \int_{E_K}^{E_{K+1}} M(E)\,\omega\left[\bar{\Omega}, \Sigma_T(E)\right] dE,$$

(normalisation)

$$\Sigma_{IK} N_K(\bar{\Omega}) = \int_{E_K}^{E_{K+1}} \Sigma_I(E)\, M(E)\, \omega\left[\bar{\Omega}\ \Sigma_T(E)\right] dE, \qquad (21)$$

(I = total, elastic etc)

$$f(\bar{\Omega}', J \to \bar{\Omega}, K) N_J(\bar{\Omega}')$$
$$= \int_{E_K}^{E_{K+1}} \int_{E_J}^{E_{J+1}} f(\bar{\Omega}', E' \to \bar{\Omega}, E)\, M(E')$$
$$\times\ \omega\left[\bar{\Omega}', \Sigma_T(E')\right] dE'\, dE \qquad (22)$$

or explicitly in terms of individual reaction (see Eq.(15)).

$$m_{IJ}\,\Sigma_{IJ}\, f_I(\bar{\Omega}', J \to \bar{\Omega}, K)\, N_J(\bar{\Omega}')$$
$$= \int_{E_K}^{E_{K+1}} \int_{E_J}^{E_{J+1}} m_I(E')\,\Sigma_I(E')\, g_I(\bar{\Omega}', E' \to \bar{\Omega}, E)$$
$$\times M(E')\,\omega\left[\bar{\Omega}, \Sigma_T(E')\right] dE'\, dE \qquad (23)$$

(I = elastic, fission etc)

Fd

Probability Table Method

The probability table method was developed to allow the cross sections to be treated statistically in the unresolved resonance region, where the amount of structure in the cross section makes it impossible or uneconomical to store discrete data for use in monte Carlo calculations.

The basic assumption in the probability table method, as applied to the unresolved energy range is that the region contains a great deal of structure that is statistically distributed so that any energy averaged property (e.g. group integral flux) is a function of the distribution of cross section values rather than the exact cross section.

In the probability table method the neutrons at each energy within the unresolved resonance region are allowed to interact with all possible values of the total and partial reaction according to the probability of each value occurring. This model is consistent with the distribution of width and spacings which defines the cross section probability density at each energy. The probability table for the total cross section and conditional probability tables for individual reactions (elastic, capture, etc.) as constructed normalized and sampled just as one would construct a probability distribution for an angular distribution to randomly sample scattering angles.

Use of probability table method has been greatly simplified by the introduction of two assumption. First the unresolved resonance region contains so much cross section structure that the probability of a neutron being born or scattered to an energy where it encounters

a total cross section $\Sigma_T$ depends only upon the probability of $\Sigma_T$ occuring. This assumption allows the probability table to be sampled after each scattering without consideration of the history of the particle through earlier events. The second assumption is that instead of compiling the conditional probability tables $P(\Sigma_T : \Sigma_I, E)$ which specify the distributions of cross section $\Sigma_I$ for any fixed $\Sigma_T$ and $E$, it is possible to average over the distribution of $\Sigma_I$ to define a single, average value of $\Sigma_I$ for each $\Sigma_T$, which will be uniquely defined without further sampling once $\Sigma_T$ is sampled from the cross section probability table.

If the cross sections within the unresolved region are interpreted as specifying a distribution of cross section at each energy instead of a unique energy dependent cross section the above assumption for the probability table method allow the flux at each energy to be within independently as a function of both $E$ and $\Sigma_T$ in which case the Boltzmann equation can be written in the form

$$\bar{\Omega} \cdot \bar{\nabla} \bar{N}(\bar{r}, \bar{\Omega}, E, \Sigma_T) + \Sigma_T \bar{N}(\bar{r}, \bar{\Omega}, E, \Sigma_T) = P(\Sigma_T, E)\, \psi(\bar{r}, \bar{\Omega}, E) \tag{24}$$

$$\psi(\bar{r}, \bar{\Omega}, E) = \sum_I \int_{\Omega'} \int_{E'} \int_{\Sigma'_T} \int_{\Sigma'_I} m_I(E') \Sigma'_I P(\Sigma'_I : \Sigma'_T, E) \Big/ P(\Sigma'_T, E') q_I(E', \bar{\Omega}' \to E, \bar{\Omega}) \times \bar{N}(\bar{r}, \bar{\Omega}', E', \Sigma'_T) dE' d\Sigma'_T d\Sigma'_I d\Omega' + \delta(\bar{r}, \bar{\Omega}, E) \tag{25}$$

The expression $\psi(\bar{r}, \bar{\Omega}, E)$ is the total number of neutron born or coming out of collision at each energy E. According to the first assumption for the probability table method $\psi(\bar{r}, \bar{\Omega}, E)$ is independent of $\Sigma_T$ and should be redistributed to a new $\Sigma_T$ according to the probability of $\Sigma_T$ occuring which is simply $P(\Sigma_T, E)$ Note that the first assumption is consistent with the continuously distributed interpretation of X-secs since $\Sigma_T$ does not appear in Eq.(25). The implications of the second assumption for the probability table method can be interpreted by examining Eq.(24). If the multiplicity $m_I(E')$ the normalized transfer kernel $g_I(E', \bar{\Omega}' \to E, \bar{\Omega})$ and the flux $N(\bar{r}, \bar{\Omega}', E', \Sigma_T')$ are not functions of the partial cross sections $\Sigma_I'$ then the integration over can be performed immediately to define

$$\Sigma_I(\Sigma_T') P(\Sigma_T', E') = \int_{\Sigma_I} \Sigma_I' P(\Sigma_I', \Sigma_T', E) \, d\Sigma_I' \quad (26)$$

which is identical to the procedure used in the probability table method for fixed $\Sigma_I'$ and $\Sigma_I'$ a uniform average even distribution of $\Sigma_I'$. Eq.(25) then becomes

$$\psi_n(\bar{r},\bar{\Omega},E) = \sum_I \int_{\bar{\Omega}'}\int_{E'}\int_{\Sigma_T'} m_I(E')\,\Sigma_I(\Sigma_T',E) \times q_I(E',\bar{\Omega}'\to E,\bar{\Omega}) \times N(\bar{r},\bar{\Omega}',E',\Sigma_T')\,dE'\,d\Sigma_T'\,d\Omega' + \delta(\bar{r},\bar{\Omega},E) \qquad (27)$$

Equation (24) can be integrated over the distribution of $\Sigma_T$ to obtain the normal Boltzmann equation (Eq.13) which in turn can be integrated over an energy interval to obtain the multigroup equation.

However if the integration is performed over energy before the integration over $\Sigma_T$ the resulting equation will define the group averaged flux as a function of $\bar{\Sigma}_T$ the self shielding factor. The solution of the resulting equation by a method analogous to the multigroup approach can be simplified by a change of variables from the flux in each total cross section interval as in Eq.(23) to the flux density per unit total cross section.

$$\bar{N}(\bar{r},\bar{\Omega},E,\Sigma_T) = P(\Sigma_T,E)\,N(\bar{r},\bar{\Omega},E,\Sigma_T)$$

The Boltzmann equation to be solved then becomes

$$\bar{\Omega}\cdot\bar{\nabla}N(\bar{r},\bar{\Omega},E,\Sigma_T) + \Sigma_T N(\bar{r},\bar{\Omega},\Sigma_T) = \psi_n(\bar{r},\bar{\Omega},E) \qquad (28)$$

$$\psi(\bar{r},\bar{\Omega},G) = \sum_I \int_{\bar{\Omega}'} \int_{E'} \int_{\Sigma_T} m_I(E') \bar{\Sigma}_I(\Sigma_T, E')$$
$$\times q_{dI}(E',\bar{\Omega}' \to E,\bar{\Omega})\, P(\Sigma_T', E)$$
$$\times N(\bar{r},\bar{\Omega},E',\Sigma_T')\, d E'\, d\Omega' d\Sigma_T'$$
$$+ \delta(\bar{r},\bar{\Omega},E) \qquad (29)$$

The multiband equations will be developed by integrating Eq.(28) over an energy group $E \in (E_K, E_{K+1})$. The resulting equation will then be integrated over the total cross section band $\Sigma_T \in (\Sigma_{TK,L}, \Sigma_{TK,L+1})$ to obtain a set of equation analogous to the multigroup equations

$$\bar{\Omega}\cdot\bar{\nabla} N_{K,L}(\bar{r},\bar{\Omega}) + \bar{\Sigma}_{TK,L} N_{K,L}(\bar{r},\bar{\Omega})$$
$$= \sum_J \sum_{\beta(J)} \int_{\bar{\Omega}'} f(\bar{\Omega}', J, \beta \to \bar{\Omega}, K, L) N_{J,\beta}(\bar{r},\bar{\Omega}')\, d\bar{\Omega}'$$
$$+ \delta_K(\bar{r},\bar{\Omega}), \qquad (30)$$

$$P_{K,L} = \int_{E_K}^{E_{K+1}} \int_{\Sigma_{TK,L}} P(\Sigma_T,E) M(E)\, d\Sigma_T\, dE \Big/ \int_{E_K}^{E_{K+1}} M(E)\, dE \qquad (31)$$

$$N_{K,L}(\bar{r},\bar{\Omega}) = \int_{E_K}^{E_{K+1}} \int_{E_{K,L}}^{E_{K,L+1}} P(\Sigma_T,E) \times N(\bar{r},\bar{\Omega},E,\Sigma_T)\, d\Sigma_T\, dE / P_{K,L} \qquad (32)$$

$$\bar{\Sigma}_{IK,L} N_{K,L}(\bar{r},\bar{\Omega}) = \int_{E_K}^{E_{K+1}} \int_{\Sigma_{TK,L}}^{\Sigma_{TK,L+1}} P(\Sigma_T,E)\Sigma_T(\Sigma_T,E) \times N(\bar{r},\bar{\Omega},E,\Sigma_T)\, d\Sigma_T\, dE \Big/ P_{K,L} \qquad (32)$$

(I = total, elastic etc)

$$f(\bar{\Omega}', J.B. \to \bar{\Omega}, K, L)\, N_{J,B}(\bar{r},\bar{\Omega}) = \int_{E_K}^{E_{K+1}} \int_{E_J}^{E_{J+1}} \int_{\Sigma_{TJ,B}}^{\Sigma_{TJ,B+1}} m_J(E')\, \bar{\Sigma}_J(\Sigma'_T, E')\, g_I(E',\Omega' \to E,\bar{\Omega})\, P(\Sigma_T,E')$$
$$\times N(\bar{r},\bar{\Omega},E',\Sigma'_T)\, dE'\, d\bar{\Omega}'\, d\Sigma'_T \qquad (33)$$

$$S_K(\bar{r},\bar{\Omega}) = \int_{E_K}^{E_{K+1}} S(\bar{r},\bar{\Omega},E)\, dE$$

The in group source $S_K(\bar{r},\bar{\Omega})$ is the normal multigroup source.

Since (26) can be made identical to the usual multigroup equations, we observe that the multigroup, multiband equations can be solved by existing transport codes.

## V. MULTIGROUP MULTIBAND CODE GROUPIE

This code calculates self shielded cross sections and multiband parameters by reading the evaluated data in the ENDF/B format. It uses arbitrary energy groups and arbitrary energy dependent neutron spectrum and performs the integrals analytically. The program preconditions that, that all cross sections should be given in tabular form with linear interpretations between tabulated values. For this it would be necessary to use two other codes LINEAR[8], RECENT[9] before using the code GROUPIE. The code LINEAR reads tabulated cross sections from the ENDF/B format, converts them to linearly interpolable form.

The code RECENT combines the output obtained from LINEAR with the resonance parameters and produces linearly interpolable tabulated

cross sections.

In addition if data are required at a temperature other than 0 kelvin, the code SIGMA1[10] may be necessary to use. This code reads the linearly interpolable cross sections, Doppler broadens them to any user specified temperature and outputs them in one ENDF/B format. The flow chart is given in Fig.1.

The output from Groupie includes the following:

1. Listings of self shielded cross sections and $\bar{J}$ factors for total, elastic, capture and fission.
2. Unshielded, group averaged cross sections for all reactions, in linearly interpolable form in the ENDF/B format. This representation can be used to evaluate the effect of multigrouping cross sections in transport calculation.
3. Calculated multiband parameters for total, elastic, capture and fission for use with a Monte Carlo transport code.

## VI. APPLICATIONS.

The following results analysed at the Lawrence Livermore Laboratory, USA using two bands per group is herewith reported[11]. These show the improved accuracy of the multiband method over the previous calculational methods.

1. $K_{eff}$ of a nickel reflected fast system.

According to Cullen, the importance of self shielding up into the MeV neutron energy range for nickel can be understood by comparing the $K_{eff}$ values calculated by the usual multigroup method with that

calculated using multiband method. Experimentally $K_{eff}$ = 1.00 for a fast critical assembly with a predominant nickel reflector. The TART 175-group calculations have always overpredicted reactivity; for a typical system the TART-calculated $K_{eff}$ was 1.018. A multiband calculation of the same system yielded a lower and acceptable answer for $k_{eff}$ of 1.004. This decrease may be understood by examining the nickel total cross section. Nickel has resonance structure well into the keV range. Self shielding of these resonances lowers the effective cross sections and increases the depth the neutrons will penetrate into the nickel reflector, which thereby has reduced reflectivity. The net effect is a decrease in the $K_{eff}$ of the system.

2. Criticality calculations:

In this process, calculations were carried out for the reactivity and neutron inducing fission energy of a homogeneous, spherical mixture ofenriched uranium and water as a function of the hydrogen to uranium atom fraction. The results tabulated below analyse the $K_{eff}$ values obtained using three different codes for various values of the hydrogen-to-uranium fractions.

| Code | Hydrogen/U-235 ratio | | |
|---|---|---|---|
| | 3/1 | 10/1 | 30/1 |
| | Calculated reactivity | | |
| TART-175 groups | 0.901 | 0.859 | 0.866 |
| TARTMM-2020 groups | 0.950 | 0.978 | 0.993 |
| ALICE 175 groups, 2 bands | 0.957 | 0.989 | 0.996 |

3. Shielding Calculations:

As an illustration of a shielding problem, a number of computer codes were used to calculate the uncollided transmission of neutrons ranging in energy from 1MeV to 20 MeV through 30.4 cms of thick iron slab.

| Code | Transmission | Ratio to Analytic |
|---|---|---|
| Analytic | 0.486 | 1.00 |
| MCN (continous energy Monte Carlo code) | 0.478 | 1.02 |
| ALICE 175 gr. 2 bands | 0.463 | 1.05 |
| TART 175 gr. | 0.065 | 7.48 |
| TART 2020gr. | 0.430 | 1.13 |

In the above table the analytic solution is the uncollided, exponentially attenuated flux using all the details of the energy dependent cross sections. Both the MCN code and the ALICE code are in excellent agreement with the analytic solution. However MCN code requires enormous storage space in the computer and lot of computer time to run. The TART 175 group answer is a factor of 7 lower than the analytic solution. Even when the number of TART groups are increased to 2020 one atreement is still not as good as with the multiband method.

4. Fusion Reactor Blanket :

This is desioned to convert fusion-neutron energy into useful form. The fusion rates were calculated per 14.1 MEV source neutron

using both multigroup and multiband methods. The table below compares the calculations at three detector positions A, B and C.

| Detector positions and distance from source | | Code ALICE | TART | ALICE/TART ratios |
|---|---|---|---|---|
| A | 309 cm | 0.465 | 0.452 | 1.03 |
| B | 324 cm | 0.727 | 0.565 | 1.29 |
| C | 334 cm | 0.355 | 0.246 | 1.43 |

It is seen that for detectors successfully farther from the source, the TART 175 group result deviates more and more from the ALICE multiband result upto a difference of 43% at the detector position labeled C. In this case self shielding has two effects. It increases the neutron's penetration depth andalso the moderating properties of the light materials. The net result is more fissions at greater distances from the source than are predicted by the multigroup method.

## VII CONCLUSION

It is clarified that the multiband method while solving a wide variety of neutron and photon transport problems accurately and economically, is very appropriate for problems in which theeffects of the cross sections are not well characterized by a single average cross section value for each group. Further in several applications the two band calculations were found to be more accurate than multigroup calculation using more than ten times as many groups. It is planned to test these claims at RRC when the inhouse computer facility will become available.

At present the LINEAR-RECENT-SIGMA1-GROUPIE code system has been successfully commissioned on IBM/370/155 system at Madras.

## ACKNOWLEDGEMENTS

The authors thank Dr. Dermott E. Cullen for supplying us with the LINEAR-RECENT-SIGMA1-GROUPIE code system and for a fruitful correspondence. The articles mentioned in the references were freely used in the preparation of this review note.

REFERENCES

1. D.E.CULLEN, Nucl. Sci. Eng. 55, 387 (1974).

2. D.E.CULLEN, Calculation of Probability Table Parameters to Include Self-Shielding and Intermediate Resonances, Lawrence Livermore Laboratory, Rept. UCRL-79761 (1977).

3. D.E.CULLEN, Nucl. Sci. Eng. 58, 261 (1975).

4. D.E.CULLEN, Trans. Amer. Nuc. Soc. 23, 526 (1976).

5. D.E.CULLEN et al., CrossSection Probability Tables in Multigroup Transport Calculations, Lawrence Livermore Laboratory, Rept. UCRL-80655 (1978).

6. D.E.CULLEN, 'Application of the Probability Table method to multigroup calculations' in Proceedings of the CSEWG Resonance Region Subcommittee Meeting; Multilevel Effects in Reactor Calculations and the Probability Table Method, Brookhaven National Laboratory, Rept. BNL-50387 (ENDF-187) p.90 (1973).

7. D.E.CULLEN, 'Program GROUPIE (Ver.79-1): UCRL-50400 Vol.17, Part D.

8. D.E.CULLEN 'Program LINEAR (Ver 79-1): UCRL-50400 Vol.17, Part A Rev.2.

9. D.E.CULLEN 'Program RECENT (Ver 79-1) : UCRL-50400 Vol.17, Part C.

10. D.E.CULLEN 'Program SIGMA-1 (Ver.79-1): UCRL-50400 Vol.17, Part B Rev.2.

11. E.F.PLECHATY, J.R.KALLEMEYN, TART Monte Carlo Neutron Transport Code, Lawrence Livermore Laboratory Rept. UCID-522 (1971).

12. R.L.HAMBLETT and J.E. CAHN, 'Energy-Dependent Self Shielding Factors for U-235 Foils from Transmission Experiments' Nucl. Sci. Eng. 35, 350 (1969).

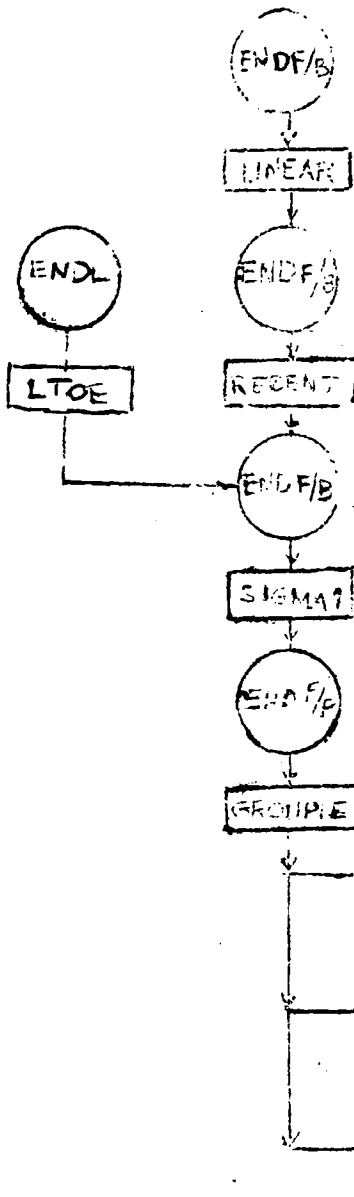


LINEARISES FILE 3

COUPLES FILE 2 FROM ENDF-B and FILE 3 OUTPUT FROM (Cross Sections may be linear interpolation) . LINEAR

Doppler broadens linearised data

Generates multibard parameters

Infinite dilution group averaged cross sections

Self shielded cross sections

Multiband parameters

# TESTING AND VALIDATION OF A MULTIGROUP CROSS-SECTION SET AGAINST INTEGRAL EXPERIMENTS

by

V.K. Shukla and S.B. Garg
Experimental Reactor Physics Section
Bhabha Atomic Research Centre
Bombay - 400 085

## 1. INTRODUCTION

The accuracies in the predictions of various physics parameters are of vital importance for the safety and economics of any reactor. The approximations made in representing the complicated neutron cross-section behaviour to account for the various competing reactions over a wide energy range as seen in fast reactors and the simplifications in the calculational model to carry out the neutronics of the complicated reactor designs introduce some uncertaintics in the predictions of various physics parameters. It is, therefore, imperative to assess the efficacy and the range of applicability of a given nuclear data set and the calculational model before using them for any design calculation.

A 27-group cross-section set[1] and the resonance self-shielding factors[2] for various reactions have been derived for different elements of interest in reactor analysis using ENDF/B library. The energy group structure of this set is identical to that of the 26-group ABBN set[3] but for an additional group in the energy range 10.5 to 15.0 MeV mainly to account for the (n, 2n), (n, p) and (n,$\alpha$) reactions which assume significance in very hard spectra fast reactors or fission-fusion systems. The present paper discusses the analysis of central reactivity worths and reaction rate measurements carried out

...2

in 11 uranium and plutonium fuelled fast critical assemblies covering a wide range of neutron energy spectrum using this cross-section set and the neutronics codes developed for fast reactor analysis.

## 2. DESCRIPTION OF CRITICAL ASSEMBLIES

Most of the assemblies selected for the present analysis are from those recommended by the Cross-Section Evaluation Working Group of BNL as benchmarks[4] for the fast reactor nuclear data testing. The assembly ZPR-3-49 has a composition identical to that of ZPR-3-48 with the exception that the sodium was removed. Similarly, ZPR-3-50 has composition identical to that of ZPR-3-49 but with additional carbon to soften the spectrum. These assemblies provide the examination of a single item and hence they are also included.

The isotopic compositions and the zone dimensions in one dimensional spherical model for these assemblies were taken from the paper of Hardie[5] et al and are given in Tables 1 and 2 for ready reference. The small quantities of $^{234}U$ and $^{236}U$ present in some of the assemblies have been included with $^{238}U$. It can be seen that these cores cover a wide range of neutron energy spectrum and hence provide a good testing bed for a cross-section set and the calculational model for the predictions of various reactor physics parameters.

## 3. CALCULATIONAL DETAILS

### 3.1 Multigroup Constants

The 27-group cross-section set[1] and the resonance self-shielding factor[2] were derived from the basic ENDF/B libraries. Version III

...3

57

of ENDF/B was used for the actinide isotopes whereas Version IV was used for the coolant and structural elements.

3.2 Multiplication Factors

The multiplication factors for all the assemblies have been calculated by 1 dimensional diffusion theory in spherical model using the code CNEDX[6]. The analysis of these assemblies limited to criticality predictions[7] was carried out earlier where we had ignored the small quantities of Si, Al and Mo present in some of these assemblies. In the present analysis we have accounted for these isotopes also.

The corrections for 1-D to 2-D, diffusion to transport and for heterogeneity have been calculated for these assemblies by Hardie et al, which have been adopted as such and have been used to obtain the $k_{eff}$'s of these assemblies.

The resonance self-shielded cross-sections for each composition zone of a reactor were generated by the usual method of iteration on the potential scattering cross-sections. The elastic slowing down cross-sections are very sensitive to the neutron energy spectrum within a group and hence iterations were further made to get the converged values of elastic slowing down cross-sections. All these iterations are incorporated in the code CNEDX.

3.3 Central Reactivity Worths and Reaction Rate Ratios

The small sample central reactivity worths of different materials have been calculated using the first order perturbation theory code PERT-5[8] in one dimensional option. The 27-group self-shielded cross-sections for different isotopes in the core spectrum, real fluxes and

...4

adjoints calculated in 1-D diffusion theory were used as input for these predictions.

The reactivity worths calculated as % $\triangle K/K$ have not been converted to inhours values (as usually quoted) to avoid the additional uncertainties in the worths of these materials due to the discrepant delayed neutron data resulting in discrepant conversion factors for $\frac{\triangle K}{K}$ to inhours. We were mainly interested in analysing the effect of our cross-section set and the computational model on the predictions of these integral parameters.

The small sample central reactivity worths for the isotopes $^{235}U$, $^{238}U$, $^{239}Pu$, Na, Fc, Cr and Ni have been calculated for these assemblies in the units of $\%\frac{\triangle K}{K}$ per kg. The central reaction rate ratios for fissions in $^{238}U$, $^{239}Pu$, $^{240}Pu$ and captures in $^{238}U$ normalised to the fissions in $^{235}U$ have also been calculated in these assemblies based on one dimensional homogeneous model.

3.4 Neutron Generation Time and Effective Delayed Neutron Fractions

The neutron generation time and effective delayed neutron fractions for these assemblies were calculated using the first order perturbation theory code PERT-5 and the 27-group 1-D diffusion theory fluxes and adjoints. The delayed neutron data required for these calculations were taken from the paper of Hardie et al (who have used the ENDF/B-IV data) except the delayed neutron energy spectrum. We have derived the 27-group delayed neutron energy spectra based on the combined data[9] of Batchelor and Bonner for the composite spectrum of delayed neutrons from $^{235}U$ fission. The same delayed neutron spectrum has been used for all the fissionable isotopes.

...5

## 4. DISCUSSION OF RESULTS

### 4.1 Multiplication Factors

The multiplication factors calculated for these assemblies using the 27-group cross-section set are given in Table 3. The $k_{eff}$ values of these assemblies obtained by Hardie et al[5] using the basic ENDF/B Version III library and those by Sharma et al[10] of RRC using the French cross-section set are also given in the same Table.

It can be seen from this Table that the 27-group cross-section set and the calculational model is quite satisfactory in predicting the criticalities of a wide range of plutonium and uranium fuelled assemblies with an average discrepancy of about 0.1% in $k_{eff}$. The maximum discrepancy occurs in ZEBRA-2 which is underpredicted by about 1.2%. This might be because it contains a small quantity of hydrogen which has been ignored in our calculations. It can be seen from this Table that the average discrepancies in the prediction of $k_{eff}$ for these assemblies by Hardie et al and Sharma et al are of the similar order with the maximum discrepancy of about 1% and 0.8% respectively. The criticality predictions using this set and the calculational model appear to be satisfactory in general. The two assemblies ZPR-6-6A and ZPR-6-7 which represent large fast uranium and plutonium fuelled fast assemblies are predicted within 0.5% using this cross-section set.

### 4.2 Central Reactivity Worth

The central reactivity worths of $^{235}U$, $^{238}U$, $^{239}Pu$, Na, Cr, Fe and Ni calculated in these assemblies using the 27-group cross-section set are given in Tables 4 to 10. The experimental values of these worths

...6

given in the paper of Hardie et al in the units of inhours/kg have been converted to % $\frac{\Delta K}{K}$ per kg., using the conversion factors given in the same paper. We have compared the calculated to experimental worth ratios of these materials in different assemblies obtained by us with those obtained by Hardie et al in 1-D model in the same Table. It may be mentioned that we have used Version III of ENDF/B for actinides and Version IV for structural and coolant materials and hence the corresponding comparisons have been made with those obtained by Hardi et al.

It is seen from Tables 4 and 5 that the central reactivity worths of fissile isotopes $^{235}U$ and $^{239}Pu$ are overestimated using this cross-section set with a discrepancy of about 8.5 and 7.9% respectively averaged over all the assemblies. The same worths have been overestimated by Hardie et al by about 14.4 and 10.3% respectively. The intercomparison of these worths for individual assemblies also indicates that the 27-group set is satisfactory for these predictions. The overestimation of about 8% in the fissile material worth appears to be quite satisfactory with the first order perturbation theory approximation.

The central reactivity worth of $^{238}U$ given in Table 6 is also overpredicted in general using this cross-section set. The average discrepancy of about 11.2% observed with this set compares favourably with 15.5% predicted by Hardie et al. Even the intercomparison of individual assemblies indicates a satisfactory trend for this set.

The reactivity worths of fissile and fertile elements are in general overestimated by all the evaluators. The reasons could be many apart from the basic cross-section set. The discrepant delayed neutron data

...7

lead t: erroneous conversion factors for $\frac{\Delta K}{K}$ values from inhours observed experimentally. The main contributions to fissile and fertile reactivity worths come from their capture and fission cross-sections which are not accounted adequately in the first order perturbation theory in homogeneous model. The atomic concentration of the isotope under consideration is always higher in the sample than in the homogenised surroundings which results in the overestimation of the effective fission and capture cross-sections of the sample. This affects the estimation of the actual reactivity worth of the sample.

The reactivity worths of the structural elements are given in Tables 7 to 9. Here again we see the over-predictions, almost consistently in all the assemblies. The average discrepancies for Cr, Fe and Ni are 45.5, 32.0 and 30.6% respectively. These discrepancies in the case of Hardie's predictions are 55.5, 32.1 and 24.1% respectively. The material worths of these elements are mainly contributed by their capture (negative) and slowing down cross-sections (negative or positive). Since these worths are consistently overestimated it appears that their capture cross-sections need some reduction. The worth of sodium is a difficult parameter to predict as can be seen from Table 10. This is because the slowing down effects become relatively very important for the central worth predictions of sodium. This component depends on the differences in the adjoint fluxes in the source and sink groups apart from the group slowing down cross-sections and the real fluxes. Small errors in the adjoint fluxes would, therefore, lead to large discrepancies in the worth predictions of sodoium. Moreover, the elastic cross-sections of Na are sensitive to energy right upto 10 MeV and hence its

...8

slowing down cross-sections are not adequately represented in a few group model. Because of a very wide variation in the calculated to experimental worth ratios in different assemblies, it is meaningless to find the average of the discrepancies over all the assemblies and, apparently, no definite conclusion can be drawn except that the sodium worths would have large uncertainties in their predictions in the present model.

4.3 Central Reaction Rate Ratios

The central reaction rates of fissions in $^{238}U$, $^{239}Pu$ and $^{240}Pu$ normalised to those in $^{235}U$ are given in Tables 11 to 13. It is seen that all these reaction rates are, in general, overestimated. The average discrepancy using the 27-group set is found to be 7.3, 3 and 11.4% for the fissions in $^{238}U$, $^{239}Pu$ and $^{240}Pu$ respectively. It may be seen that the maximum discrepancy of about 28% occurs in the fission rates of $^{238}U$ in the assemblies VERA-1B and ZPR-3-53 which are carbide fuelled cores of uranium and plutonium with high fissile to fertile ratios and reflected by $^{238}U$. It clearly indicates that the neutron spectrum in the MeV energy range has been overestimated. This may be due to the inadequate representation of inelastic scattering cross-sections of $^{238}U$ in the MeV energy range or the fission cross-sections in that energy range are given higher values. The large discrepancy in VERA-1B may partly be due to the inadequacy of the 1-D diffusion theory model used for such a small core.

The capture rates in $^{238}U$ normalised to fissions in $^{235}U$ in different assemblies are given in Table 14. They are, on the average, 3.3%

...9

23

underpredicted using 27-group cross-section set as compared to under-prediction of about 1.4% by Hardie et al.

4.4 Effective Delayed Neutron Fractions and Generation Times

The effective delayed neutron fractions and the neutron generation time calculated using 27-group cross-section set and those by Hardie et al are given in Table 15. It can be seen that the neutron generation times match very well in the two calculations for the uranium fuelled assemblies but differ upto about 10% in the case of plutonium fuelled assemblies. The effective delayed/fractions are also in agreement in the two calculations within about 10% except for VERA-1B and ZPR-3-53. The different delayed neutron spectra used in the two calculations appear to be responsible for the disagreements in the predictions of the effective delayed neutron fractions.

/neutron

5. CONCLUSIONS

The 27-group cross-section set derived from the ENDF/B library is adequate for the criticality predictions of plutonium or uranium fuelled fast reactors as the average discrepancy in $k_{eff}$ predictions of a wide ranging fast assemblies has been found to be $\simeq$ 0.1%.

The central worths of fissile and fertile elements calculated in first order perturbation theory and homogeneous model are overestimated, in tune with the usual trend, but within an average discrepancy of 8 and 11% respectively. However, there is a wide spread for the individual assemblies. The worths for the structural materials are overestimated, on the average by about 30 to 45%.

It appears that the predictions may improve in agreement with the

...10

experiments if fission cross-sections in the MeV range are slightly decreased and the inelastic cross-sections of $^{238}U$ are also suitably modified in the high energy range.

REFERENCES


1. S.B. Garg ; Report INDC (IND)-21/G + SP (1977).
2. S.B. Garg ; Report BARC-1002 (1979).
3. L.P. Abagyan et al ; Group Constants for Nuclear Reactor Calculations, Consultants Bureau, New York (1964).
4. BNL-19302 ; Cross-Section Evaluation Working Group Benchmark Specifications (1974).
5. R.W. Hardie et al ; Nucl. Sci. Engg. 57, 222 (1975).
6. R.W. Hardie and W.W. Little Jr ; BNWL-954 (1969).
7. V.K. Shukla and S.B. Garg ; "A Test of ENDF/B Library in the Criticality Predictions of Fast Assemblies", paper presented at the International Conference on Nuclear Cross-Sections for Technology, Knoxville (1979).
8. R.W. Hardie and W.W. Little Jr ; BNWL-1162 (1969).
9. L. Tomlinson ; AERE-R 6993.
10. M.L. Sharma et al ; RRC-23 (1978).

Table - 1

ATOM DENSITIES (x $10^{22}$ ATOM/CC) AND DIMENSIONS FOR URANIUM BASED ASSEMBLIES

| Isotope | VERA-1B | | ZPR-3-11 | | ZPR-3-12 | | ZEBRA-2 | | ZPR-6-6A | |
|---|---|---|---|---|---|---|---|---|---|---|
| | Core | Reflector | Core | Reflector | Core | Reflector | Core | Reflector | Core | Reflector |
| $^{235}U$ | 0.7349 | 0.0250 | 0.4567 | 0.0089 | 0.4516 | 0.0089 | 0.2526 | 0.0298 | 0.1153 | 0.00856 |
| $^{238}U$ | 0.0561 | 3.4400 | 3.4438 | 4.0025 | 1.6994 | 4.0026 | 1.5667 | 4.1269 | 0.58176 | 3.95508 |
| O | - | - | - | - | - | - | 0.01544 | - | 1.3900 | 0.0023 |
| C | 5.7540 | - | - | - | 2.6762 | - | 3.7992 | 0.0042 | - | - |
| Na | - | - | - | - | - | - | - | - | 0.92904 | - |
| Al | - | - | - | - | - | - | 0.0019 | 0.0019 | - | - |
| Cr | 0.0689 | 0.0708 | 0.1486 | 0.1196 | 0.1419 | 0.1237 | 0.0864 | 0.0864 | 0.2842 | 0.1247 |
| Fe | 0.6283 | 0.6464 | 0.5681 | 0.4925 | 0.5704 | 0.4971 | 0.36485 | 0.3323 | 1.3431 | 0.44669 |
| Ni | 0.1635 | 0.1682 | 0.0718 | 0.0536 | 0.0621 | 0.0541 | 0.0483 | 0.0483 | 0.1291 | 0.05407 |
| Mo | - | - | - | - | - | - | 0.0008 | 0.0008 | - | - |
| Si | - | - | - | - | - | 0.0060 | 0.0054 | 0.0054 | - | - |
| Radius(cm) | 19.138 | 58.59 | 31.61 | 61.61 | 28.76 | 59.26 | 45.45 | 77.15 | 95.67 | 129.48 |

Table - 2

ATOM DENSITIES (x $10^{22}$ ATOMS/CC) AND DIMENSIONS FOR PLUTONIUM BASED ASSEMBLIES

| Isotope | SNEAK-7B | | ZPR-3-48 | | ZPR-3-49 | | ZPR-3-50 | | ZPR-3-53 | | ZPR-6-7 | |
|---|---|---|---|---|---|---|---|---|---|---|---|---|
| | Core | Reflector | Core | Reflector | Core | Reflector | Core | Reflector | Core | Reflector | Core | Reflector |
| $^{235}U$ | 0.02663 | 0.01624 | 0.0016 | 0.0083 | 0.0016 | 0.0083 | 0.0016 | 0.0083 | 0.0006 | 0.0083 | 0.00126 | 0.00856 |
| $^{238}U$ | 1.45794 | 3.99401 | 0.7405 | 3.9690 | 0.7406 | 3.9556 | 0.7404 | 3.9613 | 0.2615 | 3.9770 | 0.578036 | 3.96179 |
| $^{239}Pu$ | 0.18312 | - | 0.1645 | - | 0.1644 | - | 0.1645 | - | 0.1669 | - | 0.088672 | - |
| $^{240}Pu$ | 0.01652 | - | 0.01064 | - | 0.01064 | - | 0.01064 | - | 0.0107 | - | 0.011944 | - |
| $^{241}Pu$ | 0.00149 | - | 0.0011 | - | 0.0011 | - | 0.0011 | - | 0.0008 | - | 0.00133 | - |
| O | 3.31936 | - | - | - | - | - | - | - | - | - | 1.39000 | 0.0024 |
| C | 0.00631 | 0.00135 | 2.0770 | - | 2.0766 | - | 4.5940 | - | 5.5898 | 0.0024 | - | - |
| Na | - | - | 0.6231 | - | - | - | - | - | - | - | 0.92904 | - |
| Al | 0.12112 | - | 0.0109 | - | 0.0109 | - | 0.0110 | - | 0.0111 | - | - | - |
| Cr | 0.27560 | 0.11080 | 0.2531 | 0.1225 | 0.2508 | 0.1242 | 0.1816 | 0.1161 | 0.2081 | 0.1311 | 0.2842 | 0.1295 |
| Fe | 0.98021 | 0.39549 | 1.0180 | 0.4925 | 1.0083 | 0.4626 | 0.7300 | 0.4671 | 0.7134 | 0.4496 | 1.3431 | 0.4637 |
| Ni | 0.14594 | 0.09845 | 0.1119 | 0.0536 | 0.1121 | 0.0611 | 0.0796 | 0.0508 | 0.0970 | 0.0611 | 0.1291 | 0.05635 |
| Mo | 0.00184 | 0.00100 | 0.0206 | - | 0.0206 | - | 0.0205 | - | 0.0208 | - | 0.02357 | 0.00038 |
| Si | 0.01174 | 0.00453 | 0.0124 | 0.0060 | - | - | - | - | - | - | - | - |
| Radius (cm) | 40.64 | 70.64 | 45.245 | 75.245 | 47.53 | 83.96 | 43.43 | 83.77 | 37.546 | 74.876 | 88.16 | 121.97 |

Table - 3

Calculated $k_{eff}$ Values of Critical Assemblies

($k_{eff}^{Exp} = 1.000$)

| Assembly | Fuel | Approx. Core vol. (liter) | $k_{eff}$ | | |
|---|---|---|---|---|---|
| | | | 27-Group | Hardie et al | Sharma et al |
| VERA-1B | U | 30 | 0.9950 | 1.0026 | 1.0063 |
| ZPR-3-11 | U | 140 | 1.0011 | 0.9924 | 1.0020 |
| ZPR-3-12 | U | 100 | 1.0065 | 1.0017 | 0.9960 |
| ZEBRA-2 | U | 430 | 0.9876 | 0.9902 | 0.9920 |
| ZPR-6-6A | U | 4000 | 1.0010 | 0.9988 | 0.9995 |
| SNEAK-7B | Pu | 310 | 1.0004 | 0.9893 | - |
| ZPR-3-48 | Pu | 410 | 1.0033 | 0.9997 | 1.0067 |
| ZPR-3-49 | Pu | 450 | 1.0035 | 0.9985 | 1.0071 |
| ZPR-3-50 | Pu | 340 | 0.9938 | 0.9940 | 1.0012 |
| ZPR-3-53 | Pu | 220 | 0.9903 | 1.0008 | 1.0018 |
| ZPR-6-7 | Pu | 3100 | 1.0048 | 0.9926 | 1.0010 |
| | | Average | 0.9988 | 0.9964 | 1.0014 |

...14

Table - 4

Central Reactivity Worth of $^{235}U$ (% $\frac{\Delta K}{K}$ per kg)

| Assembly | Fuel | Experimental | Calculated 27-Group | Calculated / Experimental | |
|---|---|---|---|---|---|
| | | | | 27-Group | Hardie et al |
| VERA-1B | U | 1.037 | 0.9642 | 0.928 | 0.927 |
| ZPR-3-11 | U | 0.532 | 0.5747 | 1.080 | 1.096 |
| ZPR-3-12 | U | 0.6665 | 0.6333 | 0.950 | 0.967 |
| ZEBRA-2 | U | 0.3165 | 0.3566 | 1.127 | 1.156 |
| ZPR-6-6A | U | 0.0972 | 0.1026 | 1.055 | 1.089 |
| SNEAK-7B | Pu | 0.5156 | 0.5583 | 1.083 | 1.138 |
| ZPR-3-48 | Pu | 0.3582 | 0.4182 | 1.167 | 1.232 |
| ZPR-3-49 | Pu | 0.3018 | 0.3415 | 1.131 | 1.194 |
| ZPR-3-50 | Pu | 0.4989 | 0.5344 | 1.071 | 1.135 |
| ZPR-3-53 | Pu | 0.5472 | 0.6692 | 1.223 | 1.254 |
| ZPR-6-7 | Pu | 0.1368 | 0.1533 | 1.121 | 1.213 |
| | | | Average | 1.085 | 1.144 |

...15

Table - 5

Central Reactivity Worth of $^{239}Pu$

($\% \frac{\triangle K}{K}$ per kg)

| Assembly | Fuel | Experimental | Calculated 27-Group | Calculated / Experimental | |
|---|---|---|---|---|---|
| | | | | 27 - Group | Hardie et al |
| VERA-1B | U | 1.788 | 1.688 | 0.944 | 0.944 |
| ZPR-3-11 | U | 0.888 | 0.915 | 1.030 | 1.037 |
| ZPR-3-12 | U | 1.0196 | 1.0000 | 0.981 | 0.956 |
| ZEBRA-2 | U | 0.4409 | 0.4860 | 1.102 | 1.122 |
| SNEAK-7B | Pu | 0.6922 | 0.7563 | 1.093 | 1.110 |
| ZPR-3-48 | Pu | 0.4772 | 0.5650 | 1.184 | 1.216 |
| ZPR-3-49 | Pu | 0.4441 | 0.4697 | 1.058 | 1.084 |
| ZPR-3-50 | Pu | 0.6064 | 0.6581 | 1.085 | 1.128 |
| ZPR-3-53 | Pu | 0.7166 | 0.8254 | 1.152 | 1.198 |
| ZPR-6-7 | Pu | 0.1652 | 0.1924 | 1.165 | 1.232 |
| | | | Average | 1.079 | 1.103 |

...16

Table - 6

Central Reactivity Worth of $^{238}U$

($\% \frac{\Delta K}{K}$ per kg)

| Assembly | Fuel | Experimental | Calculated 27-Group | Calculated/Experimental 27-Group | Calculated/Experimental Hardie et al |
|---|---|---|---|---|---|
| VERA-1B | U | 0.0348 | 0.0787 | 2.261 | 1.602 |
| ZPR-3-11 | U | - 0.0281 | - 0.0286 | 1.018 | 1.052 |
| ZPR-3-12 | U | - 0.0281 | - 0.0264 | 0.939 | 1.054 |
| ZEBRA-2 | U | - 0.0242 | - 0.0250 | 1.033 | 1.097 |
| ZPR-6-6A | U | - 0.0081 | - 0.0087 | 1.073 | 1.158 |
| SNEAK-7B | Pu | - 0.0287 | - 0.0340 | 1.185 | 1.251 |
| ZPR-3-48 | Pu | - 0.0253 | - 0.0259 | 1.024 | 1.164 |
| ZPR-3-49 | Pu | - 0.0198 | - 0.0206 | 1.040 | 1.158 |
| ZPR-3-50 | Pu | - 0.0453 | - 0.0398 | 0.878 | 1.023 |
| ZPR-3-53 | Pu | - 0.0790 | - 0.0628 | 0.795 | 1.062 |
| ZPR-6-7 | Pu | - 0.0112 | - 0.0110 | 0.982 | 1.088 |
| | | | Average | 1.112 | 1.155 |

...17

Table - 7

Central Reactivity Worth of Cr

($\% \frac{\Delta K}{K}$ per kg)

| Assembly | Fuel | Experimental | Calculated 27-Group | Calculated/Experimental 27-Group | Calculated/Experimental Hardie et al |
|---|---|---|---|---|---|
| VERA-1B | U | - | 0.0435 | - | - |
| ZPR-3-11 | U | - 0.0333 | - 0.0381 | 1.143 | 1.242 |
| ZPR-3-12 | U | - | - 0.0329 | - | - |
| ZEBRA-2 | U | - 0.0124 | - 0.0175 | 1.411 | 1.446 |
| ZPR-6-6A | U | - | - 0.0039 | - | - |
| SNEAK-7B | Pu | - | - 0.0298 | - | - |
| ZPR-3-48 | Pu | - 0.0132 | - 0.0195 | 1.477 | 1.546 |
| ZPR-3-49 | Pu | - 0.0126 | - 0.0170 | 1.349 | 1.429 |
| ZPR-3-50 | Pu | - 0.0141 | - 0.0224 | 1.591 | 1.728 |
| ZPR-3-53 | Pu | - 0.0106 | - 0.0190 | 1.792 | 2.014 |
| ZPR-6-7 | Pu | - 0.0046 | - 0.0066 | 1.421 | 1.483 |
| | | | Average | 1.455 | 1.555 |

...18

Table - 8

Central Reactivity Worth of Iron

($\% \frac{\triangle K}{K}$ per kg)

| Assembly | Fuel | Experimental | Calculated 27-Group | Calculated/Experimental | |
|---|---|---|---|---|---|
| | | | | 27-Group | Hardie et al |
| VERA-1B | U | - | 0.0469 | - | - |
| ZPR-3-11 | U | - 0.0309 | -0.0356 | 1.151 | 1.278 |
| ZPR-3-12 | U | - 0.0269 | -0.0294 | 1.092 | 1.108 |
| ZEBRA-2 | U | - 0.0117 | -0.0153 | 1.307 | 1.300 |
| ZPR-6-6A | U | - | -0.0029 | - | - |
| SNEAK-7B | Pu | - 0.0251 | -0.0264 | 1.050 | 1.111 |
| ZPR-3-48 | Pu | - 0.0131 | -0.0164 | 1.253 | 1.260 |
| ZPR-3-49 | Pu | - 0.0151 | -0.0145 | 0.960 | 0.992 |
| ZPR-3-50 | Pu | - 0.0142 | -0.0185 | 1.303 | 1.306 |
| ZPR-3-53 | Pu | - 0.0047 | -0.0123 | 2.595 | 2.333 |
| ZPR-6-7 | Pu | - 0.0044 | -0.00519 | 1.174 | 1.202 |
| | | | Average | 1.320 | 1.321 |

...19

Table - 9

Central Reactivity Worth of Nickel

($\%\ \frac{\Delta K}{K}$ per kg)

| Assembly | Fuel | Experimental | Calculated 27-Group | Calculated/Experimental | |
|---|---|---|---|---|---|
| | | | | 27-Group | Hardie et al |
| VERA-1B | U | - | - 0.0225 | - | - |
| ZPR-3-11 | U | - 0.0415 | - 0.0535 | 1.289 | 1.339 |
| ZPR-3-12 | U | - 0.0468 | - 0.0553 | 1.182 | 1.095 |
| ZEBRA-2 | U | - 0.0221 | - 0.0242 | 1.095 | 0.965 |
| ZPR-6-6A | U | - | - 0.0051 | - | - |
| SNEAK-7B | Pu | - | - 0.0434 | - | - |
| ZPR-3-48 | Pu | - 0.0195 | - 0.0290 | 1.486 | 1.403 |
| ZPR-3-49 | Pu | - 0.0222 | - 0.0262 | 1.180 | 1.158 |
| ZPR-3-50 | Pu | - 0.0232 | - 0.0321 | 1.384 | 1.309 |
| ZPR-3-53 | Pu | - 0.0216 | - 0.0330 | 1.528 | 1.381 |
| ZPR-6-7 | Pu | - 0.0067 | - 0.0087 | 1.304 | 1.279 |
| | | | Average | 1.306 | 1.241 |

...20

Table - 10

Central Reactivity Worth of Sodium

($\% \frac{\Delta K}{K}$ per kg)

| Assembly | Fuel | Experimental | Calculated 27-Group | Calculated/Experimental 27-Group | Calculated/Experimental Hardie et al |
|---|---|---|---|---|---|
| VERA-1B | U | 0.6235 | 0.2198 | 0.352 | 0.354 |
| ZPR-3-11 | U | - 0.0303 | - 0.0398 | 1.313 | 1.724 |
| ZEBRA-2 | U | 0.0066 | 0.0152 | 2.312 | - 0.379 |
| ZPR-6-6A | U | 0.00037 | 0.00008 | 0.228 | 0.170 |
| ZPR-3-48 | Pu | - 0.0068 | - 0.0115 | 1.707 | 2.078 |
| ZPR-3-49 | Pu | - 0.0148 | - 0.0019 | 0.126 | 1.078 |
| ZPR-3-50 | Pu | - 0.0121 | + 0.0252 | - 2.083 | 0.344 |
| ZPR-3-53 | Pu | 0.0609 | 0.0477 | 0.783 | 0.436 |
| ZPR-6-7 | Pu | - 0.0070 | - 0.0074 | 1.066 | 1.140 |

...21

Table - 11

Central Fission in $^{238}U$ Normalised to Fissions in $^{235}U$

| Assembly | Experimental | Calculated 27-Group | Calculated/Experimental | |
|---|---|---|---|---|
| | | | 7-Group | Hardie et al |
| VERA-1B | 0.0660 | 0.0846 | 1.282 | 1.190 |
| ZPR-3-11 | 0.0380 | 0.0382 | 1.005 | 0.952 |
| ZPR-3-12 | 0.0470 | 0.0488 | 1.038 | 0.982 |
| ZEBRA-2 | 0.0320 | 0.0328 | 1.024 | 0.971 |
| ZPR-6-6A | 0.0245 | 0.0238 | 0.974 | 0.926 |
| SNEAK-7B | 0.0330 | 0.0310 | 0.939 | 0.902 |
| ZPR-3-48 | 0.0326 | 0.0344 | 1.054 | 0.977 |
| ZPR-3-49 | 0.0345 | 0.0366 | 1.061 | 0.998 |
| ZPR-3-50 | 0.0251 | 0.0299 | 1.193 | 1.091 |
| ZPR-3-53 | 0.0254 | 0.0322 | 1.268 | 1.128 |
| ZPR-6-7 | 0.0230 | 0.0221 | 0.962 | 0.886 |
| | | Average | 1.073 | 1.000 |

...22

Table - 12

Central Fission Rate in $^{239}Pu$ Normalised to $^{235}U$ Fission Rate

| Assembly | Experimental | Calculated 27-Group | Calculated/Experimental | |
|---|---|---|---|---|
| | | | 27-Group | Hardie et al |
| VERA-1B | 1.070 | 1.165 | 1.089 | 1.062 |
| ZPR-3-11 | 1.190 | 1.168 | 0.982 | 0.976 |
| ZPR-3-12 | 1.120 | 1.118 | 0.999 | 0.985 |
| ZEBRA-2 | 0.987 | 1.021 | 1.034 | 0.994 |
| SNEAK-7B | 1.012 | 1.023 | 1.010 | 0.973 |
| ZPR-3-48 | 0.976 | 1.017 | 1.041 | 0.985 |
| ZPR-3-49 | 0.986 | 1.028 | 1.042 | 0.996 |
| ZPR-3-50 | 0.903 | 0.957 | 1.060 | 0.982 |
| ZPR-3-53 | 0.928 | 0.947 | 1.020 | 0.933 |
| ZPR-6-7 | 0.953 | 0.974 | 1.022 | 0.955 |
| | | Average | 1.030 | 0.984 |

...23

Table - 13

Central Fission Rate in $^{240}Pu$ Normalised to $^{235}U$ Fission Rate

| Assembly | Experimental | Calculated 27-Group | Calculated/Experimental 27-Group | Calculated/Experimental Hardie et al |
|---|---|---|---|---|
| VERA-1B | 0.399 | 0.465 | 1.166 | 1.114 |
| ZPR-3-11 | 0.340 | 0.335 | 0.985 | 0.951 |
| ZEBRA-2 | 0.237 | 0.240 | 1.013 | 0.982 |
| ZPR-3-48 | 0.243 | 0.248 | 1.019 | 0.942 |
| ZPR-3-49 | - | 0.265 | - | - |
| ZPR-3-50 | 0.159 | 0.207 | 1.303 | 1.192 |
| ZPR-3-53 | 0.174 | 0.208 | 1.198 | 1.066 |
| | | Average | 1.114 | 1.041 |

...24

Table - 14

Central Capture Rate in $^{238}U$ Normalised to $^{235}U$ Fission Rate

| Assembly | Experimental | Calculated 27-Group | Calculated/Experimental 27-Group | Calculated/Experimental Hardie et al |
|---|---|---|---|---|
| VERA-1B | 0.131 | 0.117 | 0.896 | 0.927 |
| ZPR-3-11 | 0.112 | 0.108 | 0.965 | 0.976 |
| ZPR-3-12 | 0.123 | 0.117 | 0.951 | 0.971 |
| ZEBRA-2 | 0.136 | 0.131 | 0.965 | 0.982 |
| ZPR-6-6A | 0.139 | 0.138 | 0.993 | 1.022 |
| ZPR-3-48 | 0.138 | 0.134 | 0.970 | 0.976 |
| ZPR-3-53 | - | 0.149 | - | - |
| ZPR-6-7 | 0.136 | 0.140 | 1.029 | 1.046 |
| | | Average | 0.967 | 0.986 |

Table - 15

Effective Delayed Neutron Fractions and Generation Time

| Assembly | $\bar{\beta}_{eff}$ (units of $10^{-3}$) | | Generation Time ( $\mu s$ ) | |
|---|---|---|---|---|
| | 27-Group | Hardie et al | 27-Group | Hardie et al |
| VERA-1B | 6.354 | 8.056 | 0.0996 | 0.0988 |
| ZPR-3-11 | 7.321 | 7.451 | 0.0655 | 0.0671 |
| ZPR-3-12 | 7.156 | 7.727 | 0.0955 | 0.0961 |
| ZEBRA-2 | 7.263 | 7.522 | 0.1857 | 0.1856 |
| ZPR-6-6A | 7.247 | 7.317 | 0.4671 | 0.4728 |
| SNEAK-7B | 3.564 | 4.106 | 0.1487 | 0.1551 |
| ZPR-3-48 | 3.261 | 3.588 | 0.2302 | 0.2529 |
| ZPR-3-49 | 3.283 | 3.612 | 0.2130 | 0.2267 |
| ZPR-3-50 | 3.249 | 3.550 | 0.2967 | 0.3340 |
| ZPR-3-53 | 2.592 | 3.175 | 0.3851 | 0.4429 |
| ZPR-6-7 | 3.304 | 3.373 | 0.4297 | 0.4781 |

# REMARKS ON THE VALIDATION OF NUCLEAR DATA SETS THROUGH CRITICALITY PARAMETERS

By

Anil Kumar and M. Srinivasan
Neutron Physics Division
Bhabha Atomic Research Centre
Trombay, Bombay 400 085, India.

## I. INTRODUCTION

It is an established practice to validate the multigroup nuclear data sets of reactor materials by comparing calculated integral parameters such as critical mass, $k_{eff}$, mean neutron life time, reactivity coefficients etc. to their experimentally measured values[1-4]. Of these integral parameters, critical mass ($M_c$) has been chosen more often for comparison. Critical mass ($M_c$) contained in core of a reactor assembly is crucially dependent on a number of geometrical and physical parameters of the system like shape, density, diluent fraction of the core, reflector thickness. It is shown in the subsequent section (Sec.II) that critical surface mass density ($\sigma_c$) which is defined as mass to surface area ratio of the critical core, constitutes to be a better integral parameter in that it is relatively less sensitive to the errors in density, shape description, diluent fraction, reflector thickness etc. Section III describes the dependence of $\sigma_c$ on basic nuclear parameters like infinite multiplication factor $k_\infty^*$, mean absorption probability $\Sigma_a/\Sigma_t$, weighted total mean free path ($\lambda_t$) as derived from Trombay Criticality Formula[5,6].

## II. CRITICAL SURFACE MASS DENSITY $\sigma_c$ AS INTEGRAL PARAMETER

### II. A. Dependence of Critical Surface Mass Density on System Parameters

It is quite convenient to break up critical surface mass density as the product of four factors as follows[5,6]:

$$\sigma_c = g_d \, q \, \sigma_{spc}^{b} \, Y \qquad \ldots\ldots (1)$$

where $g_d$ is dilution correction factor and is given by $g_d = F^{\frac{2-p}{3}}$; F is volume fraction of the fissile component of the core-fuel and p is diluent exponent[7]; $g_d \leq 1$. $q$, shape correction factor, is defined as the ratio of surface mass density of a bare critical core under consideration to that of the 'corresponding' (having same core composition) bare spherical critical core; $q \sim 1$. $\sigma_{spc}^{b}$ is surface mass density of the critical bare spherical core with the same core composition as that of under consideration; $\sigma_{spc}^{b}$ is specified in Kg fissile material per $m^2$. $Y$, degree of reflection parameter, is defined as the ratio of surface mass density of critical reflected core to that of the 'corresponding' critical bare core; $Y \leq 1$; for good reflectors like $^{9}Be$ and $^{12}C$ Y can be as low as $10^{-4}$ in 'infinite' slab geometry configuration.

The highlight of relation (1) is the separation of the effect of geometrical and physical system parameters on $\sigma_c$ into broadly two categories: (i) spectrum-dominated component $g_d$, and (ii) leakage-dominated components $q, \sigma_{spc}^{b}$ and Y.

Table I shows $\sigma_{spc}^{b}$, $g_d$ and Y values for bare cores of some elementary hard fast and thermal assemblies. It is to be noted that $\sigma_{spc}^{b}$ is independent of core density unlike 'corresponding' bare critical mass which varies inversely as the square of the core density for bounded systems. We can write down the effect of likely errors in $g_d, q, \sigma_{spc}^{b}$ and Y on $\sigma_c$ by:

$$\delta\sigma_c \equiv \frac{\Delta\sigma_c}{\sigma_c} = \frac{\Delta g_d}{g_d} + \frac{\Delta q}{q} + \frac{\Delta \sigma_{spc}^{b}}{\sigma_{spc}^{b}} + \frac{\Delta Y}{Y} \qquad \ldots\ldots (2)$$

112

It is to be pointed out here that out of the four error components in the right hand side of Eq.(2) that (i) $\frac{\Delta \rho_{cd}}{\rho_{cd}}$ = 0 except for error in diluent fraction, (ii) $\frac{\Delta \rho_c}{\rho_c}$ = 0 except for wrong description of shape, (iii) $\frac{\Delta Y}{Y}$ = 0 except for error in core (reflector) density and shape-description.

II. B. Critical Mass $M_c$ Versus Critical Surface Mass Density $\sigma_c$

Critical mass $M_c$ is related to $\sigma_c$ for spherical assemblies by the following relation:

$$M_c = \frac{36\pi\sigma_c^3}{\rho_{core}^2} \qquad \ldots\ldots\ldots (3)$$

where $\rho_{core}$ is core density. It can be seen from Eq.(3) that a small change in $\sigma_c$, say $\Delta\sigma_c$, amounts to the following change in $M_c$, say $\Delta M_c$, as given by

$$\delta M_c \equiv \frac{\Delta M_c}{M_c} = 3\frac{\Delta\sigma_c}{\sigma_c} - 2\frac{\Delta\rho_{core}}{\rho_{core}} \qquad \ldots\ldots (4)$$

It is obvious from Eq.(3) that limiting relative error on $M_c$ is at least equal to three times the limiting relative error on $\sigma_c$. The same is true of other geometries as well.

III. RELATIONSHIP BETWEEN CRITICAL SURFACE DENSITY $\sigma_c$ AND BASIC NUCLEAR PARAMETERS FROM TROMBAY CRITICALITY FORMULA (TCF)

Trombay Criticality Formula (TCF) consists in expressing $k_{eff}$, the effective multiplication factor, through net leakage probability ($p_L$), that is derived from 'Modified Wigner Rational (MWR)' form of collision escape probability, as follows[5,6]:

$$k_{eff} = k_\infty^* (1-p_L) \qquad \ldots\ldots (5)$$

$$\text{where } p_L = \frac{1}{1 + 4\cdot\frac{\Sigma_a/\Sigma_t}{1-\beta}\frac{\sigma}{\rho_{core}\lambda_t}\left(\xi_1 + 4\xi_2\sigma/\rho_{core}\lambda_t\right)} \qquad \ldots\ldots (6)$$

Here $\beta$ is reflector albedo. $\xi_1$ and $\xi_2$ are purely geometrical parameters. For example, for cube, $\xi_1$ = 0.699 and $\xi_2$ = 0.193. $k_\infty^*$ is akin to $k_\infty$ and is defined for the spectrum close to critical. The normalisation of $k_{eff}$ of Eq.(5) to Critical, namely,

at $\sigma = \sigma_c$ , $k_{eff} = 1$ ..... (7)

leads to the following relation between $\sigma_c$ and $k_\infty^*$ , $\Sigma_a/\Sigma_t$ , $\lambda_t$

$$\left(\Sigma_1 + 4\Sigma_2 \frac{\sigma_c}{\rho_{core}\lambda_t}\right)\frac{4\sigma_c}{\rho_{core}\lambda_t} = \frac{1-\beta}{(k_\infty^*-1)\Sigma_a/\Sigma_t} \quad \ldots(8)$$

For bare small cores, such that $4\Sigma_2\sigma_c/(\Sigma_1\rho_{core}\lambda_t) \ll 1$, Eq.(8) can be used to get the following relation between the relative error on $\sigma_c$ and the relative errors on $k_\infty^*$ , $\rho_{core}$ , $\lambda_t$ and $\Sigma_a/\Sigma_t$ :

$$\delta\sigma_c \equiv \frac{\Delta\sigma_c}{\sigma_c} = -\frac{\delta k_\infty^*}{(1-\frac{1}{k_\infty^*})} - \delta(\Sigma_c/\Sigma_t) + \delta(\rho_{core}\lambda_t) \quad \ldots(9a)$$

As $\rho_{core}\lambda_t$ is proportional to $\sigma_t$, the weighted total microscopic cross section in the core, Eq. (9a) can be rewritten as:

$$\delta\sigma_c = -\frac{\delta k_\infty^*}{(1-\frac{1}{k_\infty^*})} - \delta(\Sigma_a/\Sigma_t) + \delta\sigma_t \quad \ldots(9b)$$

Relation (9b) can be helpful for adjusting microscopic nuclear data like $\nu;\sigma_f/\sigma_a$ , $\sigma_a/\sigma_t$ , $\sigma_t$ etc. so as to predict correct surface mass density $\sigma_c$

## IV. CONCLUSION

Critical Surface Mass density $\sigma_c$ is a more dependable integral parameter than critical mass for validating the multigroup nuclear data sets as it is less sensitive to discrepancies (errors) in various geometrical and physical parameters of the system. For example, for bare critical cores $\sigma_c$ is independent of core density whereas $M_c$ varies inversely as the square of the core density. Trombay Criticality Formula (TCF) leads to a useful relation, between $\sigma_c$ and basic nuclear parameters like $k_\infty^*$, $\Sigma_a/\Sigma_t$, $\sigma_t$ , that can be of help in adjusting the multigroup nuclear data sets to make them compatible with the experimental measurements of $\sigma_c$ (or $M_c$).

References

1. G. Cecchim and A. Gandini, "Comparison between Experimental and Theoretical Data on Fast Critical Facilities", ANL - 7320 (1966).

2. H. Reif and H. Kschwendt, Nucl. Sci. Eng., 30, 395 (1967).

3. BNL - 19302: Cross Section Evaluation Working Group Benchmark Specification (1974).

4. R.W. Hardie et. al., Nucl. Sci. Eng., 57, 222 (1975).

5. Anil Kumar, "Studies on the Systematics of Neutron Multiplication and Leakage in Small Reactor Assemblies", Ph. D. Thesis, University of Bombay (1980).

6. Anil Kumar, M. Srinivasan and K. Subba Rao, "Trombay Criticality Formula for the Characterization of Neutron Leakage Variations from Small Reactor Assemblies", Part 1: Basis, and Part 2: Application, submitted to Nuclear Science and Engineering (1981).

7. W.R. Stratton, "Criticality Data and Factors Affecting Criticality of Single Homogeneous Units", LA-3612 (1967).

TABLE - I

Critical Surface Mass Density ( $\sigma_{spc}^{b}$ ), $g_d$, $k_\infty^*$ and Y for some Elementary Assemblies[+].

| Core material | Diluent | $\sigma_{spc}^{b}$ (Kg/m$^2$) | $g_d$ | $^9$Be Reflector(0.6 m) | | $H_2O$ Reflector(0.2 m) | |
|---|---|---|---|---|---|---|---|
| | | | | $k_\infty^*$ | Y | $k_\infty^*$ | Y |
| $^{239}$Pu | - | 321.63 | 1 | 2.573 | 0.572 | 2.621 | 0.778 |
| $^{239}$PuC | C | 296.26 | 0.921 | 2.528 | 0.564 | 2.560 | 0.778 |
| $^{239}$PuO2 | O | 273.86 | 0.851 | 2.473 | 0.545 | 2.541 | 0.771 |
| $^{235}$U | - | 521.24 | 1 | 2.152 | 0.530 | 2.193 | 0.764 |
| $^{235}$UN | N | 482.11 | 0.925 | 2.062 | 0.491 | 2.085 | 0.752 |
| $^{233}$U | - | 357.98 | 1 | 2.402 | 0.570 | 2.433 | 0.778 |
| $^{233}$UO2 | O | 295.20 | 0.825 | 2.329 | 0.496 | 2.373 | 0.742 |
| $^{233}$U-$H_2O$ ($H/^{233}U$ = 300) | - | 4.362 | 1 | 1.939 | 0.526 | 1.938 | 0.779 |
| $^{233}$U-$H_2O$ ($H/^{233}U$ = 500) | - | 2.949 | 1 | 1.782 | 0.554 | 1.781 | 0.807 |

+ The results presented in the table have been computed using one-dimensional transport theory code DTF-IV with angular quadrature of $S_4$ and 16 group Hansen-Roach cross section sets.

# Analysis of Selected Fast Zero Power Assemblies and Calculational Benchmarks

M.L.Sharma, M.M.Ramanadhan, V.Gopalakrishnan, S.Ganesan, R.Venkatesan and R.Shankar Singh

## 1. Introduction

'In the present state of reactor design, theorists are resigned to the need for supplementing their calculations with experimental information'. This introductory remark has been taken from the review of Kaplan[1] dealing with measurements of reactor parameters in subcritical and critical assemblies, mainly for thermal neutrons. The requirement for supplementary experimental information, stated in 1964 for thermal reactors, may have been met to a large extent in the past, but now the situation for fast reactors is similar to that encountered in 1964 for thermal reactors[2].

We had earlier analysed a set of benchmarks, as these assemblies are usually called, the data for which was available in the open literature. They were chosen on the basis of system simplicity, extent of experiments carried out, an adjudged precision of experimental results, and covering a wide spectrum range. However, most of the assemblies analysed were of comparatively smaller size.

As the reactor size is increased the spectrum becomes softer and the uncertainties in the prediction of integral parameters may not remain same. This conclusion was also brought out by a recent international comparison calculation[3] of a large sodium cooled fast breeder reactor. It was pointed out by Le Sage et al. that 'participants whose solutions disagree on the 1250 Mwe size comparison calculation have each obtained good agreement on 300 Mwe size critical experiments'.

In order to assess our predictional capability of integral parameters for large LMFBRs (Liquid Metal Fast Breeder Reactors) we have analyzed four fast zero power critical assemblies and two LMFBRs benchmark models for data testing.

## 2. Data Testing

The term data testing denotes an activity of comparison of important integral parameters, such as Keff, spectral indices, central

reactivity worths etc. measured in reactor environment with calculated values using the reference multigroupcross section library. To demonstrate how well the reference data set together with the processing codes and computational methods predicts the important reactor parameters, one usually considers the correlation of calculated quantities against measured values. Although results of such a testing program will seldom demonstrate an exacting relation between specific microscopic data and integral values, a systematic selection of test cases can show which material data consistently give poor correlation of computed and measured integral values. Analysis of such correlations can identify nuclides in need of reevaluation perhaps with some indications of reaction type and energy range(4). Thus testing plays a vital role in the validation of cross section libraries.

## 3. Description of Benchmarks

The assemblies discussed below were chosen such that they provided diagnostic information on the suitability of our cross section library in the design of reactors with softer spectra.

### 3.1 ZPR-6- Assembly 7

Assembly 7 is a large (3100 liter) fast critical assembly with a soft spectrum and other characteristics representative of current LMFBR designs. It has a single fuel zone with a length to diameter (L/D) ratio of approximately unity; it has a simple one draw unit cell; and it is blanketed both axially and radially with depleted uranium. The assembly's spectral characteristics, simple geometric configuration and simple unit cell make it well suited for a benchmark assembly. The fuel used is Pu/U/Mo (28 W/o plutonium, 69.5 W/o Uranium and 2.5W/o molybdenum). The plutonium is 11.5 W/o $^{240}$Pu. A one dimensional model with spherical geometry has been used in the analysis of the measurements made in the assembly. The benchmark specifications of the spherical model and the corresponding atom densities have been taken from Cross Section Evaluation Working Group (CSEWG) Benchmark Specifications(5)

3.2 FBR Assembly 5 Phase A

This assembly formed a part of the series of experiments performed in phase 1 of the CRBR Engineering Mockup Critical Program (EMC) to provide data base against which reactivity prediction techniques used in accident analysis could be evaluated.

The FBR-5 program was broken into two phases, A & B to simulate an initial core at end-of-cycle and beginning-of-cycle, respectively. The phase A configuration simulates the Clinch River Reactor at the end of the first cycle. Control rods are withdrawn from the core and parked in the upper axial blanket. Assembly 5 phase A configuration contains 19 sodium filled control rod positions and required 100 fuel spikes in the core toestablish criticality. The measured excess reactivity was $(1.24 \pm 0.01) \times 10^{-3}$ $\Delta K/K$. It has a core volume of about 2500 litres fuelled with $PuO_2$- $UO_2$.

Two dimensional R-Z model has been used in the analysis of the measurements made in the assembly. The specifications of this cylindrical model and the corresponding atom densities have been taken from Ref.(6,7).

3.3 SNEAK 9C-2/C and 9C-2/PCL

There is a possibility of using mixed carbide fuel in the FBTR in India so we wanted to assess the effect of such a fuel on the uncertainties in the prediction of different integral parameters. As there are only a few critical experiments with mixed carbide fuel in the open literature for the sizes of interest we selected an assembly from the SNEAK-9 series mentioned below.

The SNEAK (Schnelle Null Energie Anlage Karlsruhe, meaning zero power reactor at Karlsruhe) 9 series of critical experiments was basically designed to improve the prediction of neutronic, engineering and safety parameters for the German Be ne lux fast breeder prototype SNR-300[8]

To study the influence of higher plutonium isotopes on the prediction of fast breeder core parameters, validity of the sector substitution method etc. geometrically simple critical configurations

were designed. The reference core, SNEAK 9C-2 was a one zone $PuO_2$-$UO_2$ sodium assembly. It was built by a 360° sector substitution out of one zone uranium core, SNEAK 9C-1, that had approximately the same geometrical and neutronic characteristics.

One of the three different central zones with 'dirty' plutonium (plutonium with about 20% of $^{240}Pu$ in its isotopic vector) substituted in to the reference core 9C-2 was a 'C-zone' of 80 liter zone with ZEBRA plutonium enabled the construction of a zone simulating a carbide fuel reactor environment. The substitution assembly was called SNEAK 9C-2/C.

A second central zone called 'PUZ-zone' was also substituted in the reference core 9C-2. This zone of 90 ltr. size contained dirty plutonium metal of ZEBRA stock, combined with $Fe_2O_3$ to simulate oxide fuel. This assembly was called SNEAK 9C-2/PUZ. Reactor dimensions and atom densities for the RZ model were taken from Ref.(9).

3.4 Baker model

This is a calculational model for a 'standard' reactor in one dimension which was developed at the suggestion of the LMFBR for comparing calculations of parameters determining the criticality and conversion ratio[10]. The publication of this comparison in 1971 served as a stimulus to international co-operation in the field of fast reactor physics. We have analysed only one of the three variants in which the fuel in the core consists of only $^{239}Pu$ and $^{238}U$. In 1975 the Institute of Physics and Power Engineering at Obninsk, USSR, approached a number of laboratories with the proposal that these calculations be repeated, using the specifications proposed in Ref.(11). The composition and dimensions of the model, for our analysis, have been taken from the same reference.

3.5 NEACRP/LMBR Benchmark

The purpose of the International comparison calculation of this benchmark was to focus on the variation in parameter values, the degree of consistency among the various parameters and solutions, and the

identification of unexpected results[3].

This international comparison exercise was the first one since the so called 'Baker Model' comparison of 1970 which focussed on breeding and neutron balance. It also was the first comparison for a large 'commercial sized' LMFBR system, the first comprehensive comparison between the current adjusted data sets (eg. ENDF/B-IV, UKNDL5 and CARNAVAL-III & IV) and the unadjusted sets (e.g. ENDF/B-IV) and has been the most comprehensive of such comparisons including a number of parameters not included in previous comparisons (e.g. control rods and certain safety parameters). The benchmark reactor specification was based on a 3260 MWt conventional mixed oxide design with a 0.300 inch pin size developed at ANL in 1975. It may be noted that the reactor design model for these benchmark calculations has significantly lower enrichments ( ~ 10% and 13% fissile Pu in the two core zones) than present commercial conventional core designs (~14% and 18% for SNR-300 MOX I) which are based on smaller fuel pins and lower fuel pin inventories and fuel volume fractions. Integral experiments in a higher enrichment range (from 12% to 30%) have been used to create and validate the current adjusted libraries. In this respect, integral experiments corresponding to this lower enrichment range ( < 12%) could provide useful complementary information. The benchmark model was set up for R, Z modelling with specified homogeneous compositions[3] for each region of the reactor. The core height was 40 inches (101.6 cm) and the radii of the inner and outer core regions were 136.85 cm and 176.53 cm, respectively. The core volume fractions were 41% for fuel, 38% for total sodium and 21% for total structural.

## 4. Multigroup Cross Section Preparation and Calculation Procedure

In the present analysis we have adopted the shielding factor approach primarily due to its speed and ease of application. This method suffers however from one disability; the cross section integration for a particular isotope does not reflect the energy dependence of the other cross sections in the mixture[12].

The computer code ETOXS (SETH-512[13]) was used to generate homogeneous and composition dependent cross sections for core and

blanket regions. This code takes Cadarche Cross Section Library (Version II) as input and generates cross sections in 25 groups taking account of the resonance self shielding of heavy elements approximately and wide scattering resonances of the light materials. This energy group structure has sufficient detail at low energies to afford accurate computations of material worths and Doppler effect.

The cross section processing code MeChaOm[14] has been used for heterogeneously shielded cross sections. This code has two parts. In the first part the heterogeneously shielded cross sections are calculated for the lattice employing Tone's method[15], in which background cross section, used in self shielding factor method, is modified using collision probability equation, for each isotope and region of the lattice cell. A subsequent calculation based on the self shielding factor method will give heterogeneously shielded cross sections for all the isotopes present in the lattice cell.

In the second part of MeChaOm, using the cross sections prepared by the first part, cell eigenvalue calculation is performed to obtain the flux distribution for spatial homogenization of cross sections for the lattice. Same flux distribution is also used for computing the anisotropic diffusion coefficients using the Benoist[16] method. The directional collision probabilities are calculated using periodic boundary condition for plate lattices for use in the Benoist formula. The calculation for the cylindrical cells is based on the recent formulation of Benoist[17].

Using these cross sections in the 1D - diffusion-cum-perturbation theory code MIDI[18, 19] eigenvalues and fluxes etc. were calculated for the spherical models of critical assembly ZPR-6-7. Both homogeneous and heterogeneous cross sections were generated and used. The spherical model is expected to introduce approximately a 0.1% uncertainty in keff according to the CSEWG benchmark specifications.

Baker model calculations were also performed using 1D-diffusion code MIDI. The cell averaged cross sections and anisotropic diffusion

coefficients were used in conjunction with 2 D diffusion theory code ARCLIMI[20,21] ( - option) for the cylindrical model of ZPR-5. However for SNEAK 9C-2/C, although we used the same 2D code but we employed only the homogeneous cross sections. Same is the case with SNEAK 9C-2/ZOL assembly.

Some of the important features of the assemblies analyzed are presented in Table 1. Generally 1 and 2 cm meshes have been used in the core and blanket regions. The exact number of mesh points used for the different assemblies are given in Table 2. For the spherical models used there is a blank for the meshes in the Z direction.

Some isotopes like sulphur and phosphorus were neglected or merged with other isotopes to make up for the non availability of multigroup data. Also C concentrations were added into those of copper to obtain the comparison with KfK values. Mg was simulated with O and Ti with Cr after checking their group cross sections from ABBN set[22].

## 5. Results of Benchmark Calculations

The values of calculated $k_{effs}$ for the six benchmarks analysed are summarized in Table 3. Comparison of calculated and experimental values of reaction rate ratios at the core centre for SNEAK 9C-2/C assembly is presented in Table 4.

## 6. Evaluation of calculated Results

### 6.1 Analysis of Multiplication Constants

The earlier diffusion calculations[23] and the present results given in Table 3 show that the cross sections and computing methods used here are satisfactory in computing $k_{eff}$ for core sizes upto 3500 litres having normal $PuO_2 - UO_2$ fuel and the maximum uncertainty is about 1%. The mean value of $k_{effs}$ calculated by us 1.004. Since there is a large scatter in $k_{effs}$ a simple change in [illegible] of $^{239}Pu$ would not remove the discrepancy.

For high $^{240}Pu$ core SNEAK 9C-2/POZ the discrepancy is about 2%. This may atleast partially originate in cross sections of $^{240}Pu$ and higher plutonium isotopes. This gives an indication for the need to update the higher plutonium isotopes cross sections in our library. This observation, however, does not square withalmost negligible (<.2%) discrepancy in the $k_{eff}$ for SNEAK 9C-2/C assembly which also contains the 'dirty' plutonium. The reason for this contradiction is not known yet.

As regards the larger discrepancy in the $k_{eff}$ for LEACRP benchmark it may be attributed to the cross sections of structural materials because the main characteristics of this assembly are higher structural fraction and a very large core of about 10,000 litres. It is also possible that our adjusted set needs uplating for the cross sections in the lower energy region. There is a clear need for further analysis to obtain the definitive conclusions.

6.2 Analysis of the Central Reaction Rate Ratios in SNEAK 9C-2/C

Results in Table 4 show that the reaction rate ratios are unden-predicted in general. This observation holds for the corresponding Kfk values also.

The averaged fission cross sections ratio of $^{238}U$ relative to $^{235}U$ gives valuable information concerning the fraction of the total neutron flux having energy greater than the $^{238}U$ threshold. The discrepancy of 14% in this ratio suggests that part of the discrepancy may be caused by incorrectly calculated spectra.

As all the ratios are underpredicted we may doubt the $^{235}U$ fission cross sections which might give better results if decreased. The ratio of the capture rate in $^{238}U$ to the fission rate in $^{235}U$ suggests that capture cross sections of $^{238}U$ if increased may give better results but this may lead to more discrepancy in the $k_{eff}$ calculations. The ratio $\sigma_{c}^{9}/\sigma_{f}^{5}$ is underpredicted by 10%.

The ratio of $\sigma_f^{9}/\sigma_f^{5}$ is underpredicted by 6% which may indicate for increase in fission cross sections of $^{239}Pu$. This in conjunction with increased capture of $^{238}U$ may still keep the $k_{eff}$ in balance. Here also there is a need for further calculations for different assemblies in order to get the perspective.

## 7. Conclusions

Our results are in reasonable agreement, for $k_{eff}$ calculations, with the results obtained by independent data and code system by the French, German and U.S. teams, except for high $^{240}Pu$ cores where the discrepancies upto about 2% are noticed. The discrepancy in reaction rate ratios upto 15% is observed with our cross section library[27].

The present study has highlighted the need for further analysis in more detail including reaction rate ratios, central reactivity worths in all the critical assemblies studied for which these data are available.

References

1. I.Kaplan, Measurements of reactor parameters in subcritical and critical assemblies, Advan. Nucl. Sci. Technol. 2, 139 (1964).

2. Edgar Kiefhaber, Evaluation of integral physics experiments in fast and power facilities, Advan. Nucl. Sci. Technol. 9, 47 (1975).

3. L.C.Le Sage et al., Proceedings of the NEACRP/IAEA specialists meeting on the International Comparison Calculation of a Large Sodium Cooled Fast Breeder Reactor at Argonne National Laboratory, ANL-80-78 (NEA-CRP-L-243), Feb. 1978.

4. H.Alter, ENDF/B-2: Is it adequate for the Design and Evaluation Needs of the LMFBR Program? React. Technol., 15, 59 (1972).

5. Cross Section Evaluation Working Group Benchmark Specifications, BNL-19302 (ENDF-202) Nov. 1974.

6. C.L.Beck et al., Contributions to various ANL-RDF Reports, Argonne National Laboratory (1974-1976)

7. Liquid Metal Fast Breeder Programme, Critical Experiments and Analysis, April-June 1976, UKAEA-13771-19 (1976) p.A-29.

8. F.Helm (Compiler), Summary of results for the SNEAK-9 series of critical experiments and conclusions for the accuracy of predicted physics parameters of the SNR-300, KfK-2586, Aug. 1978.

9. W.Scholtyssek (compiler), Physics Investigations of Sodium Cooled Fast Reactors: SNEAK-Assembly 9C, KfK-2361, Apr. 1977.

10. A.I.Voropaev et al., Comparison of calculations of standard fast reactors (using the Baker model), INDC(CCP)-125/LV, Oct. 1978.

11. A.R.Baker, J.D.Harmon, Calculations for a large fast reactor, Risley, TAEA Report 2133 (d), 1971.

12. R.B.Kidman et al., Nucl. Sci. Engg, 48, 189 (1972).

13. J.Daniens and J.Lenvier, Programme SETH-512-Exploitation des Constants Multi-groupes SETH Cadarache, Report DRP/SETH No.67/746, Dec. 1967.

14. J.V.Mathews et al., MuCHidra - A Computer code for cross section processing of heterogeneous lattices, Internal Note No.RNG/RN-203, Mar. 1980.

15. T.Tone, J. Nucl. Sci. & Technol. 12, 467 (1975).

16. P.Benoist, Nucl. Sci. Engg. 32, 201 (1968).

17. J.Benoist, Trans. Am. Nucl. Soc. 33, 773 (1979).

18. T.M.John, MIDE - A one dimensional diffusion theory neutronics code Internal Note No.PRG/01100/RP-60, Jan. 1975.

19. Claude Bore et al., Resolution de l'equation multigroupe de la diffusion dans geometrie a dimension et calculs annexes: MIDE, Rapport CEA-R-2923, Dec. 1965.

20. S.M.Lee, Specifications for the code ALCIALMI, Internal Note No.FBTR/01100/70/N7, Feb. 1970.

21. J.P.Bayard et al., Specification d'un code de diffusion multigroupe à deux dimensions: ALCI, CEA Report R-2747, Feb. 1965.

22. L.P.Abagyan et al., Group Constants for calculating atomic reactors, Moscow, Atomizdat (1964).

23. M.L.Sharma et al., Analysis of Selected fast critical assemblies, RRC-23, Nov. 1978.

24. I.Y.Barre et al, Proc. of Conf. Nucl. Cross sections and Technology, Washington, NBS, 1, 51 (1975).

25. C.L.Beck et al., ZPPR Assembly-5 Calculational Models, ANL-RDP-41, (1976).

26. R.W.Hardie et al, An analysis of selected fast critical assemblies using ENDF/B-IV neutron cross sections, Nucl. Sci. Eng. 57, 222 (1975).

27. J.Y.Barre et al , Lessons drawn from integral experiments on a set of multigroup cross sections, Paper 1.15, Int. Conf. The Physics of Fast Reactor Operation and Design, BNES, London (1969).

Page no. 12 is missing in the Original Document.....

Table 1

Critical Assembly Characteristics

| Assembly | Fissile fuel | Fertile to Fissile ratio | Approximate core volume (litres) | Comments |
|---|---|---|---|---|
| SNEAK 9C-2/C | Pu | 3.78 | 240 | For simulating carbide fuel |
| SNEAK 9C-2/PUZ | Pu | 3.29 | 270 | High Pu 240 (20%) |
| BARER model | Pu | 6.53 | 2500 | Zero structural fraction |
| ZPER-5a | Pu | 6.52 | 2500 | CRER EMC Program |
| ZER-6-7 | Pu | 6.5 | 3100 | L/D ~ 0.9 |
| LAEA/NEACRP | Pu | 8.74 | 9943 | High structural fraction |

Table 2

Mesh Detail for Diffusion Theory Calculations

| Assembly | No. of Mesh Points in the R x Z direction |
|---|---|
| SNEAK 9C-2/C | 52 x 45 |
| SNEAK 9C-2/PUZ | 50 x 45 |
| BARER model | 100 x - |
| ZPER-5a | 36 x 54 |
| ZER-6-7 | 96 x - |
| LAEA/NEACRP | 25 x 58 |

Table 3

Comparison of Calculated Values of $k_{eff}$ of Critical Assemblies

| Assembly | Model of calculation | $k_{eff}$ | Source |
|---|---|---|---|
| SNEAK 9C-2/C | 2D-Diffusion | 1.0039 | Present Calculations |
| | | 1.001 | Measured Value |
| SNEAK 9C-2/PCZ | 2D-Diffusion | 0.9877 | Present Calculations |
| | | 1.0051 | Karlsruhe set (Ref.9) |
| BAKER model | 1D- Diffusion | 0.9994 | Present Calculations |
| | | 0.9992 | CARNAVAL IV (Ref.24) |
| ZPR-5A | 2D-Diffusion | 0.9968 | Present Calculations |
| | | 0.9876 | ENDF/B-IV (Ref.25) |
| ZPR-6-7 | 1D-Diffusion | 0.9979 | Present Calculations |
| | | 0.9917 | ENDF/B-IV (Ref.26) |
| IAEA/NEACRP | 2D-Diffusion | 1.03216 | Present Calculations |
| | | 1.0212 | French set (Ref.3) |
| | | 1.0223 | U.K. Set (Ref.3) |

Table 4

Comparison of Calculated and Experimental Values of Reaction Rate Ratios at the Core Centre for SNEAK 9C-2/C Assembly

| Cross Section Ratio at the Core Centre | Experiment | C/E Present calculations | C/E KfK calculations Ref.(9) |
|---|---|---|---|
| $\sigma_{f8}/\sigma_{f5}$ | 0.04445 | 0.8648 | 0.9372 (0.9154)* |
| $\sigma_{f9}/\sigma_{f5}$ | 1.114 | 0.9433 | 0.9472 (0.9592)* |
| $\sigma_{c8}/\sigma_{f5}$ | 0.1333 | 0.9073 | 0.9715 (0.9640)* |

* In brackets are values from KfK cell calculations

# Shielding Benchmark experiments and analyses

R.Indira, A.K.Jena, K.P.N.Murthy, R.Shankar Singh and R.Vaidyanathan

## Introduction

We present in this paper, our analyses of four shielding benchmark experiments. The analyses have been done with the computational techniques and cross section data available with us.

The benchmark experiments studied are relevant to fast reactor shield studies. The first benchmark studied is that of fusion source neutron transport through graphite. The measurements and our computations with one dimensional transport code are presented in section 1.

The second benchmark studied is the fast neutron transport through sodium. The experimental set-up and computations using monte Carlo code are presented in section 2.

Section 3 details the experiments and our computations for neutron transport through iron shields. Experimental details and computation using albedo monte Carlo method, for neutrons streaming through multilayered ducts are presented in section 4.

## 1.0 Neutron transport through graphite.

Neutron transport through a 80 cm sphere of graphite, with a central sphere of 4.45 cm radius, having an external neutron source originating from bombardment of depleted uranium by fast electrons, constitutes the benchmark problem. The neutron spectrum was measured at 20.3 and 35.6 cm. In addition to measurements, earlier calculations using moments method, monte Carlo (ORR ) and $S_n$ method were available[1].

Calculations were made by us using DTF-IV and DLC-2 cross section with $P_3$ - expansion for scattering cross section. To ascertain numerical

accuracy, $S_{16}$ calculations and $S_8$ calculation with 1 cm and 2 cm spatial mesh widths were made.

As the measurements are not in a readily comparable form, comparison is made with ORR calculations, which agree well with measurements. The ORR calculated spectrum and the spectrum calculated by us are presented in Table 1. The agreement is generally good, except in the region of 10 to 14 MeV, which could be attributed to discrepancy in cross section data.

## 2.0 Neutron transport through bulk sodium

This experiment was carried out at the tower shielding facility of ORNL, with the the collimated neutron beam from the reactor, asthe source. The incident neutron spectrum peaks in the energy range 2 to 3 MeV. The beam is incident normally on the flat circular face of an cylinder of eleven feet diameter, containing solid sodium, surrounded by a concrete collar. The measurements were made using Bonnerball detectors, which are spherical $BF_3$ proportional counters surrounded by polyethylene with an outer shell of Cd. The bonnerballs have responses peaking in different energy regions andhence provide good spectral indices of the transmitted neutrons.Ref.2 gives details of the experimental set up, measurements, Bonnerball detector responses and uncertainties in the measurements.

The benchmark experiment was simulated by a Monte Carlo code developed for this purpose variance reduction devices such as Russian Roullet, weighting by non-absorption probability wereused. The inter collission distance was sampled from a biassed exponential density function. Next event estimator was used for scoring the transmission at detector points. DLC-2 hundred group crosssections with $P_8$ - legendre expansion for scattering cross section, was used. Sampling of the scattering angle was done using the equiprobability group method. Transmissions through 2.5 feet thick sodium and 10 ft. thick sodium were simulated. Count rates for eight bonnerball detectors were obtained. Details of the simulation and extensive results are given in Ref.3

The Bonnerball count rates at the detector point 24" behind ten feet sodium, on centerline are given in Table 2. The measured count rates and the count rates obtained by others with calculation by MORSE and DOT are also presented for comparison. It is found that the deviation of the simulated count rates from the measurements are well within the quoted uncertainties of ± 40% in the measured values.

## 3.0 Neutron transport through iron shields

This benchmark experiment was performed in the vertical experimental column of the fast neutron source reactor YAYOI[4]. A 70 cm thick, 94 $cm^2$ iron shield was used. The shield was placed on the outer lead reflector and was surrounded by heavy concrete wall of the vertical column. The neutron and gamma distribution in the shield were measured using threshold activation detectors In, Ni, Al, Mn, Fe and Zn, sandwiched resonance foils Au, W, and Co and TLDs.

The analysis of the experiments were performed using one and two dimensional discrete ordinate transport code ANISN and TWOTRAN. The ANISN (100 + 20) energy group structure was used, in the 1-D calculation with $P_5$ approximation for the scattering cross section.

Our analysis was done with DLC-37 100 group cross section library and DTF code. The one-dimensional calculations model used is shown in table 3. 60 cm buckling was used throughout the calculations. Reaction rates measured and calculated at the inner surface the shield are given in Table 4. The measured and calculated reaction rates for $In^{115}(n,n')$ and $Au^{197}(n,\gamma)$ reactions in the iron shield are presented in Table 5.

It is seen from table 5 that In reaction rates are predicted better than that of Au. This may be due to the fact that while the fluxes are predicted well in the fast region, the thermal neutrons have a scattered contribution that deviates from the contribution given by the buckling. So two dimensional calculations are expected to predict these reaction rates better.

4.0 Thermal neutron streaming through multilegged ducts

The experiment consists of measurement of streaming neutron flux, in a straight, two-legged and three-legged square concrete duct. The neutron source was the collimated reactor neutron beam from the Dhruva tower shielding facility. The details of the experimental set-up and the measurements are given in Ref.5.

The neutron streaming through square concrete ducts was simulated by us using albedo Monte Carlo method. The thermal neutron suffer reflection at the duct walls, with the laws of reflection given by the differential albedo data[6] for the thermal neutrons. Rejection technique was used in sampling the reflected neutron direction. Variance reduction devices such as Russian Roullet, Splitting, and forward biassed density function for the reflected polar were employed. Details of the Monte Carlo code and the simulation can be found in Ref.7.

The streaming neutron fluxes were computed at various points along the duct centerline in the case of straight, two legged and three legged ducts. The simulated neutron fluxes are compared with the measured fluxes in Table 6. Comparison is found to be good in general. Calculations are found to underpredict the fluxes at dose points close to the exit of the duct. The higher flux in the case of measurements could be due to the neutrons entering from the exit face of the duct.

5.0 Conclusions

The benchmark experiments on neutron transport through sodium, iron and graphite and neutron streaming through concrete ducts have been analysed. In the case of transport through sodium, the comparison is found to be generally good, thus validating the variance reduction schemes employed in the Monte Carlo code and the cross section data. In the case of transport through graphite, the comparison is good, in the energy region below 1 MeV, which is the region of interest to us. In the case of neutron transport through steel, the discrepancies found have been attributed to choice of buckling and hence two-dimensional calculations are recommended. The albedo Monte Carlo method and the albedo data have been found to be sufficiently good in estimating the streaming thermal neutron fluxes.

References

1. A.E. Profio (Ed), 'Shielding benchmark problems', ORNL-RSIC-25 (1969).

2. R.L. Maerker, F.J. Muckenthaler et al. 'Final Report on a benchmark experiment for neutron transport in thick sodium', ORNL-4880 (1974).

3. Indira R. and K.P.N. Murthy, 'Monte Carlo Simulation of the Benchmark in neutron transport in thick sodium', MRC-48 (1981).

4. Yoshaki Oka, Shio et al. Two dimensional shielding benchmark for Iron at YAYOI, UTNL-R-0032 (1976).

5. R.L. Maerker and F.J. Muckenthaler, Nucl. Sci. and Engg. 29 (1967) 444.

6. R-L. Maerker and F.J. Muckenthaler, Nucl. Sci. and Engg. 26 (1966) 3.

Table 1

Comparison of neutron Spectrum in Graphite

| Energy Interval in MeV | Distance | 05R | $S_8P_3$ 2cm mesh | $S_8P_3$ 1 cm mesh | $S_{13}P_3$ 1 cm mesh |
|---|---|---|---|---|---|
| .247 - .408 | 20.3 | 2.789(-10) | 2.961(-10) | 3.047(-10) | 3.056(-10) |
| | 35.6 | 2.652(-11) | 2.649(-11) | 2.776(-11) | 2.814(-11) |
| .408 - .743 | 20.3 | 1.459(-10) | 1.524(-10) | 1.569(-10) | 1.575(-10) |
| | 35.6 | 1.443(-11) | 1.454(-11) | 1.52 (-11) | 1.543(-11) |
| .743 - 1.35 | 20.3 | 6.583(-11) | 7.089(-11) | 7.261(-11) | 7.277(-11) |
| | 35.6 | 8.202(-12) | 7.46 (-12) | 7.77 (-12) | 7.901(-12) |
| 1.35 - 2.02 | 20.3 | 3.114(-11) | 3.371(-11) | 3.444(-11) | 3.446(-11) |
| | 35.6 | 4.086(-12) | 3.658(-12) | 3.818(-12) | 3.893(-12) |
| 2.02 - 2.73 | 20.3 | 1.534(-11) | 1.609(-11) | 1.65 (-11) | 1.652(-11) |
| | 35.6 | 1.993(-12) | 1.695(-12) | 1.767(-12) | 1.803(-12) |
| 2.73 - 3.01 | 20.3 | 7.321(-12) | 7.248(-12) | 7.489(-12) | 7.552(-12) |
| | 35.6 | 6.7 (-13) | 7.064(-13) | 7.396(-13) | 7.579(-13) |
| 3.01 - 3.68 | 20.3 | 5.382(-12) | 4.784(-12) | 4.927(-12) | 4.95 (-12) |
| | 35.6 | 5.653(-13) | 4.867(-13) | 5.078(-13) | 5.21 (-13) |
| 3.68 - 4.07 | 20.3 | 4.056(-12) | 3.779(-12) | 3.878(-12) | 3.891(-12) |
| | 35.6 | 4.909(-13) | 4.132(-13) | 4.343(-13) | 4.446(-13) |
| 4.07 - 4.97 | 20.3 | 3.022(-12) | 3.197(-12) | 3.261(-12) | 3.262(-12) |
| | 35.6 | 3.998(-13) | 3.895(-13) | 4.029(-13) | 4.12 (-13) |

Table 2

Bonnerball Count Rates at 24" behind ten feet sodium (Comparison with experiments and other calculations)

| Detector | Code | Count rate | Deviation from expt. |
|---|---|---|---|
| Cd | Measured | 1.96 | |
| | Present calculation | 2.24 (± 13.2%) | + 14.3% |
| | DOT | 1.33 | - 16.9% |
| | MORSE | 1.66 | - 15.3% |
| 3" | Measured | 17.3 | - |
| | Present | 15.4 (± 21.6%) | - 11.0% |
| | DOT | 15.5 | - 10.4% |
| | MORSE | 16.4 | - 5.2% |
| 4" | Measured | 25.3 | |
| | Present calculation | 20.8 (± 13.9%) | - 17.8% |
| | DOT | 21.4 | - 15.4% |
| | MORSE | 23.0 | - 9.1% |
| 5" | Measured | 22.3 | |
| | Present calculation | 19.5 (± 11.5%) | - 12.6% |
| | DOT | 19.8 | -11.2% |
| | MORSE | 21.0 | - 5.8% |
| 6" | Measured | 16.7 | |
| | Present calculation | 14.5 (±10.3%) | - 13.2% |
| | DOT | 14.5 | - 13.2% |
| | MORSE | 15.5 | - 7.2% |
| 8" | Measured | 7.61 | |
| | Present calculation | 6.39 (± 9.6%) | - 16.0% |
| | DOT | 6.51 | - 14.5% |
| | MORSE | 6.88 | - 9.6% |

Table 2 contd.

| Detector | Code | Count rate | Deviation from expt. |
|---|---|---|---|
| 10" | Measured | 3.01 | |
| | Present calculation | 2.59 ( ±8.2%) | - 14.0% |
| | DOT | 2.44 | - 18.9% |
| | MORSE | 2.53 | - 15.9% |
| 12" | Measured | 1.09 | |
| | Present calculation | 0.86 (± 8.3%) | - 21.1% |
| | DOT | 0.89 | - 18.3% |
| | MORSE | 0.89 | - 18.3% |

Table 3

One dimensional Calculational Model

| Material | Zone no. | Distance (cms) | Mesh interval |
|---|---|---|---|
| | | 120.45 | |
| ↑ | 11 | | 0.973 |
| | | 109.75 | |
| Shield | 11 | | 1.0 |
| ↓ | | 99.75 | |
| | 11 | | 1.0 |
| | | 69.75 | |
| | 11 | | 0.965 |
| | | 50.45 | |
| SS | 10 | | 1.0 |
| | | 48.45 | |
| Iron+Void | 9 | | 0.85 |
| | | 46.75 | |
| Lead | 7 | | 0.985 |
| | | 32.95 | |
| Iron | 6 | | 0.875 |
| | | 27.7 | |
| Void | 5 | | 0.85 |
| | | 26.0 | |
| Reflector | 4 | | 0.9425 |
| | | 18.46 | |
| Void | 3 | | 0.9 |
| | | 16.66 | |
| Blanket | 2 | | 0.944 |
| | | 6.27 | |
| Fuel | 1 | | 0.895 |
| | | 0.0 | |

Table 4

Measured and Calculated reaction rates at the inner surface of the shield ( at 2KW)

| Reaction | Measured $sec^{-1}$ | Calculation $sec^{-1}$ | | | C/E | | |
|---|---|---|---|---|---|---|---|
| | | ANISN* | TWOTRAN* | DTF | ANISN* | TWOTRAN* | DTF |
| $^{54}Fe(n,p)$ | 2.36 ± 0.295E-18 | 1.58E-18 | 6.88E-19 | 1.42E-18 | 0.67 | 0.291 | 0.60 |
| $^{58}Ni(n,p)$ | 3.32 ± 0.225E-18 | 3.61E-18 | 1.56E-18 | 3.55E-18 | 1.09 | 0.47 | 1.07 |
| $^{24}Mg(n,p)$ | 3.04 ± 0.108E-20 | 4.86E-20 | 2.09E-20 | 4.66E-20 | 1.59 | 0.687 | 1.53 |
| $^{115}In(n,n')$ | 4.41 ± 0.288 E-17 | 4.00E-17 | 1.78E-17 | 4.24E-17 | 0.907 | 0.403 | 0.96 |
| $^{27}Al(n,p)$ | 1.465± 0.042E-20 | 2.40E-20 | 1.03E-20 | 1.84E-20 | 1.63 | 0.709 | 1.26 |
| $^{27}Al(n,\alpha)$ | 7.76 ± 1.869E-20 | 8.44E-20 | 3.65E-20 | 8.57E-20 | 1.08 | 0.47 | 1.10 |
| $^{64}Zn(n,p)$ | 1.18 ± 0.259E-18 | 9.90E-19 | 4.31E-19 | 1.0 E-18 | .839 | .365 | 0.85 |
| $^{197}Au(n,\gamma)$ | 1.21 ± 0.1 E-13 | 4.59E-13 | 1.09E-13 | 4.00E-13 | 3.79 | .393 | 3.3 |
| $^{197}Au(cd)(n,\gamma)$ | 1.21± 0.1 E-13 | 4.58E-13 | 1.09E-13 | 4.00E-13 | 3.78 | 0.893 | 3.3 |

* Japanese calculations

Table 5

Measured and Calculated Reaction Rates of $^{115}In(n,n')$ and $^{197}Au(n,\gamma)$ in iron shield at 2KW

| Thickness of shield cms | $^{115}In(n,n')$ reaction $sec^{-1}$ | | | $^{197}Au(n,\gamma)$ reaction $sec^{-1}$ | | |
|---|---|---|---|---|---|---|
| | Measured | Calculated | C/E | Measured | Calculated | C/E |
| 0 | 4.41 E - 17 | 4.24 E - 17 | 0.96 | 1.21 E - 13 | 4.00 E - 13 | 3.30 |
| 20 | 3.73 E - 18 | 3.50 E - 18 | 0.94 | 4.41 E - 14 | 9.24 E - 14 | 2.10 |
| 40 | 4.48 E - 19 | 4.22 E - 19 | 0.94 | 1.50 E - 14 | 3.28 E - 14 | 2.19 |
| 60 | 9.04 E - 20 | 8.78 E - 20 | 0.97 | 4.45 E - 15 | 1.09 E - 14 | 2.45 |

Table 6

Thermal neutron fluxes along the duct centerline

| Experiment | distance along duct centerline | measured flux | Our calculation | Deviation from expt. |
|---|---|---|---|---|
| Straight duct | 5' | 7.50 (-1) | 7.51 (-1) | 0.13% |
| | 10' | 1.52 (-1) | 1.55 (-1) | 1.97% |
| | 20' | 1.33 (-2) | 1.32 (-2) | ~~1.52%~~ 0.75% |
| | 30' | 2.34 (-3) | 2.22 (-3) | 5.13% |
| | 40' | 5.5 (-4) | 5.19 (-4) | 5.64% |
| Two legged duct | 15' | 4.4 (-2) | 4.41 (-2) | 0.23% |
| | 21' | 5.5 (-3) | 5.45 (-3) | 0.91% |
| | 27' | 1.09 (-3) | 1.05 (-3) | 3.67% |
| | 33' | 2.9 (-4) | 2.85 (-4) | 1.72% |
| | 41' | 8.7 (-5) | 9.21 (-5) | 5.86% |
| Three legged duct | 30' | 6.8 (-4) | 6.25 (-4) | 8.09% |
| | 32' | 3.4 (-4) | 3.01 (-4) | 11.4% |
| | 34' | 1.48 (-4) | 1.25 (-4) | 15.5% |
| | 36' | 7.48 (-5) | 6.23 (-5) | 16.7% |
| | 38' | 4.4 (-5) | 3.74 (-5) | 15.0% |

# FISSION PRODUCT DATA REQUIREMENT FOR BURN UP MEASUREMENT IN A FAST REACTOR.

B.Saha, R.Saikumar, N.Ravi, D.Darwin Albert Raj and C.K.Mathews
RCL, RRC, Kalpakkam 603 102

Abstract

Burn-up can be determined most accurately by monitoring a suitable fission product isotope or a group of isotopes. In FBTR burn-up has to be measured in a driver fuel, test fuel and blankets. In other words, this means suitable monitors have to be identified for fissile systems of different nature and composition. For thermal reactors $^{148}Nd$ is the best available burn-up monitor. For fast reactors a combination of rare earth isotopes is under consideration. The errors in burnup measurement on account of fission product data uncertainties are brought out in the paper.

In addition to total burn-up, one needs to know the contribution from individual fissioning nuclides towards total fission. For a fast reactor, this can be determined most accurately by monitoring the ratio of two fission product isotopes, which change significantly from one fissioning system to the other. At present the fast fission yields are available with considerable uncertainties which hardly permit one to have a suitable combination of two isotopes that can be used to monitor individual contributions within ±5% for a bi-fissioning system. In addition, there could be an additional error in using the reported data because the ratio which would be appreciably different for different fissioning nuclides might also be neutron energy sensitive.

The paper outlines how some of the problems could be overcome by irradiating pure fissile isotopes under identical situations for measuring the yields of monitor isotopes for all fissioning nuclides in general and for $^{240}Pu$ and $^{241}Pu$ in particular, for which the reported uncertainties are quite high.

143 (94 words)

# EVALUATION OF THRESHOLD REACTION INTERFERENCES IN REACTOR NEUTRON ACTIVATION ANALYSIS USING (n,γ) REACTIONS.

S.Yegnasubramanian and S.Gangadharan

Analytical Chemistry Division
Bhabha Atomic Research Centre
Trombay, Bombay 400 085.

## I. INTRODUCTION

The estimation of impurities by (n,γ) reactions in Reactor Neutron Activation Analysis can suffer from the presence of the high energy component in the reactor neutron spectrum, which can produce the same product nuclide through (threshold) nuclear reactions with the other elements constituting the matrix. Theoritical evaluation of such interferences requires knowledge of the excitation functions and the neutron spectrum in such details that it still remains not "quantitative" for analytical applications. The ultimate interest in analytical estimations is the "yield" which is a convoluted product of $\sigma(E)$ and $\bar{\Phi}(E)$, integrated over the entire neutron energy spectrum of the irradiation position. However, characterising the irradiation positions of the reactor enables the activation analyst to have an awareness of the extent of hard component present. The experimental measurement of the fast neutron reaction yield improves the accuracy in the analytical determination by the (n,γ) reaction. However, this fast neutron component itself can be used with great advantage in analytical estimations, as in the case of titanium through scandium by the (n,p) reaction[1] and its application to the estimation of titanium in steels[2]. The primary objective of the work reported here is to characterise the irradiation positions and evaluate the extent of interferences from fast neutron reac-

tions to reactor neutron activation analysis using (n,Y) reactions.

## II. CHARACTERISATION OF THE IRRADIATION POSITIONS

### II.1.Thermal (sub-cadmium) neutron flux :

The configuration of the APSARA reactor core at the time of these measurements is given in Fig.1. The positions that are characterised are those that are most commonly used for irradiations. The sub-cadmium flux was determined using the thin-foil technique[3]. Most of the measurements were performed with high-purity foils of cobalt/aluminium alloy containing 0.1% and 1.0% of cobalt, cut into discs of 8 mm diameter (thickness: 2 mil). The gamma rays from the irradiated thin foil were measured on a large volume (50 cc) Ge(Li) (and/or 7.6 cm X 7.6 cm NaI(Tl)) detector at reproducible geometries. The detector was coupled to a ND 2200 pulse height analyser. The detection systems were calibrated for the absolute full-energy peak efficiencies using NBS/IAEA reference sources. The neutron flux was then calculated from the nuclear data given in Table 1. In all cases the sub-cadmium (thermal) fluxes were obtained after correcting for the epi-cadmium contribution to the foil activity. Using the data from Table 1 for cobalt, the flux values for two in-core and three out-of-core positions of the APSARA reactor , measured , are given in Table 2.

(9)

### II.2. Fast neutron flux :

Preliminary investigations regarding the hard components of the reactor neutron spectrum were provided by values of the cadmium ratios defined as,

$$\text{Cd ratio} : \frac{(\text{sub - Cd} + \text{epi - Cd})}{\text{epi - Cd}} \quad \text{neutrons}$$

$$: \frac{\text{bare foil activity at zero-time}}{\text{Cd covered activity at zero-time}}$$

TABLE I.

(4-8)

Nuclear Data and Target Descriptions for the Reactions Studied.

| Reaction | "Q" (MeV) | $\langle\sigma\rangle$ (mb) | $E_{eff}$ (MeV) | $\sigma_{eff}$ $\sigma_{th.}$ (mb) | $T_{1/2}$ | $E_\gamma$ (MeV) | % abundance of $E_\gamma$ | Full energy peak efficiency, Ge(Li) % | Target and its purity. |
|---|---|---|---|---|---|---|---|---|---|
| $^{59}Co(n,\gamma)^{60}Co$ | | th. | th. | 37500 | 5.27 y | 1.173<br>1.332 | 100<br>100 | 0.727<br>0.626 | Co/Al alloy foil, 99.9+ |
| $^{46}Ti(n,p)^{46}Sc$ | -1.6 | 8 | 5.5 | 230 | 83.9 d | 0.889<br>1.120 | 100<br>100 | 1.536 | Ti foil 99.9+ |
| $^{48}Ti(n,p)^{48}Sc$ | -3.2 | 0.21 | 7.2 | 50 | 1.83 d | 1.312 | 100 | 0.633 | Ti foil, " |
| $^{54}Fe(n,p)^{54}Mn$ | 0.1 | 53 | 4.2 | 610 | 303 d | 0.835 | 100 | 1.570 | Fe foil, 99.9+ |
| $^{58}Ni(n,p)^{58}Co$ | 0.4 | 100 | 2.9 | 420 | 71.3 d | 0.810 | 99 | 1.582 | Ni foil, 99.9+ |
| $^{63}Cu(n,\alpha)^{60}Co$ | 1.7 | 0.73 | 9.2 | | 5.27 y | 1.173<br>1.332 | 100<br>100 | 0.727<br>0.626 | Cu foil, 99.9+ |

TABLE 2

Thermal (sub-cadmium) flux measurements (in units of $10^{12}$n.cm$^{-2}$.sec$^{-1}$)

| Reaction | Irradiation position | | | | |
|---|---|---|---|---|---|
| | A1 | A7 | C8 | E8 | D9 |
| $^{59}Co(n,\gamma)^{60}Co$ | 2.6 | 2.7 | 2.1 | 1.3 | 0.2 |

All cadmium ratios were calculated using 1mm thick interlocking cadmium covers. As an example, one of the in-core positions, A1, offered a value of 17 as supposed to a value of 30 for a D9 position.

Five different nuclear reactions have been used to determine the integrated fast flux with effective threshold energies from 2.9 MeV to 9.2 MeV. The metallic foils (8 mm dia, 2 mil thick) of the elements were irradiated in the corresponding positions simultaneously for a period of 24 hours.

The nuclear reactions and sample materials used for the measurements as well as the nuclear data used for calculations are given in Table 1. After each irradiation, the gamma rays of interest were measured on the same calibrated detector and the fast flux calculated using the nuclear constants. Cobalt/aluminium alloy foils were used to monitor all the irradiations. Several codes are available in the literature[10] for the unfolding of the foil activation data; however, the procedure adopted is the one similar to that described in ref.[11]

Table 3 summarises the results of these measurements.

TABLE 3

Hard component of the neutron spectrum measured through threshold monitors.

| Reaction | $E_{eff}$ (MeV) | $\sigma_{eff}$ (mb) | (in units of $10^{10}$ n.cm$^{-2}$.sec$^{-1}$) | | | | |
|---|---|---|---|---|---|---|---|
| | | | A1 | A7 | C8 | E8 | D9 |
| $^{48}Ti(n,p)^{48}Sc$ | 7.2 | 50 | 0.074 | 0.084 | 0.071 | 0.046 | 0.014 |
| $^{46}Ti(n,p)^{46}Sc$ | 5.5 | 230 | 0.480 | 0.417 | 0.362 | 0.230 | 0.056 |
| $^{54}Fe(n,p)^{54}Mn$ | 4.2 | 610 | 1.96 | 1.95 | 1.22 | 1.19 | 0.130 |
| $^{58}Ni(n,p)^{58}Co$ | 2.9 | 420 | 3.05 | 2.83 | 2.45 | 1.57 | 0.357 |

The values based on $^{55}Mn(n,2n)^{54}Mn$ and $^{115}In(n,n')^{115m}In$ reactions, with $E_{eff}$ 10.3 and 1.05 respectively could not be provided as the samples got damaged in the packing.

## III. EVALUATION OF THRESHOLD REACTION INTERFERENCES [12] :

Table 4 gives some typical reactions of analytical interest, the interfering reactions to those estimations and the relevent nuclear data.

TABLE 4

Typical Nuclear Reactions Studied

| (n,γ) reaction of interest | interfering reaction yielding the same product (Q:MeV) | Product $T_{1/2}$ | $E_\gamma/\beta$ (MeV) used for measurement | Sample material and its purity |
|---|---|---|---|---|
| $^{31}P(n,\gamma)^{32}P$ | $^{35}Cl(n,\alpha)^{32}P$ (0.935) | 14.3 d | 1.7 ($\bar{\beta}$) | KCl, GR grade |
| $^{45}Sc(n,\gamma)^{46}Sc$ | $^{46}Ti(n,p)^{46}Sc$ (-1.58) | 83.9 d | 0.889<br>1.120 | Ti foil, 99.9% |
| $^{55}Mn(n,\gamma)^{56}Mn$ | $^{56}Fe(n,p)^{56}Mn$ (2.92) | 2.58 h | 0.847<br>1.811 | Fe foil, 99.9% |
| $^{59}Co(n,\gamma)^{60}Co$ | $^{60}Ni(n,p)^{60}Co$ (2.04) | 5.27 y | 1.173<br>1.332 | Ni foil, 99.9% |
| $^{59}Co(n,\gamma)^{60}Co$ | $^{63}Cu(n,\alpha)^{60}Co$ (1.71) | 5.27 y | 1.173<br>1.332 | Cu foil, 99.9% |
| $^{85}Rb(n,\gamma)^{86}Rb$ | $^{86}Sr(n.p)^{86}Rb$ (1.13) | 18.7 d | 1.077 | $SrCO_3$, GR grade |

All measurements, except on $^{32}P$, were done by gamma spectrometry. In the case of $^{32}P$, which is a pure $\beta$ emitter, a chemical separation procedure was adopted. Phosphorous was precipitated as ammonium phospho molybdate and counted in a GM counter. To check for (n,γ) impurities in these targets, these samples were enclosed in 1mm thick cadmium (interlocking) covers and irradiated. The foils of Ti, Fe, Ni and Cu yielded no significant contribution from the (n,γ) reactions while KCl and $SrCO_3$ contributed as much as 10% to the total measured activity. All samples were irradiated for a duration of 24 hours

except iron, used to evaluate the $^{56}Fe(n,p)^{56}Mn$ reaction; in this case the irradiation was done for 1 hour. The activities of the irradiated samples were compared with hte activities of known amounts of standards, all activities being normalised to zero-time (end of irradiation). The threshold reaction interferences are then expressed as the quantity, in mg, of the element, which through the fast neutron reaction 'would' produce the activity of the product nuclide equivalent to that from 1 ug of the impurity element by (n,γ) reaction. Table 5 summarises these observations, for one in-core (A7)

TABLE 5

Few of the Evaluated Threshold Reaction Interferences

| Reaction | (n,γ) equivalents,mg Position A7 | Position C8 |
|---|---|---|
| $^{35}Cl(n,\alpha)^{32}P$ | 0.06 | 0.13 |
| $^{46}Ti(n,p)^{46}Sc$ | 99 | 212 |
| $^{56}Fe(n,p)^{56}Mn$ | 6.5 | ND |
| $^{60}Ni(n,p)^{60}Co$ | 120 | 180 |
| $^{63}Cu(n,\alpha)^{60}Co$ | 500 | 450 |
| $^{86}Sr(n,p)^{86}Rb$ | 26 | 97 |

and one out-of-core position (C8). The observations are in accordance with the expectations that the in-core position (A7) with a higher fast component, requires much less amount of the interfering element compared to C8 to yield the same activity as would be produced by 1 ug of the (n,γ) element, except in the case of $^{63}Cu(n,\alpha)^{60}Co$ reaction, which has a high positive 'Q'value.

IV. SUMMARY :

This type of characterisation has proved to be much useful in our 'routine' analysis of varieties of samples; for example, estimation of cobalt in copper matrix at sub-ppm levels , estimation of manganese in matrixes with iron as a major/minor component, estimation of scandium in geological samples with high concentration of titanium etc., This exercise of characterisation has to be revised to reflect significant core (fuel) changes.

ACKNOWLEDGEMENTS

It is a pleasure to thank Dr.M.Sankar Das, Head, Analytical Chemistry Division, for his continued interest and encouragement.

REFERENCES

1. Sankar Das, M., Ph.D. Thesis, University of Bombay, 1964

2. Athavale, V.T., Desai, H.B., Gangadharan, S., Pendharkar, M.S., and Sankar Das, M., Analyst, 91 (1966) 638.

3. ASTM publication E-262-65T, "Measuring thermal neutron flux by Radioactivation techniques" ASTM, 1965.

4. "Handbook on Nuclear Activation Cross-Sections", Technical Reports Series No. 156, IAEA, 1974.

5. Moteff, J., Nucleonics 20 (1962) 56.

6. Zijp, W.L., "Reviews of Activation Methods for the Determination of Fast Neutron Spectra", RCN-37, 1965.

7. Data from literature of Reactor Experiments Inc., California.

8. Lederer, C.M., and Shirley, V.S., "Table of Isotopes", seventh edition, Wiley Interscience, 1978.

9. ASTM publication E-264-65T "Measuring Fast Neutron Flux by Radioactivation of Nickel" ASTM, Philadelphia, Pa, 1965.

   Becker, D.A.,and La Fleur, P.D., J.Radioanal.Chem. 19 (1974) 149.

10. Schmotzer, J.K., and Levine, S.H., Trans. Am. Nucl. Soc.,18('74)37(

    Perey, F., "Spectrum unfolding by the least squares method", IAEA meeting on neutron spectra unfolding, Oak Ridge, TN (Oct,'77)

    Routti, J.T., "Mathematical considerations of determining neutron spectra from activation measurements", UCRL-19375, 1969.

Berg, S., and Hawkins, R.G., " A computer- automated iterative method for neutron flux spectra determination by foil activation Vol.I, a study of the iterative method", AFWL-TR-67 41,1967.

11. "Neutron Fluence Measurements" Technical Reports Series No. 107 IAEA, 1970.

12. Durham, R.W., Navalkar, M.P., and Ricci, E., "threshold Reaction Interference in Neutron Activation Analysis", AECL-1434, 1962.

Fig. 1

| | | | | | | | |
|---|---|---|---|---|---|---|---|
| LT | GR | 25 | 8/1 | 6 | GR | FC | G |
| LT | 10 | 13 | 9 | 15 | 10/5C | G | F |
| Plug | 17 | 10/3C RC | 18 | RB~~13~~ 10/2C | 22 | R | E |
| LT | 14 | 19 | 12 | 4 | 7 | 8/2 | D |
| 3 | 10/4C RF | 8 | 23 | 10/1C RA | 11 | B | C |
| LT | 2 | 20 | 5 | 16 | 26 | e 0 | B |
| LT | GR | 21 | Sb.Be source | 1 | GR | ST | A |
| 7 | 6 | 5 | 4 | 3 | 2 | 1 | |

T.C

C.R.

# EVALUATION OF (n,2n) AND (n,3n) CROSS SECTIONS FOR THORIUM ISOTOPES

R.P. Anand, M.L. Jhingan*, S.K. Gupta and M.K. Mehta,

Nuclear Physics Division, Bhabha Atomic Research Centre,

Bombay 400 085.

*Member of T.I.F.R., Colaba, Bombay 400085.

Abstract:

As a part of the IAEA sponsored Co-ordinated Research Programme on the Actinide Neutron Data, evaluation of $\sigma$ (n,2n) and $\sigma$ (n,3n) cross-sections for $^{232}$Th and $^{233}$Th was undertaken. All the available experimental data for $^{232}$Th were compiled, examined and renormalized wherever possible. A computer code "SPLINE" was used to fit a smooth curve to the accepted experimental points. The "SPLINE" code fits to the data points with a set of cubic polynomials such that the value of the function, its first and second derivatives are continuous. The present evaluation compares well with those by Meadows J. et al (1978) and by Vasiliu et al. (1979). As there exists only one inferred value for $\sigma$ (n,3n) on $^{232}$Th and no measured data for $\sigma$ (n,2n) and $\sigma$ (n,3n) on $^{233}$Th, these cross-sections were calculated theoretically taking into account statistical as well as pre-equilibrium emission. Experimental evaluation agrees quite well with the theoretical calculations for $\sigma$ (n,2n) of $^{232}$Th. All the evaluated cross-sections are given in graphs as well as in tables.

1. Introduction:

A programme has been initiated to carry out data evaluation for the isotopes of importance for Th-U fuel cycle as a part of the IAEA/NDS sponsored Co-ordinated Research Programme on the Intercomparison of Evaluation of Actinide Neutron Nuclear Data. To start with an evaluation of thorium isotopes has been carried out. The present report describes the evaluation of (n,2n) and (n,3n) cross sections on $^{232}Th$ and $^{233}Th$.

The data for the (n,2n) and (n,3n) reaction cross-sections were compiled from all the sources referred to in 'CINDA' till June 1979 and the data tapes supplied by the Nuclear Data Section of IAEA. Each data-set was critically examined and cross-sections were renormalized whereever necessary and possible. The new standard cross-sections were taken from ENDF/B-IV file. Each data-set was assigned with an appropriate error, decided by the experimental details and evaluators judgement. Some of the data measurements are rejected completely. A computer xcode "SPLINE" was used to fit a smooth curve to the accepted experimental data points which were weighted in inverse proportion to the errors quoted or reassigned in the present work. This code fits the data points with a set of cubic polynomials, such that the value of the function and its first and second derivatives are

continuous throughout the whole range, while only the third derivatives are discontinuous at all the joining points of polynomials, which are called knots. Even the discontinuities in the third derivatives are not allowed to have abrupt changes through the use of a smoothing-term in the 'SPLINE' code. If there are more than one data point at the same energy, their weighted average was taken as this code does not allow more than one data point at the same energy.

2. <u>(n,2n) cross section evaluation</u>:

The (n,2n) data from the following references were scrutinized: Batchler et al (1965), Butler et al (1961); Cochran et al (1958); Halperin et al (1958); Karius et al (1976); Perkin et al (1961); Phillips et al (1956); Prestwood et al (1961); Tewes et al (1958) and Zisin et al (1960). It can be seen that all of the data available are quite old except that of Karius et al (1976).

The data of Halperin et al (1958), Tewes et al (1959) and Zysin et al (1960) have been rejected for one or more of the following reasons: 1) The data are preliminary, 2) The data points are descrepant with other measurements by several times the quoted errors, 3) The data-set contains unexplainable large fluctuations not corroborated by other measurements.

The recent 9-point measurement of Karius et al (1976) from 13-18 MeV is the only new set which has not been consi-

dered so far by earlier evaluators. For this data the cross-sections were measured with the activation technique using a high resolution Ge(Li) detector to count $\gamma$ -rays. The errors quoted are about $\pm 9\%$.

The data set of Butler et al (1961) is the only one which covers an energy range from threshold to 20.4 MeV. Although the quoted errors are 5% (except at low energies where it is $\approx$ 10%), they do not include the errors in the standard $^{32}S(n,p)$ cross-section. The data were renormalized with ENDF/B-IV values for the standard cross section which is uncertain to an extent of 10%. Further these data are quite old and hence to reduce their weightage, $\pm 20\%$ error was assigned for them. The measurements at 12.53, 18.52 and 20.4 MeV were performed with a T(d,n) neutrons and a different technique for the flux measurements. Thus they would have to be renormalised differently for which sufficient information is not available. These points disagree very much with Karius (1976) data at similar energies and hence are not included in the evaluation.

The measurements of Prestwood et al (1961) from 13.33 to 14.93 MeV are absolute, hence are not renormalized. According to authors, absolute errors are difficult to calculate. Quoted errors of $\pm 10\%$ are obtained only from estimates obtained by comparing the data to statistical model predictions. Hence,

considering various factors we have assigned an error of ±20% to these data. The point at 12.13 MeV was rejected as it was measured with a different technique relative to $^{238}U$ fission cross section and was not possible to renormalize as the value used is not given.

The measurement of Perkin et al (1961) at 14.1 MeV is a good measurement but for us it was not possible to renormelize it as the value of the cross section for $^{27}Al$ (n,$\alpha$) reaction, used as his standard, was not given. We assigned an error of ±25% to this point.

The measurements of Cochran et al (1958) and Phillips (1956) are old and none of their experimental details are available, our assigned errors to them were ±25%. One data point of Batchelor et al (1965) at 7 MeV has also been rejected as it not a measurement but $\sigma$ (n,2n) has been deduced from measured $\eta$ .

These data were fitted with the 'SPLINE' code at BESM-6 computer and the recommended values for the (n,2n) reaction cross-sections are the final fit obtained using 20 knots. The Spline fitted and experimental values are given in Table I and shown in Figure 1. The final evaluated errors estimated for the fitted values are about ± 10% except at 6.5 MeV which is very close to the threshold where the error is ±50%.

For $^{233}Th$ measured data does not exist on (n,2n) cross-sections.

3. (n,3n) cross-section evaluation:

(n,3n) reaction cross sections for $^{232}Th$ has not been measured as the half life of the rasidual nucleus $^{230}Th$ is $8x10^4$ years which is too large for activation measurements. However, there is one indirect measurement of McJaggert et al (1963) where $\sigma$ (n,3n) has been deduced from the measured value of $\eta$ for $^{232}Th$ at 14 MeV only. And there is no measured data for $\sigma$ (n,3n) for $^{233}Th$. Hence these unmeasured cross-sections were calculated based on a theoretical model developed by us.

4. Theoretical Calculation:

In our previous (Jhingan et al 1978) calculations of (n,2n) and (n,3n) cross-sections all non-equilibrium effects were presumed to be accounted by an empirical factor. The calculations for $^{232}Th$ and $^{238}U$ agreed well upto 15 MeV while at higher energies it deviated significantly and systematically from the experimental data due to the inadequacy of the empirical factor. In the present work we have overcome this shortcoming by considering the pre-equilibrium effects in the emission of first particle. Subsequent particle emissions are calculated according to the statistical model only. Emission

of protons is also considered but only in the pre-equilibrium part.

The general expression for (n,xn) , x = 2,3,4 cross-section may be written as

$$\sigma(n,xn) = \sigma_M \int_0^{L_1} P_1(\epsilon_1) \int_0^{L_2} P_2(\epsilon_1,\epsilon_2) \cdots \int_0^{L_{x-1}} P_{x-1}(\epsilon_1,\epsilon_2 \cdots \epsilon_{x-1}) \int_0^{L_x} (1-P_x)\, d\epsilon_1 d\epsilon_2 \cdots d\epsilon_x \cdots \text{I}$$

where $L_x = E_n - EB_x - \sum_{i=1}^{(x-1)} \epsilon_i$ ; $EB_x$ is the Binding Energy, and $\epsilon_i$ is energy of $i^{th}$ neutron; $E_n$- Energy of the incident neutron. For nonfissile nuclei $\sigma_M = \sigma_R(E_n)$ and for fissile nuclei $\sigma_M = \{\sigma_R(E_n) - \sigma_f(E_n)$ and $P_1(\epsilon_1)$ is the probability that the first particle is emitted with energy between $\epsilon_1$ and $(\epsilon_1 + d\epsilon_1)$ and is given by

$$P_1(\epsilon_1) = \left\{ \frac{d f_{P.E}(\epsilon_1)}{d\epsilon_1} + (1-\delta) \frac{\epsilon_1 . \sigma_{inv}(\epsilon_1) . \rho_1(E_n - \epsilon_1)}{\int_0^{E_n} \epsilon_1 . \sigma_{inv}(\epsilon_1) . \rho_1(E_n - \epsilon_1) d\epsilon_1} \right\} \cdots \text{II}$$

Here the first term is due to pre-equilibrium and is given by

$$\frac{d f_{P.E}(\epsilon_1)}{d\epsilon_1} = \frac{(2S+1) . m . \epsilon_1 . \sigma_{inv}(\epsilon_1)}{2\pi . \hbar^2 . |M|^2 . g^4 . E^3} \sum_{n=3}^{n} \left(\frac{U}{E}\right)^{n-2} . (n+1) . (n-1) . Q_b \cdots \text{III}$$

where the symbols have the usual meaning. $g = A/13\ MeV^{-1}$. $\sigma_{inv}(\epsilon_1)$ are taken from reaction cross-sections based on Wilmore-Hodgson optical potential. The squared Matrix

element $|M|^2$ is adopted from Kalbach. C.(1978) where it is given as a function of excitation energy per exciton (E/n).

The second term in eq.(2) represents the equilibrium part. $\delta$ represents the total pre-equilibrium component. After the emission of first neutron, the second one is emitted with an energy between $\epsilon_2$ and $(\epsilon_2 + d\epsilon_2)$ with a probability $P_2(\epsilon_1, \epsilon_2) d\epsilon_2$ and similarly for subsequent neutrons.

The level density at energy $E$ is given as $\rho(E) \sim \exp(2\sqrt{a.E})$ where '$a$' is the Pearlstein level density parameter and it is lower by a factor of about 2.7 for each nucleus from that of Gilbert and Cameron as discussed by Jhingan et al (1978). The effect of neglecting gamma emission, particularly near the threshold, is compensated by using the apparent level density parameter given by Pearlstein(1965). A computer code has been developed for (n,xn), x = 2,3,4 cross-sections. Calculations have been performed using this code from threshold to 28 MeV for 13 nuclei viz. $^{89}Y$, $^{90}Zr$, $^{93}Nb$, $^{103}Rh$, $^{107}Ag$, $^{151}Eu$, $^{169}Tm$, $^{175}Lu$, $^{181}Ta$, $^{191}Ir$, $^{197}Au$, $^{203}Tl$ and $^{209}Bi$. For two fissionable nuclei $^{232}Th$ and $^{238}U$ the cross-sections are calculated upto 20 MeV. The values of $|M|^2$ given in ref. were increased twofold to obtain a satisfactory agreement with the measured data. The calculations agree well with the recent measurements within 10-15% for all

the above mentioned nuclei.

Thus after testing this model for medium to heavy nuclei successfully, it was used to calculate (n,3n) cross-sections for $^{232}Th$ and (n,2n) and (n,3n) cross-sections for $^{233}Th$. The fission cross-sections for $^{233}Th$ are based on a semi-empirical formula proposed by Jhingan et al (1979). Figure 1 shows the experimental evaluations as well as theoretical calculations for $\sigma$ (n,2n) and $\sigma$ (n,3n) for $^{232}Th$ and figure 2 shows the theoretical evaluations for $\sigma$ (n,2n) and $\sigma$ (n,3n) for $^{233}Th$. Table I gives the experimental-evaluation values at equal energy interval.

References:


Batchelor R. et al. (1965) Nucl. Phys. - 65, 236

Butler J.P. et al. (1961) Can. Jour. of Chem - 39, 689

Cochran D.R.F. et al. (1958) WASH-1006,22 and WASH-1013,34

Helperin J. et al. (1958), WASH-1006,25 (1958)

Jhingan M.L. et al. Proc. Int. Conf. on Neutron Physics and Nuclear Data for Reactors and other applied purposes, Harwell, 1049, Sept. 1978

Jhingal et al. (1979) Annals of Nuclear Energy-6,495

Kalbach C, (1978) Z. Physik A 287,319

Karius H. et al. (1976) Prog. NEANDC (E), 172

McJaggart M.H. and Goodfellow H. (1963) J.N. E-17, 437

Meadows J. et al. (1978), ANL/NDM-35

Pearlstein S. (1965) Nucl. Sci. Engg. 23, 238

Perkin J.L. et al. (1961) J. Nucl. Energy - 14, 69

Phillips J.A. (1956) Report - AERE-NP/R-2033

Prestwood R.J. et al. (1961) Phys. Rev. - 121, 1438

Tewes H.A. et al. (1961) BNL-653, 2(N-3)

Zisin Yu. A. et al. (1960) Atom. Energ. - 8, 360

TABLE - I

$^{232}Th$ : $\sigma(n,2n)$ Experimental Evaluation at equal energy interval

| Sr. No. | Neutron-Energy MeV | $\sigma(n,2n)$ Barns | Sr. No. | Neutron-Energy MeV | $\sigma(n,2n)$ Barns |
|---|---|---|---|---|---|
| 1. | 6.50 | 0.002 | 26 | 12.75 | 1.794 |
| 2 | 6.75 | 0.064 | 27 | 13.00 | 1.735 |
| 3 | 7.00 | 0.252 | 28 | 13.25 | 1.671 |
| 4 | 7.25 | 0.535 | 29 | 13.50 | 1.602 |
| 5 | 7.50 | 0.831 | 30 | 13.75 | 1.528 |
| 6 | 7.75 | 1.095 | 31 | 14.00 | 1.444 |
| 7 | 8.00 | 1.304 | 32 | 14.25 | 1.346 |
| 8 | 8.25 | 1.458 | 33 | 14.50 | 1.232 |
| 9 | 8.50 | 1.566 | 34 | 14.75 | 1.105 |
| 10 | 8.75 | 1.650 | 35 | 15.00 | 0.974 |
| 11 | 9.00 | 1.722 | 36 | 15.25 | 0.843 |
| 12 | 9.25 | 1.788 | 37 | 15.50 | 0.721 |
| 13 | 9.50 | 1.847 | 38 | 15.75 | 0.613 |
| 14 | 9.75 | 1.899 | 39 | 16.00 | 0.527 |
| 15 | 10.00 | 1.940 | 40 | 16.25 | 0.468 |
| 16 | 10.25 | 1.971 | 41 | 16.50 | 0.431 |
| 17 | 10.50 | 1.991 | 42 | 16.75 | 0.408 |
| 18 | 10.75 | 2.001 | 43 | 17.00 | 0.393 |
| 19 | 11.00 | 2.003 | 44 | 17.25 | 0.380 |
| 20 | 11.25 | 1.996 | 45 | 17.50 | 0.364 |
| 21 | 11.50 | 1.981 | 46 | 17.75 | 0.345 |
| 22 | 11.75 | 1.958 | 47 | 18.00 | 0.319 |
| 23 | 12.00 | 1.928 | | | |
| 24 | 12.25 | 1.891 | | | |
| 25 | 12.50 | 1.846 | | | |

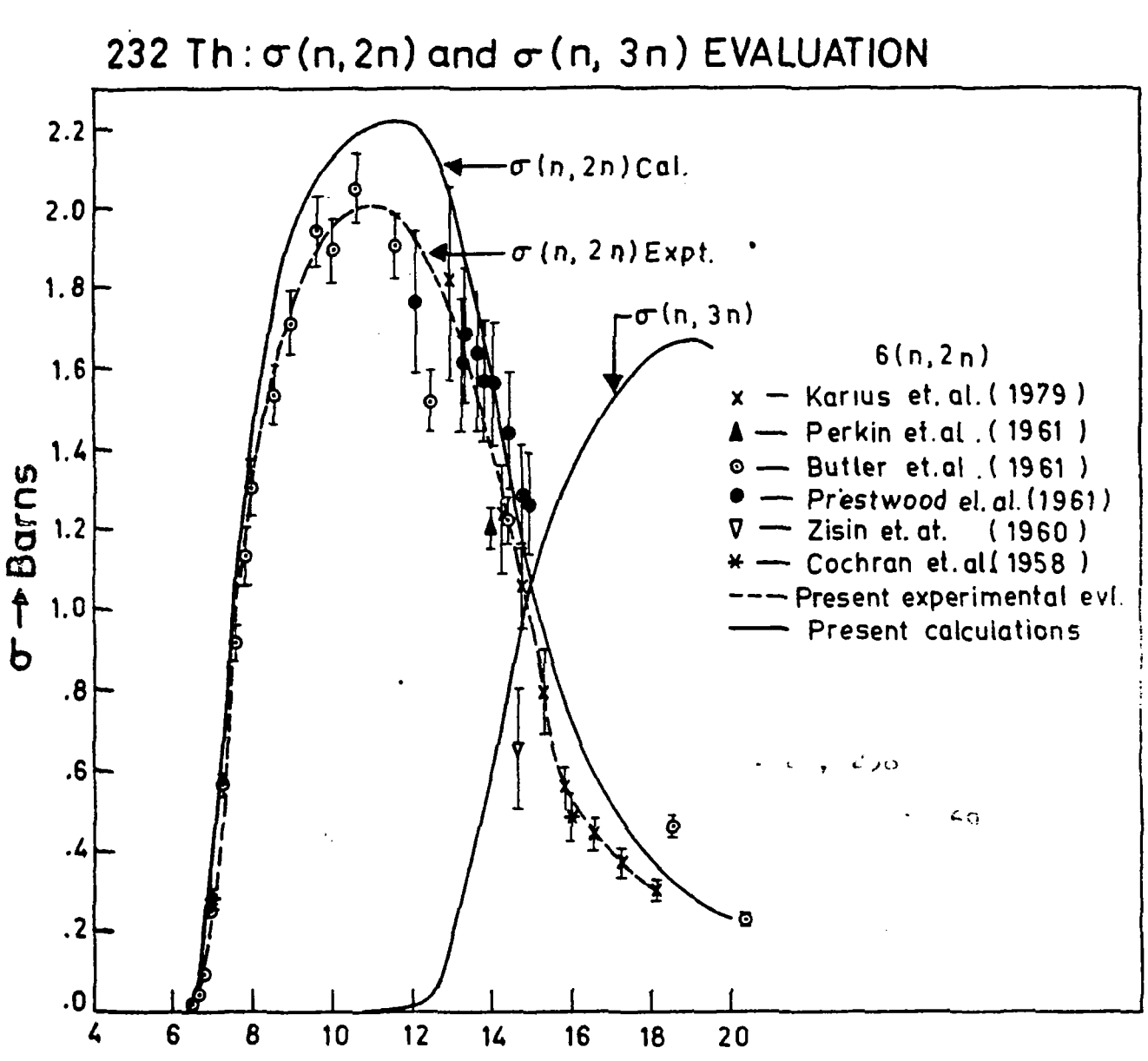
232 Th : σ (n, 2n) and σ (n, 3n) EVALUATION
σ (n, 2n) Cal.
σ (n, 2n) Expt.
σ (n, 3n)
6 (n, 2n)
x — Karius et. al. ( 1979 )
▲ — Perkin et.al . ( 1961 )
⊙ — Butler et.al . ( 1961 )
● — Prestwood el. al. (1961)
▽ — Zisin et. at. ( 1960 )
✱ — Cochran et. al ( 1958 )
--- Present experimental evl.
—— Present calculations
σ → Barns
En → MeV
2.2
2.0
1.8
1.6
1.4
1.2
1.0
.8
.6
.4
.2
.0
4
6
8
10
12
14
16
18
20

FIG. 1.

# RESOLUTION OF DISCREPANT (n,2n) AND (n,3n) EVALUATED CROSS SECTIONS FOR $^{239}Pu$

S.K. Gupta*, M.L. Jhingan**, R.P. Anand* and S. Ganesan***

* Nuclear Physics Division, Bhabha Atomic Research Centre, Bombay 400085.

** Tata Institute of Fundamental Research, Colaba, Bombay 400005.

*** Reactor Research Centre, Kalpakkam 603102.

**Abstract:**

It is observed that the existing Japanese, Los Alamos, ENDF B-IV and Russian evaluations differ by as much as a factor of four from each other for $^{239}Pu(n,2n)$ and $^{239}Pu(n,3n)$ cross sections. We have carried out a calculation using the statistical-cum-preequilibrium model for obtaining these cross sections. The nonelastic and fission cross sections are also input to our calculation. The nonelastic cross sections are taken from the Japanese evaluation while the fission cross sections are taken from the experiment of Kari and Cierjacks. Our calculation yields values similar to those of the Japanese and also agree with the experimental results of Mather et al.

Hunter[1], Prince[2], Sukhovitskij[3] and Kikuchi[4] have evaluated $^{239}Pu(n,2n)$ cross sections. These evaluations differ considerably as is clear from fig.1. For example according to Sukhovitskij maximum (n,2n) cross section is 130 mb, according to Kikuchi it is about 600 mb which is nearer to the measured maximum cross section by Mather[5].

Jhingan et al[6,7] have developed a method to calculate (n,2n) and (n,3n) cross sections. According to this model neutrons are emitted in successive steps and after emission of a neutron if the residual nucleus is left with sufficient energy, a further neutron is emitted and the process is (n,2n). Similarly a third neutron is emitted if residual nucleus is left with sufficient energy after the emission of two neutrons resulting in (n,3n) process. This is in contrast with the method used by Pearlstein[8] who assumes that after emission of first neutron if sufficient energy is available for two neutron emission, they are emitted with a unit probability. Thus he overestimates (n,3n) and underestimates (n,2n) cross sections above the threshold of (n,3n) reactions. For the emission of first particle both the pre-equilibrium and the compound nucleus processes have been considered while subsequent emissions are considered to be due to only the compound nuclear process. Accordingly the expression for the cross

section is given as follows:

$$\sigma(m,in) = (\sigma_R - \sigma_b) \int_{E_n - EBi}^{E_n} \left\{ \frac{d\,bPE}{d\epsilon} + \frac{(1-\delta)\epsilon\rho P_i}{\int_0^{E_{n'}} \epsilon_1 \sigma \rho d\epsilon_1} \right\} d\epsilon$$

where $i = 2$ stands for (n,2n) events and $i = 3$ for (n,3n) events. Above the threshold competition due to (n,4n) is also taken into account. $P_2(\epsilon)$ is the probability that after emission of the first particle with energy $\epsilon$ only one more neutron is emitted and there is not sufficient energy for emitting the third neutron. $P_3(\epsilon)$ is the probability of emitting the third neutron when the second residual nucleus is left with sufficient energy. $P_2$ and $P_3$ are given as follows:

$$P_2 = \frac{\int_{E_n - EB2 - \epsilon}^{E_n - EB1 - \epsilon} \epsilon_2 \sigma_2 \rho_2 d\epsilon_2}{\int_0^{E_n - EB1 - \epsilon} \epsilon_2 \sigma_2 \rho_2 d\epsilon_2}$$

and

$$P_3 = 1 - P_2 = \frac{\int_0^{E_n - EB2 - \epsilon} \epsilon_2 \sigma_2 \rho d\epsilon_2}{\int_0^{E_n - EB1 - \epsilon}}$$

$EB1$ and $EB2$ are separation energies for one and two neutrons respectively. $\rho$ is the level density and is taken of the form $\sim e^{2\sqrt{a u}}$, $u$ is the excitation energy of the residual nucleus and $a$ is the level density parameter taken

from Pearlstein[8] which in this case comes out to be $10.750\ MeV^{-1}$.

$\frac{d\sigma_{PE}}{d\epsilon}$ is the term due to preequilibrium emission and is given by

$$\frac{d\sigma_{PE}}{d\epsilon} = \frac{(2S+1)m\epsilon\sigma_{inv}(\epsilon)}{2\pi\hbar^2|M|^2 g^4 E^3} \sum_{n=3}^{\bar{n}} \left(\frac{U}{E}\right)^{n-2} \times (n-1)(n+1)\rho_n$$

where symbols have the usual meaning. The last factor $\rho_n$ arises due to neutron-proton distinguishability. $g$ is single particle level density and is chosen as $A/13\ MeV^{-1}$. The inverse cross section is calculated using the parametrized form given by Chatterjee et al[9]. $|M|^2$ is the average interaction metrix element and is taken to be dependant on average exciton energy ( $E/n$ ) as given by Kalbach[10]

$$M^2(n,E) = \frac{K'}{A^3 e}\left(\frac{e}{7MeV}\right)^{\frac{1}{2}}\left(\frac{e}{2MeV}\right)^{\frac{1}{2}} \qquad e < 2MeV$$

$$M^2(n,E) = \frac{K'}{A^3 e}\left(\frac{e}{7MeV}\right)^{\frac{1}{2}}, \qquad 2MeV \le e < 7MeV$$

$$M^2(n,E) = \frac{K'}{A^3 e}, \qquad 7MeV \le e < 15MeV$$

$$M^2(n,E) = \frac{K'}{A^3 e}\left(\frac{15MeV}{e}\right)^{\frac{1}{2}}, \qquad 15MeV < e$$

$e$ is the average exciton energy $E/n$, $E$ being the exciton number. However Kalbach has given the value of $a$ as $135\ MeV^3$, We used $K' = 270\ MeV^3$ as determined by an

extensive comparison of (n,xn) (n = 2,3) cross-sections in medium and heavy nuclei[7].

For non-fissionable nuclei $\sigma_f$ is zero, for fissionable nuclei $\sigma_f$ is required. A computer code has been developed to calculate (n,xn) cross section including the competition due to (n,4n) process. Calculations have been performed using this code from threshold to 28 MeV for about 15 nuclei in the mass region 89 to 238. However in case of $^{232}Th$ and $^{238}U$ the calculation was done upto 20 MeV as fission cross sections for these two cases were taken from ENDF-B-IV where data are given upto 20 MeV only. Calculatedcross sections were found to agree well within 10-15% with the recent measurements.

The method can be used to calculate (n,2n) and (n,3n) cross sections in cases where measurement does not exist or is very poor. $\sigma_{n,2n}$ and $\sigma_{n,3n}$ were calculated for $^{239}Pu$. In case of $^{239}Pu$ $\sigma_f$ is quite large and is about 80% of $\sigma_R$. Thus an accurate knowledge of $\sigma_R$ and $\sigma_f$ is essential. Kari et al[11] have measured fission cross section for $^{239}Pu$ with an accuracy of 3%. Patrick[12] has compared different measurements on fission cross sections on $^{239}Pu$ and found that Kari's measurements agree well with other

measurements. $\sigma_R$ is calculated as the difference of the total and the elastic cross sections listed in JAERI[13].

Calculated results are compared with the evaluations of Hunter[1], Prince[2], Sukhovitskij[3] and Kikuchi[4] alongwith the measurements of Mather[5] in fig.1. The results of first three authors are too low as compared to our results. In case of Hunter inelastic scattering comes out to be quite large. Even at 15 MeV (about 9 MeV above the threshold of (n,2n) reaction) inelastic scattering cross section is 52% of total neutron emission cross section. Sukhovitskij's values are very low. Our results agree reasonably well with Kikuchi's evaluations and also with the measurements of Mather. Pre-equilibrium contribution is not considered by other authors. Below 15 MeV it is not very significant. The present calculations are estimated to be accurate within 20%.

References:

1. R.E. Hunter et al LA-5172 (1973).
2. A. Prince et al BNL-50388 (1973)
3. E. Sh. Sukhovitskij and V.A. Kon'shin INDC (CCP)-63/L Feb. (1975)
4. Y. Kikuchi, T. Nakagarwa, H. Motsunobu, Y. Kanda, M. Kawai and T. Murata. JAERI-M 6996 (Feb.1977)
5. D.S. Mather, P.F. Bampton, R.E. Coles, G. James and P.J. Nind. AWRE O 72/72, EANDC (UK) 142-AL
6. M.L. Jhingan, R.P. Anand, S.K. Gupta and M.K. Mehta, Proc. International Conf. on Neutron Phys. and Nucl. Data, Harwell (1978) pp-1049
7. M.L. Jhingan, R.P. Anand, S.K. Gupta and M.K. Mehta, Proc. Nucl. Phys. & Solid State Phys. Symposium, Delhi (1980).
8. S. Pearlstein, Nucl. Sc. Eng. 23, 238 (1965).
9. A. Chatterjee, K.H.N. Murthy and S.K. Gupta, Pramana 16, 391 (1981).
10. C. Kalbach, Z. Physik A 287, 319 (1978).
11. K. Kari and S. Cierjacks, Progress report on Nucl. Data Research in F.R.G. NEANDC(E)-192, Vol.5 pp.6 (1978)
12. B.H. Patrick. Proc. Int. Conf. on Neutron Phys. and Nucl. Data, Harwell (1978) pp.76
13. JAERI 1261 March (1979).

Teble I

(n,2n) and (n,3n) cross section for $^{239}Pu$.

| $E_n$ | $\sigma_R$ | $\sigma_t$ | $\sigma_{n,2n}$ | $\sigma_{n,3n}$ |
|---|---|---|---|---|
| 5.50 | 2.78 | 1.720 | 0.0 | |
| 5.75 | 2.78 | 1.760 | .012 | |
| 6.0 | 2.80 | 1.803 | .0889 | |
| 6.25 | 2.82 | 1.840 | .198 | |
| 6.50 | 2.82 | 1.906 | .293 | |
| 7.0 | 2.82 | 2.033 | .418 | |
| 7.5 | 2.82 | 2.135 | .471 | |
| 8.0 | 2.82 | 2.228 | .469 | |
| 8.5 | 2.83 | 2.219 | .523 | |
| 9.0 | 2.83 | 2.219 | .547 | |
| 9.5 | 2.83 | 2.219 | .562 | |
| 10.0 | 2.83 | 2.211 | .579 | |
| 10.5 | 2.83 | 2.219 | .578 | |
| 11.0 | 2.83 | 2.219 | .582 | |
| 11.5 | 2.83 | 2.211 | .593 | |
| 12.0 | 2.83 | 2.203 | .603 | |
| 12.5 | 2.83 | 2.228 | .580 | |
| 13.0 | 2.83 | 2.270 | .541 | .0004 |
| 14.0 | 2.83 | 2.330 | .459 | .026 |
| 15.0 | 2.83 | 2.381 | .342 | .095 |
| 16.0 | 2.83 | 2.380 | .255 | .184 |
| 17.0 | 2.83 | 2.326 | .201 | .291 |
| 18.0 | 2.83 | 2.250 | .163 | .404 |
| 19.0 | 2.83 | 2.222 | .125 | .471 |
| 20.0 | 2.83 | 2.234 | .093 | .490 |

$^{239}$Pu: σ(n, 2n) and σ(n, 3n) EVALUATION

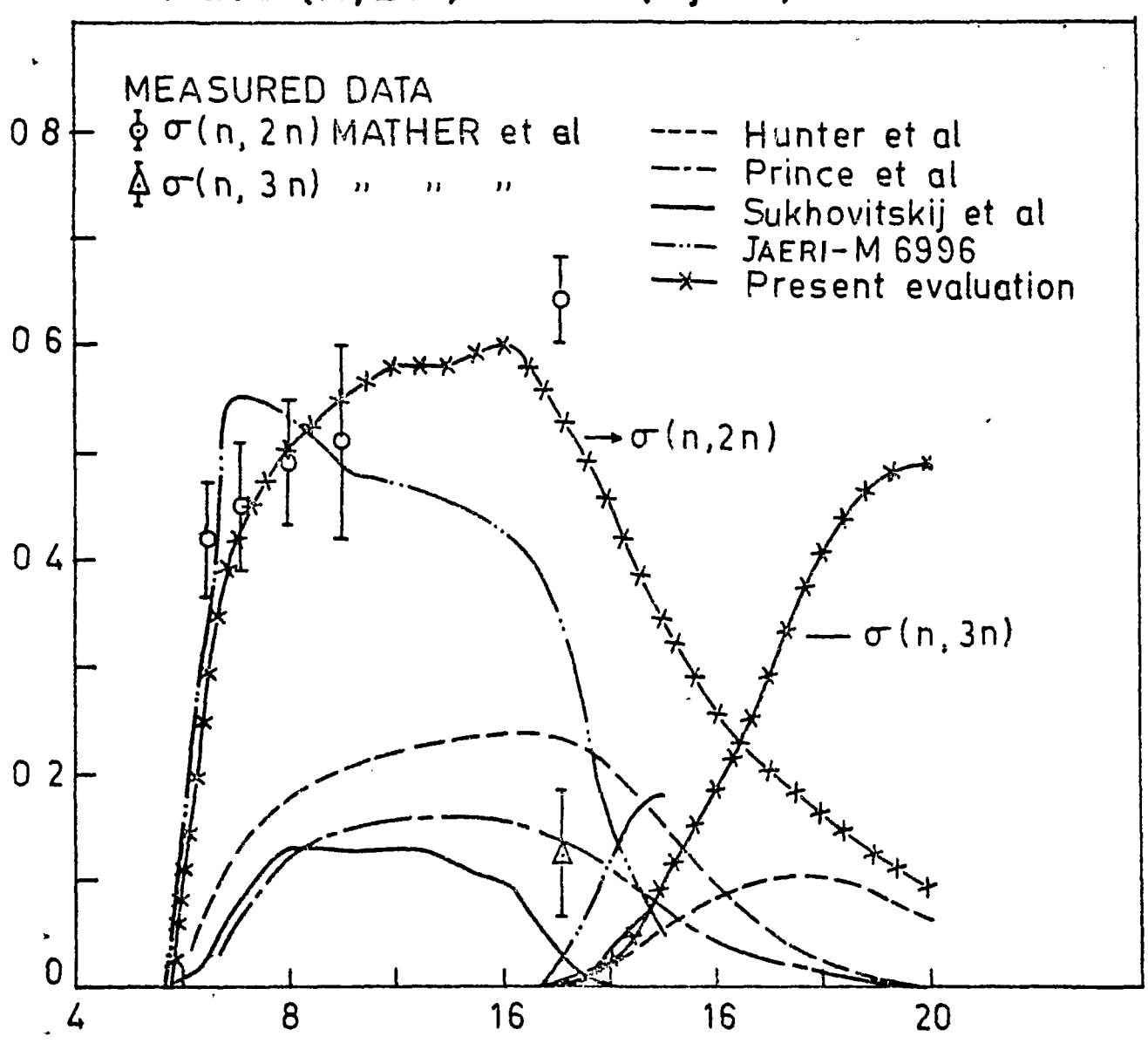


FIG. 1.

# COMMENTS ON $^{9}Be$ (n, 2n) CROSS SECTION DATA IN THE CONTEXT OF FISSION AND FUSION SYSTEMS

P.K. Job, T.K. Basu, K. Subba Rao and M. Srinivasan

Neutron Physics Division,
Bhabha Atomic Research Centre,
Trombay, Bombay 400 085.

## Introduction:

Beryllium can be used as an efficient neutron reflector/ blanket multiplier in fission/fusion systems. Because of its favourable neutronic characterstics and (n, 2n) reactions, beryllium improves neutron economy significantly and thus lowers the critical mass in fission systems and enhances breeding of fusile fuel in fusion blankets containing lithium.

In order to validate the available beryllium data, a quantity $M_{\infty}(E)$[1], defined as the net number of neutrons absorbed per neutron of energy E released into an infinite beryllium system, is calculated using the available cross section data and compared with the corresponding experimentally deduced quantities. $M_{\infty}(E)$ is a unique constant which eliminates the leakage and spatial dependence of neutron flux and is less sensitive to anisotropic scattering.

## Beryllium Cross Section Data for Fission Systems

In the case of fission systems, $M_{\infty}$ was calculated using the DTF-IV (transport theory) code for fission neutrons in an infinite beryllium assembly with the Hansen and Roach (HR) cross section set. $M_{\infty}$ was calculated as the total number of absorptions + leakage per fission neutron introduced at the centre of a large Be (40 cm radius) sphere. $M_{\infty}$ was also deduced for fission spectrum using the latest ENDL-78 data[2]. The $M_{\infty}$ values obtained by the ENDL-78 set compared very well with the experimental value of $1.12 \pm .05$ quoted by Krasin et al[3]. However, the HR set gave much higher $M_{\infty}$ value of 1.21. The overestimation of $M_{\infty}$ by HR set is attributed to the incorrect inelastic transfer cross sections of the first two groups,

( > 3.0 MeV and from 3.0 to 1.4 MeV).

Since in general HR set showed excellent agreement with experimental $k_{eff}$ values in the case of bare $^{233}U$ uranyl nitrate solution systems[4], we decided to modify only the inelastic scattering cross section of beryllium. The (n, 2n) inelastic scattering group cross sections of beryllium was derived from ENDL-78 point cross section data by collapsing over the fission spectrum between 1.4 to 10 MeV. Table I gives the deduced (n, 2n) cross sections of Be for the 16 group HR set. The quantities given in the brakets are original values of HR set. $M_{\infty}$ calculation with the modified set for a 40 cm radius Be sphere gave a value of 1.13 ± .01 which is in very good agreement with the experimental result. Using the modified 16 - group cross section set for beryllium, $M_{\infty}$ value for BeO due to a fission source was estimated as 1.085 ± .01 which is lower than the $M_{\infty}$ value for Be. This lower value is presumably due to the elastic scattering in oxygen which brings down the energy of some of the fission neutrons below (n, 2n) threshold.

Beryllium Cross Section Data for Fusion Systems

An integral measurement of the multiplication of 14-MeV neutrons in beryllium has indicated a 25% lower value than the calculated one using the present day cross section data[5]. This discrepancy could be attributed either to the secondary neutron spectra being softer than presently assumed or the (n, 2n) cross section being slightly overestimated.

In order to understand the influence of the secondary neutron spectra on the overall neutron multiplication, the variation of $M_{\infty}(E)$ as a function of incident neutron energy E was studied. The detailed analysis of this study is reported in Ref.[6]. Values of M for 14-MeV neutrons in $^{9}Be$ using different available cross section sets was found to be 2.5 ± 0.1.

To study the upper and lower limits of $M_{\infty}$ due to changes in secondary neutron spectra, $M_{\infty}$ was calculated in four different stages:

(i) It is assumed in the first stage that the elastic scattering and (n, 2n) reaction leaves the neutrons at energies less than the $^{9}Be$ (n, 2n) threshold so that secondary (n, 2n) reactions are not possible. In this case, the multiplication is simply given by,

$$M_{\infty} \quad (E) \quad = \quad 1 + \frac{\sigma_{n,2n}}{\sigma_{f}}$$

The $M_{\infty}$ value for a 14-MeV neutron is 1.34.

(ii) In the second stage, the elastic scattering is treated properly, i.e. the energy loss in an elastic event is considered and the group transfers are calculated accordingly. The neutrons which are emitted in (n, 2n) reactions however, are assumed to have energies less than the reaction threshold.

(iii) In the third stage, the energy of the 'first neutron' (direct neutron) from (n, 2n) reaction is considered properly whereas the 'second neutron' (from compound nucleus) is assumed to have energies less than the reaction threshold energy.

(iv) In the last stage, the 'second (n, 2n) neutron' is also considered to have energies as given in the cross section data file.

The values of $M_{\infty}$ at different stages using the data set of LLL - ENDL (1978) are shown in Fig. 1. For 14-MeV neutrons the $M_{\infty}$ varied from 1.9 for stage 2 to 2.5 for stage 4. Therefore, the maximum contribution from second and subsequent generations of (n, 2n) multiplication to the $M_{\infty}$ (14) value is ~25%. Thus the secondary neutron spectrum has a strong influence on the $M_{\infty}$ value and this in turn depends upon the various partial cross sections of the (n, 2n) decay mode.

Conclusion

The conclusions are, for fission system the latest $^{9}Be$ cross section data is quite adequate whereas for fusion systems,

the evaluated secondary (n, 2n) spectra is harder than the actual spectra. However, it is found that the uncertainties in the (n, 2n) neutron spectra alone can not explain the discrepancy of about 25% between the experimental and calculated values of multiplication in beryllium. It is therefore possible that part of the discrepancy may be attributed to a slight overestimation of the $^{9}$Be (n, 2n) cross section for energies greater than 8 MeV. This calls for further measurements to determine the (n, 2n) cross section and the secondary neutron emission spectra for a number of incident neutron energies of interest to fusion reactor blankets.

References:

1. Basu, T.K., "Studies on Multiplication of 14 MeV Neutrons in Be Assemblies for Fusion Reactor Blankets", Ph. D. Thesis, University of Bombay (1980).

2. Perkins, S.T., Private Communication (1979)

3. Krasin, A.K., et. al., "Physics Characteristics of Beryllium Moderated Reactor", Proc. Second International Conference on the Peaceful Uses of Atomic Energy, V 12 (1958).

4. Job, P.K., "Neutron Multiplication Studies in a BeO Reflected $^{233}$U Uranyl Nitrate Solution Subcritical Assembly", M. Sc. thesis, University of Bombay (1980).

5. Basu, T.K., Nargundkar, V.R., Cloth, P., Filges, D. and Taczanowski, S., Nucl. Sci. Eng., 70, 309 (1979).

6. Basu, T.K., Subba Rao, K. and Srinivasan, M., Atomkernenergie - Kerntechnik, 36, 30 (1980).

TABLE I

Modified (n, 2n) Be Cross Sections For HR Set

| Energy Range (MeV) | $\sigma_{(n, 2n)}$ | $\sigma^{*}_{g \to g}$ | $\sigma^{*}_{g \to g+1}$ | $\sigma^{*}_{g \to g+2}$ |
|---|---|---|---|---|
| 10 - 3.0 | 0.41 | 0.447 | 0.920 | 0.355 |
| | (0.35) | (0.432) | (0.818) | (0.35) |
| 30 - 1.4 | 0.037 | 0.898 | 0.469 | 0.037 |
| | (0.12) | (0.934) | (0.509) | (0.12) |

* Includes elastic transfers also.

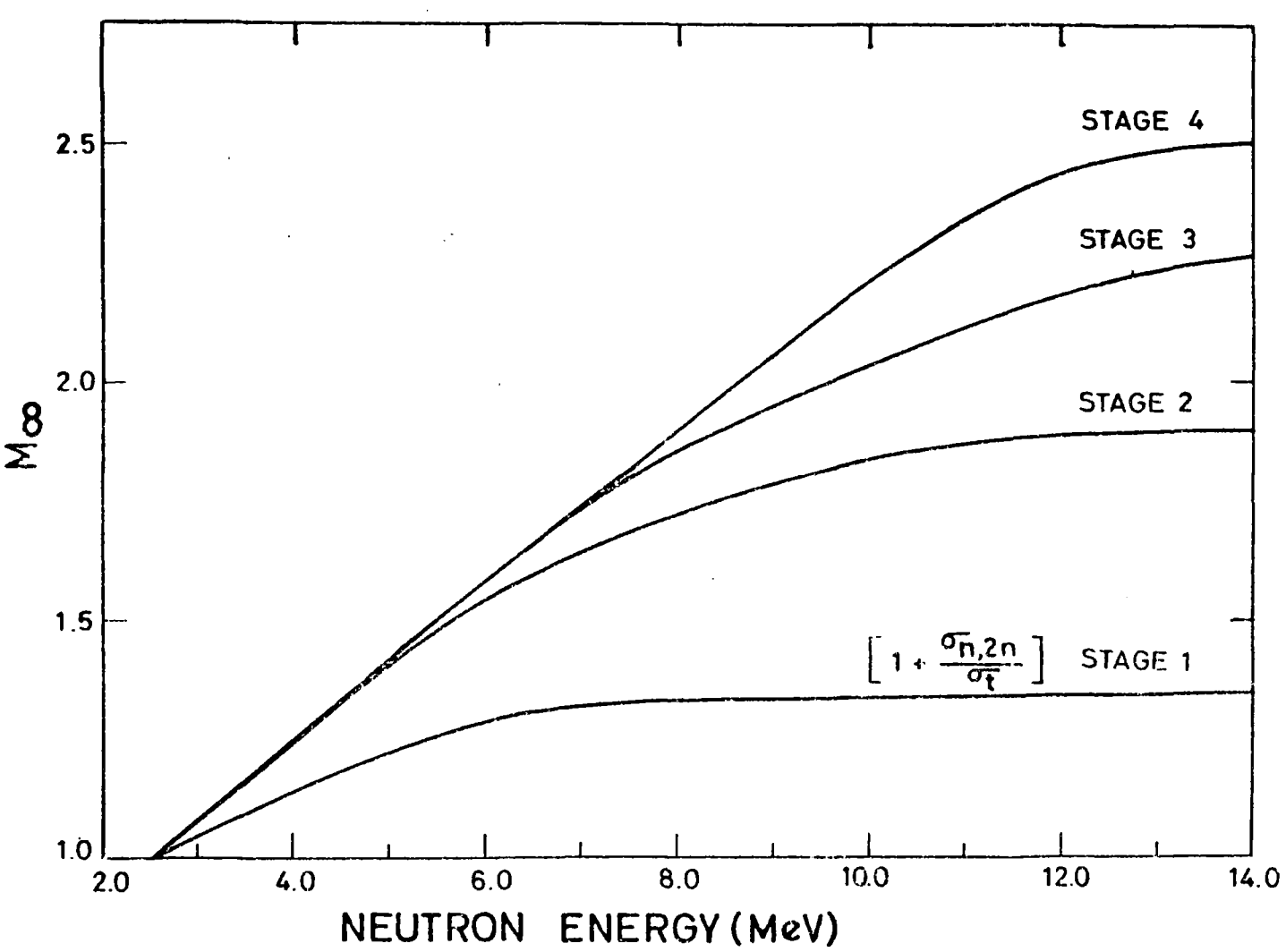


$M_\infty$ AS FUNCTION OF INCIDENT NEUTRON ENERGY FOR DIFFERENT STAGES USING ENDL DATA

FIG.

GOVERNMENT OF INDIA

BHABHA ATOMIC RESEARCH CENTRE

# EVALUATION OF THERMAL REACTOR CROSS-SECTIONS THROUGH INTEGRAL MEASUREMENTS

by

H.C.Huria, P.D.Krishnani, H.K.Bhatia, P.Mohanakrishnan and

B.P.Rastogi

Theoretical Reactor Physics Section

PAPER TO BE PRESENTED IN THE WORKSHOP ON NUCLEAR DATA EVALUATION, PROCESSING AND TESTING, REACTOR RESEARCH CENTRE, KALPAKKAM, AUGUST 4-5, 1981.

# Evaluation of Thermal Reactor Cross-Sections through Integral Measurements

## Abstract

Integral measurements of various types provide valuable data to assess the adequacy of the cross-sections used in predicting the nuclear characteristics of reactors. In this context, measurements of reactivity, relative reaction rates and neutron balance assume fundamental importance. The lattice physics calculational model of TRPS uses the 69-group WIMS library or its collapsed versions, for light water and heavy water moderated systems. The library has been generated using the fundamental nuclear data from UKNDL and weighting spectra typical of thermal reactors.

The accuracy of the physical formulation of the model, which uses interface currents, has been established by comparisons with results from more sophisticated approaches, and also with Monte-Carlo calculations. A broad spectrum of experimental data was selected to evaluate the adequacy of the cross-sections used in the code. The selected experiments include natural uranium, enriched uranium, $U^{233}$- enriched and plutonium oxide fuelled lattices in $D_2O$ and $H_2O$ moderator, and they cover a wide range of parameters. The analyses included, not only reactivity prediction, but also comparison of measured and calculated reaction rate ratios. Internationally recommended benchmarks for thermal reactors have also been extensively analysed. The observed discrepencies did lead to modifications in some areas of basic nuclear data for fissile and fertile materials. However, the work with regard to the suspected uncertainties in the data for moderating materials is in progress.

# EVALUATION OF THERMAL REACTOR CROSS-SECTIONS THROUGH INTEGRAL MEASUREMENTS

H.C.Huria, P.D.Krishnani, H.K. Bhatia, P.Mohanakrishnan, and B.P. Rastogi

## I. INTRODUCTION

For a thorough understanding of the behaviour of thermal reactors, under all operating conditions, a detailed assessment of various physical processes has to be carried out. This essentially calls for an accurate nuclear data together with exact calculational procedures. Thus, the accuracy of predicting the nuclear characteristics of reactors is contributed both by uncertainties in the basic cross-sections and by the limitations of the physical formalism.

In this paper, we report on the results of the analyses of a wide variety of integral experiments in thermal systems. The selected experiments cover a broad spectrum of parameters such as fuel enrichment, isotopic composition, lattice pitch, buckling,etc. The analysis includes not only the reactivity prediction, but also comparison of calculated and measured relative reaction rates and spectral indices wherever available. This study was undertaken to evaluate the multi-group cross-sections generated by us using nuclear data from ENDF/B-IV and also those from WIMS library. The uncertainties from the calculational prôcedures were also evaluated through intercomparisons with more sophisticated models. The emphasis in this paper is, however, on the evaluation of uncertainties coming from nuclear data.

## II. CROSS-SECTIONS AND METHODS OF ANALYSIS

The methods of analysis used in the physics design aspects of thermal reactors make use of multigroup integral transport theory. The spatial coupling in obtaining the spatial distribution of neutrons is realised through different means, namely, interface currents (MURLI Code) [1], first flight collision probabilities (COP) [2], a combination of interface currents and first flight probabilities (CLUB) [3], For intercomparison of methods, we have also considered the differential transport theory-$S_N$ method- also (DTF-IV) [4].

For the treatment of energy variable, we have used the 69-group structure of WIMS code [5], and the associated cross-sections library. The group structure as shown in Table-1, was designed primarily for thermal reactors. The fast range (defined to lie between 10 MeV and 9.118 KeV), is divided into 14 groups of equal lethargy width; the resonance range (9.118 KeV-4 eV) is covered by 13 groups, while the thermal range (below 4eV) is described by 42 groups. The group boundaries of 13 resonance groups were decided keeping the locations of important resonances of main fissile and fertile isotopes in view. The thermal range has groups clustered around the peak of thermal spectrum and also around the thermal energy resonances of plutonium isotopes.

The group constants have been derived from UKNDL using appropriate weighting spectra-typical of thermal systems. However, a special treatment was accorded to the resonance range, where the cross-sections

depend on composition (geometry) and on temperature. Here, the slowing down equations in an infinite homogeneous mixture of absorber and a moderator were solved numerically in the relevant energy range. The tables of resonance integrals in terms of composition and temperature were derived from there. The library has the tables for $U^{235}$, $U^{236}$, $U^{238}$ and $Pu^{239}$. $Th^{232}$ and $U^{233}$ cross-sections were not available in the original WIMS library. These were generated using resonance parameters from ENDF/B-IV.

With 69 group library as base, 27-group libraries were generated using representative spectra for light water and heavy water moderated systems as the weighting functions. This was done with a view to reduce the computational time. However, for the benchmarks recommended by cross-section evaluation working group (CSEWG) the basic 69-group library was used as such.

Extensive analyses of some typical thermal reactor lattice experiments by the sophisticated WIMS [6,7] code which also uses the same library had indicated some areas of cross-sections, where modifications in the original UK data were necessary. These were

(i) changes in $U^{238}$ resonance integral (a reduction of 4%)

(ii) reduction in the epithermal capture to fission ratio of $U^{235}$ (0.67 to 0.5)

(iii) hardening of fission spectrum

(iv) some minor changes in the epithermal scattering cross-sections of H and D.

These changes have since been confirmed by full 3D Monte-Carlo [8] simulations of some thermal reactor benchmarks. Our present analyses incorporate all these modifications.

...4

There are of course still some areas which call for adjustments as we will presently see.

## III. RESULTS

### III.1 LIGHT WATER MODERATED SYSTEMS

We have examined more than 150 lattice experiments with enriched U-metal or oxide rods in light water moderator. Majority of these were critical experiments with enrichment varying from 1wt% to 5.7wt% $U^{235}$, and a wide range of other relevant parameters. Besides, enriched uranium fuel, we have also studied critical experiments with mixed oxide ($PuO_2$) fuel and ($U^{233}$-$Th^{232}$)$O_2$ fuel bearing rods in light water moderator to examine the data for the plutonium isotopes and thorium. The results of these extensive analyses have been presented in reference 9. Here we will be presenting results mainly for the benchmarks recommended by Cross-Sections Evaluation Working Group [10] to evaluate data for thermal reactors. These include

(i) 4-TRX Lattices-Slightly enriched uranium metal rods in light water (BNL-experiments)

(ii) 3-erriched $UO_2$ fuelled lattices (BAPL-experiments)

(iii) $H_2O$ moderated thorium oxide exponential experiments.

The parameters compared for TRX Lattices are

(i) $\rho^{28}$ - epithermal to thermal captures in $U^{238}$

(ii) $\delta^{25}$ - epithermal to thermal fission in $U^{235}$

(iii) $\delta^{28}$ - fissions in $U^{238}$ to those in $U^{235}$

(iv) CR* - captures in $U^{238}$ to fissions in $U^{235}$

(v) k - effective multiplication factor

The results are indicated in Table-2. It will be noticed that all the ratios are predicted correctly, the difference between the calculated and measured being within ± 5mk (0.5%) of unity which is quite satisfactory. This last point has also been confirmed by the reactivity calculations of a large number of other experiments.

Let us now have a look at the calculations for $H_2O$ moderated $UO_2$ criticals. Here also the parameters compared, are the same as for the TRX Lattices except the modified conversion ratio CR*. The calculated parameters are compared with the measured ones in Table-3. Once again, we notice a good comparison, the differences lying between ± 5%.

These two comparisons indicate that the data being used by us for relevant materials are quite adequate. We have, in fact, also ascertained the uncertainties because of the method of calculation by comparing the results of same lattices, by different formulations. These discrepancies were not significant leading to the aforesaid conclusions.

As regards the experiments with thorium-$U^{233}$ oxide fuel, we are again quoting the results for the recommended benchmarks.[11] . These are three exponential experiments done at BNL. The parameters compared are

(i) $\rho^{02}$ - ratio of epithermal to thermal captures in $Th^{232}$

..6

(ii) $\xi_{Dy}$ - Dysprosium-164 disadvantage factor - ratio of activations of $^{164}Dy$ in the moderator to those in the fuel

(iii) k - the effective multiplication factor

The results are shown in Table-4. It is observed that the k-values are predicted extremely well-within 0.6% of unity and that $\xi_{Dy}$ is calculated correctly. However, $\rho_{02}$ is under predicted by 7-14%. Similar results on the same lattices have been reported earlier also. One could thus cast some doubt on the data for $Th^{232}$ particularly, the epithermal one.

## III.2 HEAVY WATER MODERATED LATTICES

### III.2.1 SINGLE ROD LATTICE EXPERIMENTS

The benchmarks recommended for heavy water moderated single rod lattices are small subcritical exponential experiments [10] with natural or slightly enriched uranium metal rods. We tried to analyse these also, but the exact simulation presented some difficulties in the absence of complete geometrical and physical parameters. Moreover, analyses have shown that the experimental bucklings are inconsistant in the sense that measured relative reaction rates are not able to reproduce the measured bucklings. So we are not presenting those results, till we are able to resolve those inconsistencies.

190

We have however, carried out reactivity calculations for nearly 100 single rod critical experiments [12] with natural uranium rods in $D_2O$ moderator. The results are quite satisfactory - the deviations lying between ±5mk over most of the range of moderator to fuel volumes ratios.

III.2.2 EXPERIMENTS WITH CLUSTER FUEL ASSEMBLIES

In view of the aforesaid observation on single rod lattices, we have concentrated our efforts on the analysis of experiments using rod cluster type fuel assemblies. Measurements have been made in Chalk River, Canada, in ZED-2 reactor for various lattice arrangements, that is, different lattice pitches, different sizes of clusters and different coolant materials to provide a broad experimental background to evaluate the calculational models. We have selected 7-, 19- and 28-rod cluster experiments [13,14,15, 16,17] with $D_2O$ and air as coolant materials. The parameters compared are

(i) $\delta^{28}$ - ratio of fissions in $U^{238}$ to those in $U^{235}$

(ii) $\gamma$ - ratio of captures in $U^{238}$ to absorptions in $U^{235}$

(iii) k - the effective multiplication factor

(iv) $\nu_m/\nu_f$ - neutron density disadvantage factor

The clusters are geometrically more complex and hence, difficult to simulate. We have done these calculations by three different approaches in increasing order of sophistication ( or

..6

accuracy). They are

(i) Interface currents (MURLI)

(ii)Combination of interface currents and Pij method (CLUB)

(iii) Complete Pij method (COP)

This study of intercomparison of formulation was helpful in assessing the uncertainties coming from limitations of physical formulation.

Tables 5 through 10 give the results for 7-, 9-. and 28-rod cluster experiments with $D_2O$ and Air coolants. The calculated parameters from both the approaches (MURLI and CLUB) are quoted along with the experimental values. The study involving the comparison of these approaches with the most accurate one (3rd approach) had shown a maximum difference of 0.2% in k while the reaction rates matched exactly.

The calculated values of the relative reaction rates are leakage corrected using the measured buckling. In principle, one should use the critical buckling for this purpose. But since the calculated k's are very close to unity, it is immaterial which buckling to use.

It will be seen that the predictions for the modified conversion ratio are very good for the majority of cases, the errors are well within the experimental uncertainties. This shows once again the soundness of the resonance cross-sections of $U^{238}$ in conformity with our earlier observations. However, the fast fissions ratios are generally over-estimated. The deviations are ofcourse not very large except at the lowest pitch. It is worthwhile pointing here, that

even the experimental values differ in two publications of the same set of experiments, in particular, for the lattices where the deviations are largest. If we recall that even for light water moderated lattices $\delta^{28}$ was slightly over-predicted for both TRX and BAPL benchmarks, this observation is not surprising. One could thus, say that the hardening of the fission spectrum as recommended by WIMS group was on a slightly higher side.

## IV. CONCLUSIONS

The most prominent observation that could be made from a scrutiny of the analyses presented in this paper is that the cross-sections library being used at present is quite adequate in predicting the nuclear characteristics of thermal reactors. This is true for all the systems studied in general and more so for light water moderated ones. The discrepancies noticed for the heavy water moderated experiments point towards a close re-examination of thermal scattering data for $D_2O$. The overestimate of fast fission ratios for all types of lattices also suggests a further check of fission spectrum for $U^{235}$. Another point that comes out is that the resonance cross-sections of $Th^{232}$ (and probably those of $U^{233}$ as well) should be looked at more thoroughly.

## V. REFERENCES

1. Huria H.C. : MURLI - A Multigroup Integral Transport Theory Code for Thermal Reactor Lattice Studies, Atomkernenergie 31(1978) 37.

2. Carlvik I. : A Method for Calculating Collision Probabilities in General Cylindrical Geometry and Applications to Flux Distribution and Dancoff Factors, Proc. 1964 Int.Conf.Peaceful Uses of Atomic Energy, 2 (1965) 225.

3. Krishnani P.D. : CLUB - A Multigroup Integral Transport Theory Code for the Analysis of Cluster Lattices, to be published.

4. Lathrop K.D. : A FORTRAN IV Program for Solving Multigroup Transport Equations with Anisotropic Scattering. Report LA-3373 (1965).

5. Askew, J.R. et al: A General Description of the Lattice Code WIMS, Journal of Brit.Nucl.Energy Soc. 5(1966) 564.

6. Hemshell, P.B. : Some Integral Properties of Nuclear Data Deduced from WIMS Analysis of Well Thermalised Uranium Lattices, Report AEEW-R-786 (1972).

7. Chawla, R. : An Assessment of Methods and Data for Predicting Integral Properties of Thermal Reactor Physics Experiments, Report AEEW-R-797 (1972)

8. Hardy J : The Performance of ENDF/B Data in Thermal Reactor Benchmark Testing - Some results with Version IV and Prospects for Version V, Trans. Am.Nucl. Soc. 28 (1978) 736.

9. Huria, H.C. : Evaluation of the Lattice Physics Code 'MURLI' for Light Water Lattices, Annals of Nuclear Energy 8 (1981) 183.

10. Cross-Section Evaluation Working Group. Benchmark Specifications, Report BNL-19302 (ENDF-202) (1974)

11. Windsor, H.H. et al : Exponential Experiments with Lattices of $U^{233}$ oxide and Thorium oxide in Light and Heavy Water, Nuc.Sc.Engg. 42 (1970) 150.

12. Honeck H.C.et al: The Physics of Heavy Water Lattices, Reactor Technology, Selected Reviews - 1965.

..11

13. Green R.E. et al: Highlights of Chalk river Work on the Physics of Heavy Water Lattices Since the 1959 IAEA Panel Meeting -Report AECL - 1684 (1962).

14. Green R.E. et al: Lattice Parameters Measurements in ZED-2,IAEA Symposium on Exponential and Critical Experiments, Vol.II(1964)457.

15. Green, R.E. et al: Lattice Studies at Chalk River and their Interpretation - Report AECL 2025 (1964).

16. Serduda K.J. - Lattice Measurements with 28-element $UO_2$ Fuel Assemblies Part I - Buckling for a Range of Spacing with Three Coolants - Report AECL 2686 (1966).

17. De Lange P.W. et al : Experimental Initial Conversion and Fast Fission Ratios for Clusters of Natural U and $UO_2$ in $D_2O$ - Report AECL - 2636 (1966).

## T A B L E - 1

ENERGY BOUNDARIES FOR 69-GROUP LIBRARY

Upper energy limit of the first group-10.0 MeV

| Group | Lower Energy Limit MeV | Energy Width. MeV | Lethargy Width |
|---|---|---|---|
| 1. | 6.0655 | 3.9545 | 0.5 |
| 2. | 3.679 | 2.3865 | 0.5 |
| 3. | 2.231 | 1.448 | 0.5 |
| 4. | 1.353 | 0.878 | 0.5 |
| 5. | 0.821 | 0.532 | 0.5 |
| 6. | 0.500 | 0.321 | 0.5 |
| 7. | 0.3025 | 0.1975 | 0.5 |
| 8. | 0.183 | 0.1195 | 0.5 |
| 9. | 0.111 | 0.072 | 0.5 |
| 10. | 0.06734 | 0.4366 | 0.5 |
| 11. | 0.04085 | 0.02649 | 0.5 |
| 12. | 0.02478 | 0.01607 | 0.5 |
| 13. | 0.01503 | 0.00975 | 0.5 |
| 14. | 0.00912 | 0.00591 | 0.5 |
| | eV | eV | |
| 15. | 5530.0 | 3588.0 | 0.5 |
| 16. | 3519.1 | 2010.9 | 0.452 |
| 17. | 2239.45 | 1279.65 | 0.452 |
| 18. | 1425.1 | 814.35 | 0.452 |
| 19. | 906.9 | 518.20 | 0.452 |
| 20. | 367.26 | 359.64 | 0.904 |
| 21. | 148.73 | 218.53 | 0.904 |
| 22. | 75.501 | 73.23 | 0.678 |
| 23. | 48.052 | 27.45 | 0.452 |
| 24. | 27.70 | 20.35 | 0.551 |
| 25. | 15.968 | 11.73 | 0.551 |
| 26. | 9.877 | 6.09 | 0.480 |
| 27. | 4.000 | 5.877 | 0.904 |

| Group | Lower Energy Limit eV | Energy Width eV | Lethargy Width |
|---|---|---|---|
| 28. | 3.30 | 0.700 | 0.1924 |
| 29. | 2.60 | 0.700 | 0.2384 |
| 30. | 2.10 | 0.500 | 0.2136 |
| 31. | 1.50 | 0.600 | 0.3365 |
| 32. | 1.30 | 0.200 | 0.1431 |
| 33. | 1.15 | 0.150 | 0.1226 |
| 34. | 1.123 | 0.027 | 0.0237 |
| 35. | 1.097 | 0.026 | 0.0234 |
| 36. | 1.071 | 0.026 | 0.0240 |
| 37. | 1.045 | 0.026 | 0.0246 |
| 38. | 1.020 | 0.025 | 0.0242 |
| 39. | 0.996 | 0.024 | 0.0238 |
| 40. | 0.972 | 0.024 | 0.0244 |
| 41. | 0.950 | 0.022 | 0.0229 |
| 42. | 0.910 | 0.040 | 0.0430 |
| 43. | 0.850 | 0.060 | 0.0682 |
| 44. | 0.780 | 0.070 | 0.0859 |
| 45. | 0.625 | 0.155 | 0.2215 |
| 46. | 0.500 | 0.125 | 0.2231 |
| 47. | 0.400 | 0.100 | 0.2231 |
| 48. | 0.350 | 0.050 | 0.1335 |
| 49. | 0.320 | 0.030 | 0.0896 |
| 50. | 0.300 | 0.020 | 0.0645 |
| 51. | 0.280 | 0.020 | 0.0690 |
| 52. | 0.250 | 0.030 | 0.1133 |
| 53. | 0.220 | 0.030 | 0.1278 |
| 54. | 0.180 | 0.040 | 0.2007 |
| 55. | 0.140 | 0.040 | 0.2513 |
| 56. | 0.100 | 0.040 | 0.3365 |
| 57. | 0.080 | 0.020 | 0.2231 |
| 58. | 0.067 | 0.013 | 0.1773 |
| 59. | 0.058 | 0.009 | 0.1442 |
| 60. | 0.050 | 0.008 | 0.1484 |
| 61. | 0.042 | 0.008 | 0.1743 |
| 62. | 0.035 | 0.007 | 0.1823 |
| 63. | 0.030 | 0.005 | 0.1541 |
| 64. | 0.025 | 0.005 | 0.1823 |
| 65. | 0.020 | 0.005 | 0.2231 |
| 66. | 0.015 | 0.005 | 0.2877 |
| 68. | 0.005 | 0.005 | 0.6931 |
| 69. | 0.0 | 0.005 | - |

T A B L E - 2

ENRICHED U - METAL BENCHMARKS

| PARAMETER PITCH | METHOD | $f^{28}$ | $\delta^{25}$ | $\delta^{28}$ | CR* | k |
|---|---|---|---|---|---|---|
| cm 1.606 | EXPT | 3.01 ± 0.05 | 0.230 ± 0.03 | 0.163 ±0004 | 1.255 ±0.011 | 1.000 |
| | MURLI | 2.94 | 1.225 | 0.170 | 1.238 | 0.998 |
| 2.174 | EXPT | 1.311± 0.02 | 0.0901± 0.001 | 0.0914±0.002 | 0.792 ±0.008 | 1.000 |
| | MURLI | 1.276 | 0.0936 | 0.0948 | 0.783 | 1.005 |
| 1.447 | EXPT | 0.830±0.015 | 0.0608±0.0007 | 0.0667±0.002 | 0.646 ±0.002 | 1.000 |
| | MURLI | 0.796 | 0.0577 | 0.0670 | 0.634 | 0.999 |
| 2.882 | EXPT | 0.466±0.010 | 0.0352±0.0004 | 0.0452±0.0007 | 0.526±0.004 | 1.000 |
| | MURLI | 0.465 | 0.0336 | 0.0466 | 0.527 | 0.997 |

T A B L E - 3

ENRICHED $UO_2$ BENCHMARKS (BAPL - 1 to 3)

| PARAMETER | | $\rho^{28}$ | $\delta^{25}$ | $\delta^{28}$ | k |
|---|---|---|---|---|---|
| PITCH cm | METHOD | | | | |
| 1.557 | EXPT | 1.39 ± 0.01 | 0.084 ± 0.002 | 0.078 ± 0.004 | 1.0000 |
| | MURLI | 1.433 | 0.0021 | 0.0813 | 0.9934 |
| 1.851 | EXPT | 1.12 ± 0.001 | 0.068 ± 0.001 | 0.070 ± 0.004 | 1.0000 |
| | MURLI | 1.151 | 0.0671 | 0.0719 | 0.9937 |
| 1.805 | EXPT | 0.906 ± 0.01 | 0.052 ± 0.001 | 0.057 ± 0.003 | 1.0000 |
| | MURLI | 0.921 | 0.0516 | 0.058 | 0.9941 |

## T A B L E - 4

## ($Th^{232}$ - $U^{233}$) BENCHMARKS

| PARAMETER PITCH cm | METHOD | $\xi$ Dy | $\beta$02 | k |
|---|---|---|---|---|
| 1.5923 | EXPT | 1.219 ± 0.024 | 1.380 +0.042 | 1.000 |
| | MURLI | 1.216 | 1.233 | 1.005 |
| 1.7188 | EXPT | 1.257 ± 0.024 | 0.928 ±0.038 | 1.000 |
| | MURLI | 1.247 | 0.849 | 1.000 |
| 2.1697 | EXPT | 1.325 ± 0.024 | 0.435 ±0.013 | 1.000 |
| | MURLI | 1.342 | 0.386 | 0.998 |

T A B L E-5

7 - ROD CLUSTER - $D_2O$ COOLANT

| PARAMETER PITCH (cm) | METHOD | k | $\delta^{28}$ | $\gamma$ | $n_m/n_f$ |
|---|---|---|---|---|---|
| 18 | EXPT | 1,0000 | 0.056 | 0.916 | 1.792 |
| | CLUB | 1.0017 | 0.062 | 0.923 | 1.774 |
| 22 | EXPT | 1.0000 | 0.056 | 0.810 | 1.919 |
| | CLUB | 1.0019 | 0.058 | 0.816 | 1.933 |
| 28 | EXPT | 1.0000 | 0.056 | 0.730 | 2.121 |
| | CLUB | 1.0025 | 0.057 | 0.746 | 2.120 |
| 36 | EXPT | 1.0000 | 0.052 | 0.699 | 2.347 |
| | CLUB | 1.0050 | 0.056 | 0.713 | 2.275 |

T A B L E - 6

7 - ROD CLUSTER - AIR COOLANT

| PARAMETER / PITCH | METHOD | k | $\delta^{28}$ | $\gamma$ | $n_m/n_f$ |
|---|---|---|---|---|---|
| cm 19 | EXPT | 1.0000 | 0.058 | 0.873 | 1.728 |
| | CLUB | 0.9971 | 0.0637 | 0.897 | 1.754 |
| 22 | EXPT | 1.0000 | 0.058 | 0.794 | - |
| | CLUB | 1.0016 | 0.0607 | 0.816 | - |
| 28 | EXPT | 1.0000 | - | - | 2.049 |
| | CLUB | 0.9997 | - | - | 2.049 |
| 36 | EXPT | 1.0000 | - | - | 2.225 |
| | CLUB | 1.0040 | - | - | 2.200 |

T A B L E - 7

19 - ROD CLUSTERS - $D_2O$ COOLANT

| PARAMETER | | k | $\delta^{28}$ | $\gamma$ | $n_n/n_f$ |
|---|---|---|---|---|---|
| PITCH cm | METHOD | | | | |
| 18 . . | EXPT. | 1.0000 | 0.0564 | 0.967 | 1.658 |
| | MURLI | 0.9950 | 0.0601 | 0.981 | 1.595 |
| | CLUB | 0.9949 | 0.0589 | 0.975 | 1.602 |
| 21 | EXPT | 1.0000 | 0.0543 | 0.858 | 1.782 |
| | MURLI | 1.0007 | 0.0559 | 0.863 | 1.714 |
| | CLUB | 0.9993 | 0.0548 | 0.860 | 1.784 |
| 24 | EXPT | 1.0000 | 0.0528 | 0.806 | 1.856 |
| | MURLI | 1.0030 | 0.0539 | 0.798 | 1.815 |
| | CLUB | 1.0010 | 0.0531 | 0.797 | 1.888 |
| 28 | EXPT | 1.0000 | 0.0481 | 0.749 | 1.989 |
| | MURLI | 1.0020 | 0.0529 | 0.750 | 1.926 |
| | CLUB | 0.9993 | 0.0522 | 0.750 | 2.003 |
| 36 | EXPT | 1.0000 | 0.0475 | 0.709 | 2.192 |
| | MURLI | 1.0016 | 0.0525 | 0.711 | 2.097 |
| | CLUB | 0.9981 | 0.0519 | 0.711 | 2.179 |

202

T A B L E - 8

19 - ROD CLUSTER - AIR COOLANT

| PARAMETER PITCH cm | METHOD | k | $\delta^{28}$ | $\gamma$ | $n_m/n_f$ |
|---|---|---|---|---|---|
| 18 | EXPT | 1.0000 | 0.0659 | 0.991 | 1.607 |
| | MURLI | 1.0103 | 0.0670 | 0.982 | 1.585 |
| | CLUB | 1.0088 | 0.0650 | 0.982 | 1.646 |
| 21 | EXPT | 1.0000 | 0.0623 | 0.843 | 1.713 |
| | MURLI | 1.0032 | 0.0606 | 0.854 | 1.695 |
| | CLUB | 1.0022 | 0.0593 | 0.855 | 1.737 |
| 24 | EXPT | 1.0000 | 0.0565 | 0.788 | 1.820 |
| | MURLI | 1.0029 | 0.0579 | 0.786 | 1.791 |
| | CLUB | 1.0020 | 0.0571 | 0.787 | 1.837 |
| 28. | EXPT | 1.0000 | 0.0549 | 0.734 | 1.946 |
| | MURLI | 1.0023 | 0.0566 | 0.736 | 1.898 |
| | CLUB | 1.0013 | 0.0559 | 0.738 | 1.947 |
| 36 | EXPT | 1.0000 | 0.0532 | 0.687 | 2.117 |
| | MURLI | 1.0004 | 0.0561 | 0.694 | 2.064 |
| | CLUB | 0.9989 | 0.0555 | 0.696 | 2.119 |

T A B L E - 2

28 - ROD CLUSTERS - $D_2O$ COOLANT

| PARAMETER | | k | $\delta^{28}$ | $\gamma$ | $n_u/n_f$ |
|---|---|---|---|---|---|
| PITCH cm | METHOD | | | | |
| 24 | EXPT | 1.0000 | 0.0580 | 0.9258 | 1.947 |
| | MURLI | 0.9994 | 0.0598 | 0.9068 | 1.861 |
| | CLUB | 1.0002 | 0.0586 | 0.9040 | 1.918 |
| 28 | EXPT | 1.0000 | 0.0582 | 0.8457 | 2.115 |
| | MURLI | 0.9985 | 0.0575 | 0.8260 | 2.012 |
| | CLUB | 0.9986 | 0.0569 | 0.8247 | 2.081 |
| 32 | EXPT | 1.0000 | 0.0554 | 0.8054 | 2.215 |
| | MURLI | 0.9993 | 0.0567 | 0.7838 | 2.112 |
| | CLUB | 0.9993 | 0.0562 | 0.7830 | 2.214 |
| 40 | EXPT | 1.0000 | 0.0547 | 0.7663 | 2.452 |
| | MURLI | 0.9991 | 0.0564 | 0.7488 | 2.352 |
| | CLUB | 0.9983 | 0.0560 | 0.7487 | 2.432 |

T A B L E - 10

28-ROD CLUSTERS - AIR COOLANT

| PARAMETER PITCH cm | METHOD | k | $\delta^{28}$ | $\gamma'$ | $n_m/n_f$ |
|---|---|---|---|---|---|
| 24 | EXPT | 1.0000 | 0 0691 | 0.9144 | 1.893 |
| | MURLI | 1.0040 | 0 0689 | 0.8867 | 1.832 |
| | CLUB | 1.0015 | 0.0675 | 0.8886 | 1.890 |
| 28 | EXPT | 1.0000 | 0.0632 | 0.8177 | 2.050 |
| | MURLI | 1.0016 | 0.0653 | 0.8009 | 1.974 |
| | CLUB | 0.9990 | 0.0646 | 0.8035 | 2.045 |
| 32 | EXPT | 1.0000 | 0.0619 | 0.7663 | 2.175 |
| | MURLI | 1.0039 | 0.0642 | 0.7561 | 2.098 |
| | CLUB | 1.0013 | 0.0636 | 0.7590 | 2.172 |
| 40 | EXPT | 1.0000 | 0.0624 | 0.7312 | 2.422 |
| | MURLI | 1.0015 | 0.0638 | 0.7128 | 2.304 |
| | CLUB | 0.9982 | 0.0633 | 0.7215 | 2.397 |

# Evaluation of Gamma Production Cross Sections in Coupled Neutron-Gamma Cross Section Sets

M. S. Kalra
Nuclear Engineering and Technology Programme
I.I.T., Kanpur - 208 016

ABSTRACT

Gamma energy deposition is a major source of heating in the blanket of an FBR, particularly at the beginning-of-life conditions prior to build-up of fissile isotopes. In the reflector external to the blanket, it is always the dominant fraction of total heating rate [1 ].

Stenstrom [2] used a multigroup transport approach, separately for neutrons and gammas, to obtain gamma heating rates in fast reactor environments. With the development of coupled neutron-gamma cross section sets [3,4,5 ] , the two transport calculations can be combined into one. The coupled cross section sets were used extensively for gamma heating analysis of FBR by Kalra and Driscoll [1] .

It is found that there is considerable amount of mismatching in the coupled neutron-gamma cross section sets. The gamma energy yield in the fissionable/fertile isotopes is found to range from 5 to 34 MeV per fission, and 2 to 13 MeV

per capture,indifferent neutron spectra appropriate to fast reactor environments. This is unreasonable in view of the fact that gamma energy from fission and fission product decay is in the range of approximately 14 to 16 MeV per fission, and from nonfission neutron capture, in the range of 4.8 to 6.5 MeV per capture in isotopes of uranium and plutonium. Gamma energy production per capture from sodium and iron is also observed to vary over unrealistic ranges.

Inelestic scattering gamma energy, which should not be more than 10 per cent of total gamma energy production in most fast reactor spectra [1] , is found to be highly overpredicted by coupled neutron-gamma cross section sets. For this purpose, an independent evaluation of inelastic gamma energy production was made using a 26 group cross section set [6] . Gammas produced from other reactions, for example (n,2n), (n, charged particle) etc, were ignored.

From the above mentioned observations, it can be concluded that the coupled neutron-gamma cross section data requires further evaluation, and at its present state of development, the calculations using this data may not be highly reliable.

References:

[1] Kalra, M.S. and M.J. Driscoll, "Gamma Heating in LMFBR Media," MITNE-179, COO-2240-18, February 1976.

[2] Stenstrom, D.G., "Calculation of Gamma Heating in a Fast Reactor Environment, "Trans. Am. Nucl. Soc., 15, 1, 551, June 1972.

[3] Oak Ridge National Laboratory, "40 Group Coupled Neutron and Gamma-Ray Cross Section Data, "DLC-23,April 1974.

[4] Sandmeier,H.A., et.al., "Coupled Neutron-Gamma Multigroup-Multitable Cross Sections for 29 Materials Pertinent to Nuclear Weapons Effect Calculations Generated by LASL/TD Division, "Los Alamos Scientific Laboratory, LA-5137, February 1974.

[5] Morrison, G.W. et al, " A Coupled Neutron and Gamma-Ray Multigroup Cross Section Library for Use in Shielding Calculations, " Trans. Am. Nucl. Soc., 15,1,535, June 1972.

[6] Bondarenko, I.I., et al, "Group Constants for Nuclear Reactor Calculations, " Consultants Bureau, New York (1964).

# Effect of Gamma Source Spectra on Gamma Transport near Interfaces

M. S. Kalra
Nuclear Engineering and Technology Programme
I.I.T., Kanpur-208 016

ABSTRACT

Data on neutron-energy-dependent gamma production spectra from all reactions and for various materials of interes in FBR design is practically non-existent. Where it exists, the uncertainties are likely to be large. For example, the spectrur of gammas produced subsequent to the capture of a thermal neutron in U-238 [1,2] , even when examined in a coarse gamma group structure [3] , shows upto a factor-of-two uncertainty ir particular groups.

To see the effect of gamma source spectra on gamma transport near interfaces/boundaries, where source and material discontinuities are encountered, one dimensional $S_8P_1$ transport calculations [4] with 18 gamma groups were done for typical LMFBR core-blanket-reflector assemblies. The space dependence of the gamma source chosen was appropriate for a large LMFBR, and was obtained by multigroup neutronic calculations accounting for gamma productions in fission, capture and inelastic scattering.

Three types of gamma interactions were considered, namely, Compton scattering, photoelectric effect and pair production [5,6] . Gamma source spectra were arbitrarily varied, while preserving the gamma energy source at each spatial point throughout the reactor. Gamma energy range from zero to 10 MeV was considered. Attention was focussed mainly on two hypothetical spectra - one introducing most of the gammas in the middle of the energy range, and the other at low and high energies.

The results obtained indicate that the gamma heating calculations in LMFBR media are insensitive to a large extent to gamma source spectra. The uncertainties in the source spectra are largely mitigated in gamma heating calculations if the total amount of gamma energy produced in any event is preserved. The maximum difference in gamma deposition rates is found to be $\pm$ 4% near the core-blanket and blanket-reflector interfaces, where a spike of as much as 100% in the deposition to source ratio can occur.

Thus it appears that the uncertainties in gamma source spectra are not likely to be the major source of error in gamma heating calculations for FBR media.

REFERENCES:

[1] Booth, R.S., et al., "A comparison of Calculated and Measured Yields of Neutron-Energy-Dependent Capture Gamma Rays from Uranium-238", Nucl.Sci.Eng., 47, 8-18 (1972).

[2] Takahashi, H., "Gamma-Ray Production Cross Sections of Neutron-Induced Uranium-238 Reactions", Nucl.Sci. Eng., 51, 296-315 (1973).

[3] Kalra, M.S. and M.J. Driscoll, "Gamma Heating in LMFBR Media", MITNE-179, COO-2250-18, February 1976.

[4] Engle, W.W., Jr., "A User's Manual for ANISN," K-1693, Union Carbide Corporation, Nuclear Division (1967).

[5] Davisson, C.M. and R.D. Evans, "Gamma-Ray Absorption Coefficients," Reviews of Modern Physics, 24,2,79-107, April 1952.

[6] Weise, K.E., and A. Foderaro, " Legendre Polynomial Expansion of Klein-Nishina Differential Cross Section," Nucl. Sci, Eng., 54, 1, 85-93, May 1974.

ABSTRACT

## Fusion Blanket Neutronics

(V.R. Nargundkar and M.P. Navalkar, Neutron Physics Division, Bhabha Atomic Research Centre, Trombay, Bombay 400 085, India).

Monte Carlo calculations were done using MORSE-E code to study the neutron multiplication for fusion neutrons in Beryllium, Beryllium Oxide and Lead. Los-Alamos 30 group cross-section set, with P1 scattering approximation was used. Some calculations were done using 99 group ENDF/B-III file with GAM-II structure for comparisons.

Tritium production in natural lithium blanket with and without graphite reflector has been also calculated for typical fusion blanket systems.

Object

Fusion blanket neutronics calculations are done using MORSE code and 99 group - ENDF B IV cross-section set. This requires a fairly large amount of memory on the computer and puts restrictions on the number elements that can be used. It was therefore thought necessary to find out whether reasonably accurate neutronics calculations can be done with a small group cross-section set. The Los-Alamos 30 group cross-section set was chosen for this purpose because of its group structure being suitable for fusion blanket neutronics studies.

Neutron Multiplication

In thermal blanket studies beryllium is considered to be the most efficient neutron multiplier for fusion neutrons. It is a very costly material and its oxide is more suitable from the manufacturing point of view. Practically all the intermediate and heavy metals have a fairly good (n,2n) cross-section at a reasonable threshold energy. Lead is one of the common materials and had the added advantage of being a good gamma shield. As such neutron multiplication was studied for Be, BeO and lead using MORSE-E code and 30 group Los-Alamos cross-section set. Only P1 scattering approximation was used, as it was found that it does not make appreciable change in the accuracy using higher approximations. Though, anisotropy of in-elastic scattering may be important, it was not considered. For beryllium alone, 99 group P3 approximation calculations were made for comparison purposes. The results

are shown in Table 1. It is seen that for beryllium there is very good agreement between 99 group P3 and 30 group P1 calculations. From neutron multiplication point of view, it is seen that BeO is a poor choice. For Be, which has highest neutron multiplication, saturation occurs at 20 cm thickness, whereas for lead neutron saturation does not occur even at 40 cm. The neutron spectra for Be, BeO and lead for 20 cm radius sphere ane shown in figure 1. It is seen that Be spectrum is superior from tritium breeding point of view when compared to that of lead because

1. At higher energies (T7 breeding) neutron flux is much higher in beryllium

2. Lead has a very prominent peak in 100 KeV region and a sharp cut-off around 160 eV.

3. Beryllium has a pronounced thermal peak.

Thus it may be inferred that even if, lead and beryllium have comparable neutron multiplications, only beryllium has a neutron spectrum suitable for tritium breeding. For using lead as a neutron multiplier, it would be necessary to tailor its spectrum for tritium breeding. These inferences have been verified by tritium breeding calculations in a loocm thick natural lithium blanket, using lead/ beryllium as multipliers. The results are shown in Table 2.

Tritium Breeding

Calculations were done for T6 and T7 breeding in natural lithium blanket for two different geometries using 99 group P3 approximation and 30 group P1 approximation. The results are shown

in Table 3. It is seen that T7 breeding is over-estimated by 12% in 30 group set compared to 99 group set. This may be due to the fact that for Li-7, 30 group library uses ENDF/B-II Library based on 1965 results, compared to ENDF/B-IV library of 1977 used in 99 group set. It is desirable to suitably amend 30 group lithium-7 cross-sections.

By using a suitable reflector like graphite, T-6 breeding in lithium can be very considerably enhanced. This was studied for natural lithium blanket with lead/beryllium multipliers. The results are shown in Table IV. It is seen that with lead (12 cm or 20 cm) multiplier, a maximum tritium breeding of 1.50 can be obtained which is smaller than 1.58 obtained without any multiplier (i.e. nat. lithium with graphite reflector). A maximum tritium breeding of 1.78 is obtained with 12 cm thick beryllium multiplier and 40 cm thick graphite reflector, which is only 12% higher than that obtained without any multiplier.

TABLE 1

MULTIPLICATION IN SPHERES

| Sphere Radius cm | Beryllium | | BeO | Lead |
|---|---|---|---|---|
| | 99 group P3 | 30 group P1 | 30 group | P1 approx. |
| 8 | 1.54 | 1.50 | 1.19 | 1.41 |
| 12 | 1.70 | 1.73 | 1.27 | 1.53 |
| 20 | 2.14 | 2.03 | 1.36 | 1.67 |
| 40 | 2.14 | 2.03 | 1.25 | 1.79 |

TABLE 2

COMPARISON OF TRITIUM PRODUCTION IN NATURAL LITHIUM, FOR LEAD AND BERYLLIUM AS MULTIPLIERS (spherical geometry)

NAT. Li THICKNESS = 100 cm

| Multiplier | Thickness Cm | T6 | T7 | Total |
|---|---|---|---|---|
| Lead | 12 | 0.98 | 0.29 | 1.18 |
| Beryllium | 12 | 1.11 | 0.36 | 1.47 |
| Lead | 20 | 1.03 | 0.13 | 1.16 |
| Beryllium | 20 | 1.36 | 0.19 | 1.55 |

TABLE 3

NATURAL LITHIUM COMPARISON OF RESULTS 30 GROUP AND 99 GROUP

| Geometry | | 99 group P3 | 30 group P1 | 99/30 gr. ratio |
|---|---|---|---|---|
| 100 cm radius 200 cm height cylinder | T6 | 0.48 | 0.51 | 0.94 |
| | T7 | 0.72 | 0.82 | 0.88 |
| 50 cm radius sphere | T6 | 0.105 | 0.104 | 1.00 |
| | T7 | 0.55 | 0.64 | 0.86 |

TABLE 4

TRITIUM PRODUCTION IN 100 CM RADIUS LITHIUM BLANKET

| Multiplier | Graphite Reflector Thickness | T6 | T7 | T total |
|---|---|---|---|---|
| - | 0 cm | 0.45 | 0.80 | 1.25 |
| - | 40 cm | 0.78 | 0.81 | 1.59 |
| 12 cm lead | 0 cm | 0.89 | 0.29 | 1.18 |
| " | 40 cm | 1.23 | 0.27 | 1.50 |
| 12 cm beryl. | 0 cm | 1.11 | 0.36 | 1.47 |
| " | 40 cm | 1.40 | 0.38 | 1.78 |
| 20 cm lead | 0 cm | 1.03 | 0.13 | 1.16 |
| " | 40 cm | 1.36 | 0.14 | 1.50 |
| 20 cm beryl. | 0 cm | 1.36 | 0.19 | 1.53 |
| " | 40 cm | 1.49 | 0.18 | 1.67 |

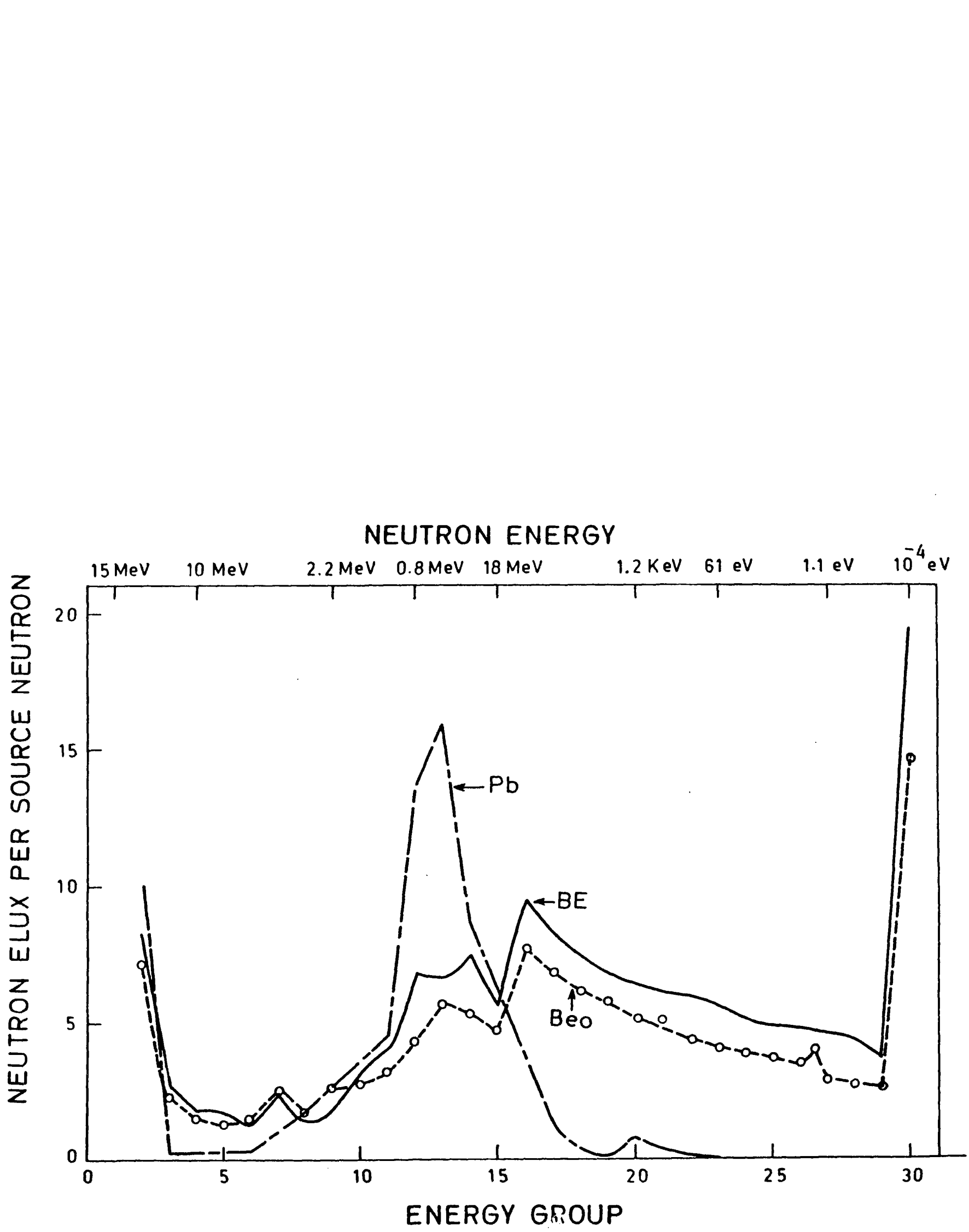
NEUTRON ENERGY
15 MeV
10 MeV
2.2 MeV
0.8 MeV
18 MeV
1.2 KeV
61 eV
1.1 eV
10⁻⁴ eV
NEUTRON ELUX PER SOURCE NEUTRON
20
15
10
5
0
Pb
BE
Beo
0
5
10
15
20
25
30
ENERGY GROUP